UNIVERSIDADE FEDERAL DO RIO GRANDE DO SUL

INSTITUTO DE GEOCIÊNCIAS

PROGRAMA DE PÓS-GRADUAÇÃO EM GEOCIÊNCIAS

INTERAÇÕES VULCANO-SEDIMENTARES - UMA CHAVE PARA COMPREENDER OS PALEOAMBIENTES DO JURÁSSICO SUPERIOR E CRETÁCEO INFERIOR NA BACIA DO PARANÁ, SUL DO BRASIL

FERNANDO RODRIGUES RIOS

ORIENTADORA - Profª. Drª. Ana Maria Pimentel Mizusaki

COORIENTADORA - Profª. Drª. Cassiana Roberta Lizzoni Michelin

Porto Alegre, 2023

UNIVERSIDADE FEDERAL DO RIO GRANDE DO SUL
INSTITUTO DE GEOCIÊNCIAS
PROGRAMA DE PÓS-GRADUAÇÃO EM GEOCIÊNCIAS

INTERAÇÕES VULCANO-SEDIMENTARES - UMA CHAVE PARA COMPREENDER OS PALEOAMBIENTES DO JURÁSSICO SUPERIOR E CRETÁCEO INFERIOR NA BACIA DO PARANÁ, SUL DO BRASIL

FERNANDO RODRIGUES RIOS

ORIENTADORA - Profª. Drª. Ana Maria Pimentel Mizusaki
COORIENTADORA - Profª. Drª. Cassiana Roberta Lizzoni Michelin

BANCA EXAMINADORA
Drª. Carla Klein – Serviço Geológico do Brasil, Companhia de Pesquisas de Recursos Minerais (CPRM)
Prof. Dr. Giovani Matte Cioccari – Centro de Engenharias, Universidade Federal de Pelotas (UFPel)
Prof. Dr. Rogério Roque Rubert – Faculdade de Geociências, Universidade Federal do Mato Grosso (UFMT)

Tese de Doutorado apresentada como requisito para a obtenção do Título de Doutor em Geociências.

Porto Alegre, 2023

CIP - Catalogação na Publicação

Rios, Fernando Rodrigues
Interações vulcano-sedimentares - uma chave para compreender os paleoambientes do Jurássico Superior e Cretáceo Inferior na Bacia do Paraná, Sul do Brasil / Fernando Rodrigues Rios. -- 2023.
154 f.
Orientadora: Ana Maria Pimentel Mizusaki.

Coorientadora: Cassiana Roberta Lizzoni Michelin.

Tese (Doutorado) -- Universidade Federal do Rio Grande do Sul, Instituto de Geociências, Programa de Pós-Graduação em Geociências, Porto Alegre, BR-RS, 2023.

1. Interação vulcano-sedimentar. 2. Jurássico Superior - Cretáceo Inferior. 3. Formação Guará. 4. Formação Botucatu. 5. Formação Serra Geral. I. Mizusaki, Ana Maria Pimentel, orient. II. Michelin, Cassiana Roberta Lizzoni, coorient. III. Título.

Elaborada pelo Sistema de Geração Automática de Ficha Catalográfica da UFRGS com os dados fornecidos pelo(a) autor(a).

Aos meus amados,

Neusa, José Edmilson e Eduardo.

AGRADECIMENTOS

Agradeço primeiramente aos meus pais que sempre priorizaram a educação de qualidade como um agente transformador de nós mesmos. Sou grato por sempre estarem de braços abertos, por toda ajuda financeira e emocional, pelas discussões, risos, questionamentos e incentivos que me trouxeram até aqui. Pela confiança e liberdade depositadas em mim. Essa tese é a cristalização do esforço de vocês.

Agradeço imensamente a minha orientadora Profª. Drª. Ana Maria Pimentel Mizusaki pela amizade, oportunidade, por toda a dedicação e confiança depositadas em mim e neste trabalho. Pelos sábios conselhos, paciência e pelos valores éticos repassados. Seus ensinamentos me mostraram o tipo de profissional que pretendo ser.

Agradeço a minha coorientadora Profª. Drª. Cassiana Roberta Lizzoni Michelin pelos inúmeros ensinamentos, pela amizade, por conselhos, recomendações e oportunidades. Por acreditar no projeto apesar de todos as dificuldades e desafios enfrentados.

Agradeço aos amigos que estiveram em quase todos ou em algum momento me acompanhando numa cerveja, num churrasco, num chimas, nos inúmeros campos, na escadinha, no RU, me emprestando algum livro, um martelo, uma bússola, um pendrive, me dando carona, uma ajuda, em longas e maravilhosas conversas sobre a vida: Isaque Rodrigues, Vivianne Bastos, Rayane Bastos, Igor Flesch, Amanda Massuda, Eduardo Trein, Débora Sayuri, Dionatan Padilha, Henrique Redivo, Larissa Tononi, Rafaela Kunrath, Catherine Goulart, Edgar Amaral, Edvaldo Oliveira...

Agradeço ao professor Dr. Rualdo Menegat pelos ensinamentos e conhecimentos repassados durante as fases de escrita e correção do artigo. Foi uma rotina de grande aprendizado.

Agradeço aos professores Dr. Luiz Fernando De Ros e Drª. Amanda Goulart Rodrigues pelos ensinamentos transmitidos durante a minha estadia no Laboratório de Petrologia Sedimentar.

Agradeço ao professor Dr. Heinrich Theodor Frank pelo suporte com o microscópio durante a pandemia.

Agradeço ao Gilberto pela grande ajuda na preparação das amostras para DRX.

Estendo meus agradecimentos também ao Conselho Nacional de Desenvolvimento Científico e Tecnológico (CNPq) pela concessão de bolsa de doutorado (Processo 141345/2017-9). Agradeço a todos os profissionais que fazem o Programa de

Pós-Graduação em Geociências da Universidade Federal do Rio Grande do Sul (PPGGEO – UFRGS) uma referência internacional. Agradeço pela educação pública, gratuita e de qualidade, pela estrutura intelectual e laboratorial disponíveis e pelas inúmeras oportunidades.

Ao meu melhor amigo e namorado Jonas, pelo companheirismo e amor em todos os momentos. Que me acompanhou nessa longa e exaustiva caminhada, que aguentou meus momentos de mau humor e que fez jantares maravilhosos durante esse longo período alegrando os meus dias. Muito obrigado pela compreensão, incentivo, pelas inúmeras ajudas com o Excel e pela verificação de todas as referências.

“Tudo no mundo começou com um sim. Uma molécula disse sim a outra molécula e nasceu a vida. Mas antes da pré-história havia a pré-história da pré-história e havia o nunca e havia o sim. Sempre houve. Não sei o quê, mas sei que o universo jamais começou.”

A hora da Estrela, Clarice Lispector.

RESUMO

O intervalo entre o Jurássico Superior e o Cretáceo Inferior na Bacia do Paraná foi caracterizado pela acumulação do sistema eólico seco, a Formação Botucatu, inteiramente preservado pelos derrames vulcânicos, da Formação Serra Geral, contemporâneos à fragmentação do Gondwana. O intenso vulcanismo básico e, secundariamente, ácido recobriu o erg. A interface entre essas duas unidades registra um ambiente eólico atuante durante os estágios iniciais do vulcanismo caracterizada por feições e depósitos vulcano-sedimentares. As interações vulcano-sedimentares se originaram pela mistura de sedimentos consolidados ou inconsolidados, saturados ou não em água, com os derrames vulcânicos. As feições e depósitos de interação foram classificadas como concomitantes ao vulcanismo, formando feições e depósitos vulcanoclásticos, ou apenas feições de recobrimento com ausência de interações; e podem ser posteriores ou em intervalos de quiescência do vulcanismo e retorno da sedimentação, formando feições e depósitos epiclásticos. Através das diferentes particularidades dos processos de interação, entre as rochas vulcânicas e os sedimentos analisados nas feições e depósitos vulcano-sedimentares, o ambiente eólico da Formação Botucatu pôde ser, por analogia, comparado aos ambientes eólicos atuais. O paleoambiente proposto indica um ambiente sedimentar com diferentes domínios, categorizados por sua saturação em água. Os diferentes componentes siliciclásticos encontrados em cada domínio permitiram a formação das diferentes feições e depósitos vulcano-sedimentares encontrados. Por meio da petrografia quantitativa, amostras da matriz arenosa desses depósitos foram analisadas, a fim de discutir a paragênese das interações vulcano-sedimentares. Processos diagenéticos normais de soterramento foram discutidos para os arenitos epiclásticos e de diagênese de contato para os arenitos vulcanoclásticos. A principal distinção entre eles é a presença de indicativos texturais de fluidização encontrados nos arenitos vulcanoclásticos, ao longo da interface lava-sedimento. Tais características apontam que os sedimentos se encontravam inconsolidados e provavelmente úmidos ou saturados em água no momento da interação com o derrame vulcânico. Os arenitos epiclásticos possuem como principais constituinte diagenético as argilas infiltradas e esmectitas neoformadas, enquanto que os arenitos vulcanoclásticos são cimentados principalmente por calcedônia e zeólita. Devido ao volume intergranular ocupados pela calcedônia e zeólita, principalmente na interface lava-sedimento, suas gêneses por meio do soterramento é improvável, indicando condições precoces e de diagênese de contato. Além do mais, na região central do Rio Grande do Sul, limite sudeste atual da borda da Bacia do Paraná, há ocorrência de depósitos flúvio-eólicos da Formação Guará em contato com as rochas vulcânicas da Formação Serra Geral. Considerando, portanto, uma nova compreensão das relações temporais e espaciais entre os sistemas flúvio-eólicos (Formação Guará), eólicos (Formação Botucatu) e vulcânicos (Formação Serra Geral) que se instalaram nesse intervalo temporal. Mediante a análise de fácies e de elementos arquiteturais, a fim de reconstituir a evolução desse pacote vulcano-sedimentar, foi demonstrado que os sistemas sedimentares Guará e Botucatu permaneceram ativos durante o início do Serra Geral. Consequentemente, não houve hiato entre essas unidades, demonstrando uma contemporaneidade dos sistemas sedimentares com o vulcanismo em pelo menos uma de suas fases de desenvolvimento.

Palavras-chave: Interação vulcano-sedimentar, Jurássico Superior-Cretáceo Inferior, Formação Guará, Formação Botucatu, Formação Serra Geral.

ABSTRACT

The period between the Upper Jurassic and Lower Cretaceous in Paraná Basin was characterized by a dry aeolian system accumulation, the Botucatu Formation, entirely preserved by the volcanic flows of Serra Geral Formation, contemporaneous with the Gondwana fragmentation. Intense basic and, secondarily, acidic volcanism covered the erg. The interface between these two units records an active aeolian environment during the initial stages of volcanism characterized by features and volcanic-sedimentary deposits. Volcano-sedimentary interaction originated from the mixing of consolidated or unconsolidated sediments, saturated or not in water, with volcanic flows. Interaction features and deposits were classified as concomitant to volcanism, forming volcanoclastic features and deposits, or just covering features with no interaction; and it can occur later or during the volcanism quiescence and sedimentation return, forming epiclastic features and deposits. Through the different particularities of the interaction processes analyzed in the features and in the volcanic-sedimentary deposits, the aeolian environment of the Botucatu Formation could be, by analogy, compared to the current aeolian environments. The proposed paleoenvironment indicates a sedimentary environment with different domains, categorized by their water saturation. The different siliciclastic components found in each domain allowed the formation of different features and volcano-sedimentary deposits. Through quantitative petrography, sandy matrix samples of these deposits were analyzed, in order to discuss the paragenesis of volcano-sedimentary interaction. Regular burial diagenetic processes were discussed for epiclastic sandstones and contact diagenesis processes for volcanoclastic sandstones. The main distinction between them is the presence of fluidization in texture found in the volcano-clastic sandstones, along lava-sediment interface. Such characteristics indicate that the sediments were unconsolidated and probably wet or saturated in water during the interaction with the volcanic flow. Epiclastic sandstones hold infiltrated clays and neoformed smectites as their main diagenetic constituent, while volcanoclastic sandstones are cemented mainly by chalcedony and zeolite. Due to the intergranular volume occupied by chalcedony and zeolite, mainly at the lava-sediment interface, their genesis through burial is unlikely, indicating early conditions and contact diagenesis. Furthermore, in the central region of Rio Grande do Sul, the current southeast limit of Paraná Basin's border, there are occurrences of fluvio-aeolian deposits from the Guará Formation in contact with volcanic rocks of Serra Geral Formation. Considering, therefore, a new understanding of the temporal and spatial relationships between the fluvio-aeolian (Guará Formation), aeolian (Botucatu Formation) and volcanic (Serra Geral Formation) systems that were installed at that period. Through the analysis of facies and architectural elements, in order to reconstitute the evolution of this volcanic-sedimentary successions, it was demonstrated that the Guará and Botucatu sedimentary systems remained active during the beginning of Serra Geral. Consequently, there was no gap between these units, demonstrating that the sedimentary systems are contemporaneous with volcanism, in at least one of its development phases.

Keywords: Volcano-sedimentary interaction, Upper Jurassic-Lower Cretaceous, Guará Formation, Botucatu Formation, Serra Geral Formation.

LISTA DE FIGURAS

SUMÁRIO

ESTRUTURAÇÃO DA TESE

A presente tese de doutorado, cujo título é *"Interações vulcano-sedimentares - uma chave para compreender os paleoambientes do Jurássico Superior e Cretáceo Inferior na Bacia do Paraná, Sul do Brasil"*, está estruturada em torno de três artigos científicos submetidos em periódicos classificados pela CAPES como *Qualis* A. Assim, a organização deste trabalho compreende a seguinte sequência:

Capítulo 1 - Apresenta a introdução e a justificativa com os principais questionamentos que levaram ao desenvolvimento da pesquisa, bem como os objetivos.

Capítulo 2 - Estado da Arte com as principais discussões na literatura a respeito da contemporaneidade entre sedimentação e magmatismo e seus produtos gerados.

Capítulo 3 - Expõe as Metodologias empregadas durante as investigações aqui apresentadas.

Capítulo 4 - Contextualização geológica da Bacia do Paraná e as unidades litoestratigráficas da Sequência Gondwana III, foco da pesquisa.

Capítulo 5 - Exibe uma síntese integradora das discussões resultantes dos artigos científicos submetidos.

Capítulo 6 - Apresenta três artigos científicos resultantes da pesquisa submetidos em revistas especializadas, contendo as cartas de submissão e os manuscritos:

6.1 "Volcano-sedimentary interactions - a key to understand Cretaceous paleoenvironments in the Paraná Basin (southern Brazil)" - Journal of Volcanoglogy and Geothermal Research (A2).

6.2 "Evolution of the Upper Jurassic and Lower Cretaceous vulcano-sedimentary register - southeast portion of Paraná Basin, Brazil" - Cretaceous Research (A2).

6.3 "Volcanoclastic and epiclastic diagenesis of sandstones associated with volcano-sedimentary deposits from the Upper Jurassic and Lower Cretaceous, Paraná Basin, southern Brazil"- Journal of South American Earth Sciences (A3).

Capítulo 7 - Conclusões.

Capítulo 8 - Engloba as referências bibliográficas que apoiaram o estudo e que estão citadas no corpo da tese.

CAPÍTULO 1 - FUNDAMENTAÇÃO DA TESE

1. INTRODUÇÃO

Aspectos tanto do ponto de vista ígneo quanto do sedimentar controlam a formação de rochas e feições por meio da interação vulcano-sedimentar, como: o ambiente de colocação, tipo de lava, grau de cristalização, granulometria, consolidação e grau de saturação em água dos sedimentos. No entanto, os processos e produtos de tais interações ainda não estão totalmente compreendidos, posto que o modo como a lava interage com os sedimentos consolidados ou inconsolidados com ou sem a presença de água é complexa. A interação entre vulcânicas e sedimentos pode ocorrer de forma concomitante com as extrusões, com temperaturas relativamente elevadas e lavas parcialmente cristalizadas – feições e depósitos vulcanoclásticos; ou em ambientes expostos, com intemperismo, erosão e sedimentação, consequentemente, em derrames já cristalizados e em temperatura ambiente - feições e depósitos epiclásticos (Kokelaar, 1982; Lorenz, 1984; Busby-Spera & White, 1987; McPhie *et al.*, 1993; Hanson & Hargrove, 1999; Dadd & Van Wagoner, 2002; Jerram & Stollhofen, 2002; Lorenz *et al.*, 2002; Skilling *et al.*, 2002; Squire & McPhie, 2002; Zimanowski & Büttner, 2002; Rawcliffe, 2016; Rios *et. al.*, 2018).

As feições e litologias geradas a partir da interação vulcano-sedimentar são fundamentais em reconstruções paleoambientais, além de serem marcadores estratigráficos importantes, já que sua presença fornece uma idade relativa, pois possuem como eventos contemporâneos sedimentação e magmatismo. Diversas pesquisas vêm sendo realizadas com o objetivo de entender os processos de formação de feições vulcano-sedimentares nos mais diversos ambientes (MacDonald, 1939, Branney & Suthren, 1988; Allen, 1992; Boulter, 1993; McPhie, *et al.*, 1993; Jerram & Stollhofen, 2002; Erkül *et al.*, 2006; Petry *et al.*, 2007; Arioli *et al.*, 2008; Holz et al., 2008; Perinotto et al., 2008; Waichel *et al.*, 2008; Ballén *et al.*, 2013; Hole *et al.*, 2013; Michelin, 2014; Reis *et al.*, 2014; Rabelo & Nogueira, 2015; McLean *et. al.*, 2016; Gihm & Kwon, 2017; Kwon & Gihm, 2017; Rios *et al.*, 2018; Rabelo, 2019; Rabelo *et al.*, 2019; Famelli *et al.*, 2021; Nogueira *et al.*, 2021; Jeon & Sohn, 2022)

Na Plataforma Sul-Americana, destaca-se a Bacia do Paraná, onde houve um importante evento vulcânico no Cretáceo Inferior, relacionado com a quebra do

Gondwana e a formação do Oceano Atlântico Sul. É a denominada Formação Serra Geral, caracterizada por um enorme volume de lavas e intrusões associadas que recobriram e interagiram com um extenso sistema eólico ativo, a Formação Botucatu, formando depósitos e feições vulcano-sedimentares (Milani *et al.*, 1998; Scherer, 2002; Petry *et al.*, 2007; Waichel *et al.*, 2008; Michelin, 2014; Reis *et al.*, 2014; Rios *et al.*, 2018).

Durante muito tempo o intervalo Jurássico-Cretáceo da Bacia do Paraná foi subdividido em três unidades: unidade basal flúvio-eólica (Formação Guará); unidade intermediária francamente eólica (Formação Botucatu); e unidade de topo totalmente vulcânica (Formação Serra Geral) (Milani, 1997; Milani *et al.*, 1998; Scherer, 2002; Scherer & Lavina, 2005, 2006; Zerfass *et al.*, 2007; Godoy *et al.*, 2011, 2016, 2018; Reis, 2016, 2020; Reis *et al.*, 2019). Recentemente, trabalhos demonstraram que o sistema eólico foi progressivamente recoberto pelos basaltos, resultando na preservação de dunas eólicas. As intercalações sedimentares, denominadas de intertraps, são abundantes na base da sucessão vulcânica e evidenciam períodos de quiescência da atividade magmática (Waichel *et al.*, 2008; Michelin, 2014; Reis *et al.*, 2014; Rios *et al.*, 2018). Por conta disso, esses trabalhos associaram a Formação Botucatu como contínua à Formação Serra Geral, posicionando a Formação Guará como uma unidade separada e anterior as outras duas. Entretanto, na região central do estado Rio Grande do Sul, os basaltos estão diretamente em contato com uma unidade de semelhante posicionamento estratigráfico e características faciológicas, sugerindo-se tratar da Formação Guará (Zerfass *et al.*, 2007; Godoy *et al.*, 2011, 2016, 2018)

1.1 JUSTIFICATIVA

Enfoque inovador na proposição de paleoambientes utilizando as feições e depósitos de interação lava-sedimento presentes na interface entre as unidades Botucatu e Serra Geral, e, também, no contato entre a Formação Guará com a Formação Serra Geral. Discutindo, portanto, a contemporaneidade entre essas três formações.

As interações lava-sedimento estão cada vez mais bem documentadas na literatura. Há na literatura, no entanto, uma ênfase na descrição e interpretação dos aspectos relacionados a lava/magma na formação das diferentes litologias e feições (Kokelaar, 1982; Lorenz, 1984; Busby-Spera & White, 1987; Hanson & Hargrove, 1999; Dadd & Van Wagoner, 2002; Jerram & Stollhofen, 2002; Lorenz et al., 2002; Skilling et

al., 2002; Squire & McPhie, 2002; Zimanowski & Büttner, 2002; Petry et al., 2007; Waichel et al., 2007; Hole et al., 2013; McLean et. al., 2016; Rawcliffe, 2016; Gihm & Kwon, 2017; Kwon & Gihm, 2017; Famelli et al., 2021; Jeon & Sohn, 2022). Em contrapartida, os argumentos abordados para os controles, do ponto de vista sedimentar, que influenciam nos processos de interação são mínimos (Ballén et al., 2013; Rabelo & Nogueira, 2015; Rabelo, 2019; Rabelo et al., 2019; Nogueira et al., 2021). Portanto faz-se necessária uma maior discussão a respeito de que forma os sedimentos inconsolidados ou não, insaturados ou saturados em água, conduzem essas interações em conjunto com os controles ígneos.

Diversas pesquisas vêm sendo realizadas investigando o impacto da fluidização e a redistribuição de partículas e dos fluidos existentes nos poros em depósitos de fluxo piroclástico (Wilson, 1980, 1984; Druitt, 1995; Roche et al., 2001; Druitt et al., 2004; Ross & White, 2005; Druitt et al., 2007; Girolami et al., 2008). Ao passo que, os efeitos da fluidização e do calor atuantes nos sedimentos durante a formação das feições e depósitos vulcano-sedimentares em derrames efusivos raramente são investigados. Tornando necessário estudos que aprofundem de que forma a fluidização e o calor da lava contribuem para a diagênese das feições e depósitos vulcano-sedimentares.

1.2 OBJETIVOS

O objetivo geral deste trabalho é reconhecer os depósitos e feições vulcano-sedimentares do Jurássico Superior - Cretáceo Inferior, da Bacia do Paraná, buscando os mecanismos que influenciaram os processos de interação. Utilizar interpretações estratigráficas e análises petrográficas afim verificar e obter modelos paleoambientais a partir das interações vulcano-sedimentares.

Como objetivos específicos, busca verificar a existência de água ou umidade para os modelos paleoambientais por meio das interações lava-sedimento. Bem como discutir e explicar a origem, distribuição e cronologia das alterações diagenéticas dessas interações. Além de investigar o posicionamento estratigráfico das Formações Guará, Botucatu e Serra Geral.

CAPÍTULO 2 - ESTADO DA ARTE

2. CONTEMPORANEIDADE MAGMATISMO E SEDIMENTAÇÃO

As interações lava-sedimento podem ocorrer concomitantes ao vulcanismo formando feições e depósitos vulcanoclásticos, ou apenas feições de recobrimento com ausência de interações; e podem ser posteriores, ou em intervalos de quiescência do vulcanismo e retorno da sedimentação, originando feições e depósitos epiclásticos.

Intercalados aos derrames vulcânicos, os denominados *intertraps* caracterizam-se por camadas sedimentares de dimensões centimétricas a métricas que geralmente apresentam estruturas sedimentares e feições características do ambiente sedimentar no qual foi formado. Os *intertraps* são interpretados como indicativos de que a sedimentação persistiu durante o evento vulcânico e são importantes não só por demonstrarem intervalos de quiescência entre os diferentes derrames vulcânicos em um determinado local da bacia, mas também pela possibilidade de associarem-se a feições e depósitos de interação vulcano-sedimentar.

2.1 FEIÇÕES DE RECOBRIMENTO

Rawcliffe (2016) investigou em kinghorn, Fife, costa leste da Escócia, a deformação por carga nos sedimentos sem a presença de brechas vulcanoclásticas associadas. Os sedimentos foram compactados pela lava sobrejacente e, devido aos contrastes de densidade e à presença mínima de água nos poros, estruturas em chama se desenvolveram (Figura 1). O estado do sedimento no momento da colocação da lava foi interpretado como: ligeiramente compactado e consolidado, com o mínimo de água nos poros. A consolidação do sedimento indicou que as estruturas do acamamento foram preservadas e que a fluidização e a liquefação foram inibidas (Busby-Spera & White, 1987; Skilling *et al.,* 2002). A combinação de todas as propriedades dos sedimentos impediu a fragmentação da lava e, portanto, a interação lava-sedimento não ocorreu. Ao passo que, Gihm & Kwon (2017) em estudos na porção ocidental dos vulcões de Buan, sudoeste da Coreia, relataram a deformação por carga e a presença de brechas vulcanoclásticas em sedimentos lacustres, saturados em água e inconsolidados. O contato lava-sedimento, marcado pelas brechas vulcanoclásticas, é ondulado devido ao

desenvolvimento de uma série de estruturas de carga e chama. Ao contrário do estudo anterior, neste, o processo de fluidização foi fundamental.

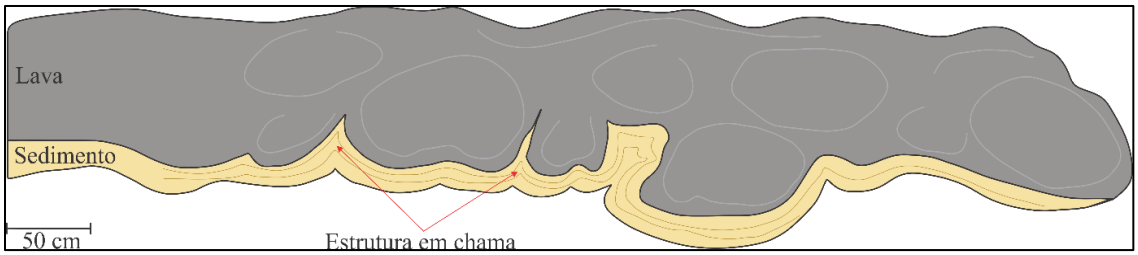

Figura 1: Esquema de deformação por carga em uma unidade sedimentar sobreposta por derrame vulcânico. Modificado de Rawcliffe (2016).

Pesquisas na Bacia do Paraná têm demonstrado a presença de dunas do paleodeserto Botucatu completamente preservadas ao longo da pilha vulcânica pelos derrames basálticos da Formação Serra Geral (Figura 2). A preservação da paleotopografia das dunas é ocasionada pelo seu recobrimento por lava em temperaturas elevadas, com sedimentos consolidados ou inconsolidados e ausência de interação vulcano-sedimentar ao longo da interface lava-sedimento (Scherer, 2002; Petry *et al.*, 2007; Waichel *et al.*, 2007, Holz *et al.*, 2008; Waichel *et al.*, 2008; Reis, 2013; Luchetti *et al.*, 2014; Michelin, 2014; Rios, 2017; Rios *et al.*, 2018). A preservação da das dunas eólicas, requer uma rápida velocidade de fluxo do derrame e ausência de água e ou umidade nos sedimentos. Estruturas de superfície no dorso da duna como estrias de fluxo (Figura 3) e lobos de lava foram formadas pelo fluxo da lava sobre um substrato de areia não consolidado (Jerram *et al.*, 2000; Jerram & Stollhofen, 2002; Rios, 2017; Rios *et al.*, 2018).

Figura 2: Duna eólica com morfologia preservada. Município de Novo Hamburgo, Rio Grande do Sul (RS) (Modificado de Rios *et al.,* 2018).

Figura 3: A) Contato (linha tracejada) entre a duna eólica e o derrame vulcânico. B) Estrias de fluxo localizadas na interface lava-sedimento formada pelo arrasto do derrame sobre o sedimento inconsolidado. Modificado de Rios (2017).

2.2 DIQUES DE ARENITO

O dique de arenito, também conhecido como dique clástico, é formado através do processo de fluidização sendo caracterizado como uma feição vulcanoclástica. O fraturamento, devido ao rápido resfriamento do corpo magmático, reduz a pressão litostática e permite a fluidização dos sedimentos adjacentes e sua posterior injeção nas fraturas (Kokelaar, 1982). A mobilização dos sedimentos em subsuperfície e a fluidização têm sido reconhecidas em muitos ambientes geológicos: reservatórios pressurizados, interface lava-sedimento em derrames vulcânicos e metamorfismo de contato ao redor de

intrusões magmáticas (Nichols *et al.,* 1994; Jolly & Lonergan, 2002; Mazzini *et al.,* 2003; Jamtveit *et al.,* 2004; Svensen *et al.,* 2006, 2010). É uma feição comumente encontrada em bacias sedimentares afetadas por grandes eventos magmáticos, como a Bacia do Paraná (Figuras 4A-C) (Picheler, 1952; Suguio & Fulfaro, 1974; Petry *et al.,* 2007; Arioli *et al.,* 2008; Perinotto *et al.,* 2008; Machado *et al.,* 2009; Hartmann *et al.,* 2012a, b; Michelin, 2014; Rios, 2017; Rios *et al.,* 2018).

Petry (2006) e Petry *et al.* (2007) investigando os limites entre as Formações Botucatu e Serra Geral, Bacia do Paraná, na cidade de Torres (RS), relataram que os diques de arenito podem vir a ser formados pela da injeção de sedimento para o interior do derrame vulcânico durante a sua movimentação, dado o peso do pacote ígneo e seu fluxo. Deste modo, a areia injetada ao encontrar porções rúpteis originaria os diques de arenito. Entretanto, Hartmann *et al.* (2012b), para a mesma área de estudo, propõe um modelo de injeção de areia por processos hidrotermais de baixa temperatura em rochas basálticas. Já Rios *et al.* (2018), também para a mesma área, não leva em consideração os mecanismos de movimentação do derrame (tracionamento), descritos anteriormente por Petry (2006) e Petry *et al.* (2007), na formação de diques de arenito, e sim a fluidização como o principal mecanismo de formação dessas feições. Contudo, mais de um mecanismo, além da fluidização, posto que este é o principal, pode estar atrelado aos processos de formação dos diques de arenito.

Sedimentos saturados em água faz com que as interações ocorram de forma concomitante ao evento magmático (Mizusaki, 1986; Reis, 2013; Reis *et al.,* 2014). Diques de arenito podem se formar pelo contraste de temperatura da lava com o sedimento úmido, contraste este que faz com que o processo de fluidização se inicie. A água é vaporizada e confina-se na interface sedimento-derrame. Com o resfriamento progressivo da lava diaclases começam a surgir, fazendo com que o vapor juntamente com o sedimento, que estava confinado a altas pressões, escape por essas zonas de menor pressão. Ao longo do contato com a rocha encaixante o dique pode apresentar bordas de reação, indicando uma interação a temperaturas elevadas (Michelin, 2014; Rios, 2017; Rios *et al.,* 2018). Ademais, nota-se a presença de clastos com diferentes morfologias imersos no dique de arenito, provavelmente oriundos do processo de fragmentação magmática durante a fluidização (Figuras 4A-C).

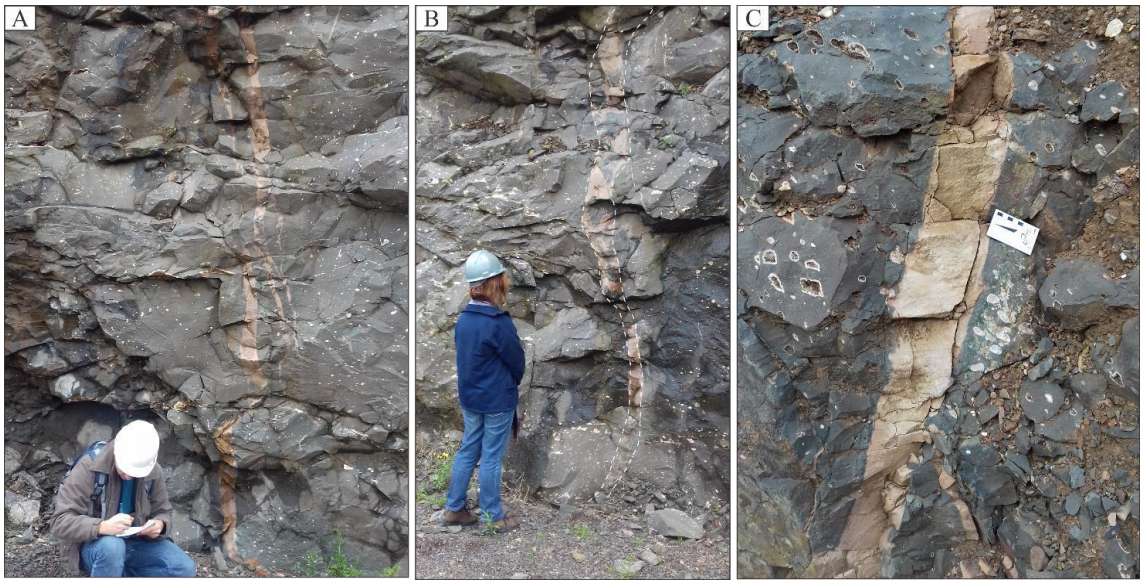

Figura 4: Diques de arenito em algumas regiões da borda sudeste da Bacia do Paraná (RS). A) B) Diques de arenito no município de Novo Hamburgo. C) Diques de arenito em Santa Cruz do Sul.

Svensen *et al.* (2010) em estudos a respeito de diques de arenito em *sills* de dolerito na Bacia de Karoo, África do Sul, conseguiram modelar, através de dados de campo, petrográficos e numéricos, como estas feições podem ser originadas (Figura 5).

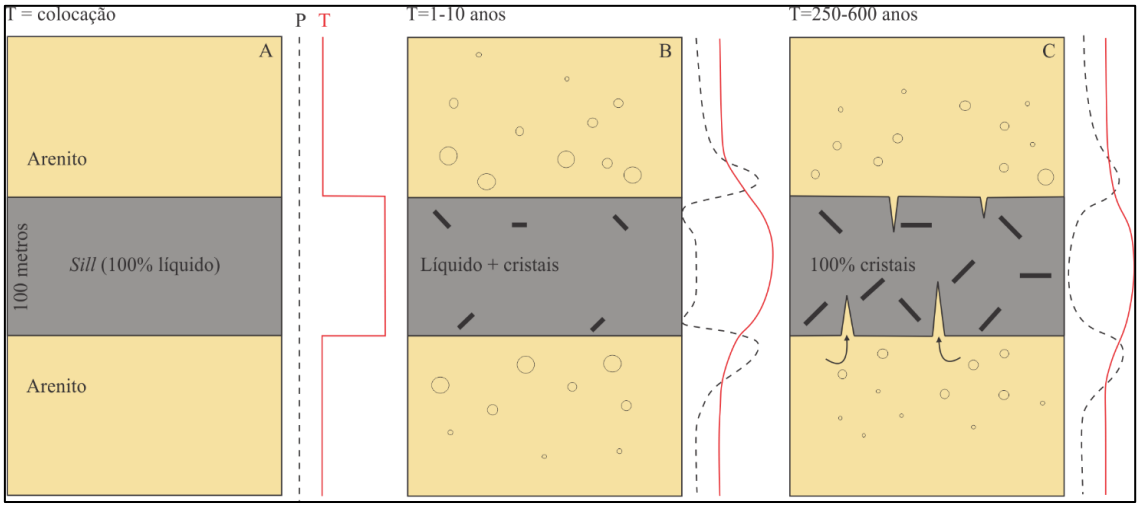

Figura 5: Evolução esquemática de um sistema sill-aureola com diques de arenitos. A) colocação inicial do sill em rochas hospedeiras sedimentares. B) Metamorfismo de contato em torno do sill e expansão dos fluidos de poros sedimentares (simbolizados por círculos). C) Cristalização do sill seguida de fraturamento devido à enorme diferença de pressão entre o sill e a auréola. O sill ainda é quente o suficiente para causar metamorfismo de alta temperatura nos sedimentos injetados (Traduzido de Svensen *et al.*, 2010).

Os autores demonstraram que os diques de arenito são comuns tanto no topo quanto na base das intrusões e que os sedimentos foram injetados enquanto os *sills* ainda estavam quentes, produzindo assembleias minerais típicas de metamorfismo (> 300 °C). As anomalias de pressão negativa no *sill* se formam devido ao resfriamento, enquanto que as de alta pressão se desenvolvem nas auréolas devido à expansão térmica. A modelagem térmica mostra que os diques de arenito foram formados 100 anos após a colocação da soleira. A sobrepressão induzida pelo calor e a subsequente fluidização de sedimentos na auréola de contato é sugerida como sendo o principal mecanismo de formação dos diques de arenito na intrusão magmática.

2.3 DEPÓSITOS VULCANOCLÁSTICOS

Os depósitos vulcanoclásticos são caracterizados por brechas vulcânicas, e existem inúmeras classificações para as brechas associadas a eventos vulcânicos, entre elas: Fischer (1960), Pettijohn (1975), Cas & Wright (1987), McPhie *et al*. (1993) e White & Houghton (2006). Alguns autores sugerem o termo peperito para designá-las, sendo esta, uma terminologia genética (White *et al.,* 2000; Jerram & Stollhofen, 2002; Skilling *et al.,* 2002).

O termo “peperino” foi utilizado por Scrope (1827) para descrever rochas clásticas em Limagne d'Auvergne, região central da França, que compreendem misturas de calcário lacustre com basalto que se assemelhavam a pimenta moída.

White *et al.,* (2000) define peperito como um termo genético aplicado a uma rocha formada essencialmente *in situ* pela desintegração do magma, intrudindo e misturando com sedimentos inconsolidados ou pobremente consolidados, tipicamente úmidos. O termo também se refere a misturas semelhantes geradas pelos mesmos processos que operam nos contatos de lavas e outros depósitos vulcanoclásticos com tais sedimentos.

O termo peperito é polêmico e alguns autores, ao realizarem estudos na Bacia do Paraná (RS), optaram em utilizar uma terminologia mais descritiva para se referir aos mesmos, nomeando-os de brechas vulcânicas de matriz sedimentar (Reis, 2013; Michelin, 2014; Reis *et al.,* 2014; Rios, 2017; Rios *et al.,* 2018). Este trabalho também optou por denominar os depósitos vulcanoclásticos de maneira mais descritiva, utilizando o termo brecha associado as composições dos clastos vulcânicos e da matriz sedimentar, por

exemplo: brecha basáltica de matriz subarcósea; brecha dacítica de matriz litoarenítica (Rosa *et al.,* 2016).

As brechas vulcânicas de matriz sedimentar, classificadas como rochas autoclásticas (Fischer, 1960; McPhie *et al*., 1993), desenvolvem-se em uma variedade de ambientes onde o magmatismo e a sedimentação são contemporâneos. Sua gênese pode envolver tanto intrusões de composição máfica a ácida, como derrames andesíticos, traquíticos, dacíticos, riolíticos e máficos (Skilling *et al.,* 2002).

Investigações baseadas em campo foram realizadas para desvendar os processos de formação de brechas vulcânicas de matriz sedimentar em sequências sedimentares: submarinas (Brooks *et al.,* 1982; Busby-Spera & White, 1987; Hanson & Wilson, 1993; McPhie, *et al.,* 1993; Goto & McPhie, 1996; Hanson & Hargrove, 1999; Hunns & McPhie, 1999; Doyle, 2000; Squire & McPhie, 2002; Rawcliffe, 2016); fluviais (Hole *et al.,* 2013); lacustres (Cas *et al.,* 2001; Erkül *et al.,* 2006; Tucker & Scott, 2009; Gihm & Kwon, 2017; Kwon & Gihn, 2017); e ambientes eólicos (Almeida, 1954; Mountney *et al.,* 1998; Jerram *et al.,* 1999a, b; Mountney *et al.,*1999; Jerram *et al.,* 2000; Mountney & Howell, 2000; Jerram & Stollhofen, 2002; Scherer, 2002; Waichel *et al.,* 2006; Michelin, 2007; Petry *et al.,* 2007; Waichel *et al.,* 2007; Arioli *et al.,* 2008; Holz *et al.,* 2008; Perinotto *et al.,* 2008; Waichel *et al.,* 2008; Machado *et al.,* 2009; Hartmann *et al.,* 2012a,b; Luchetti *et al.,* 2014; Michelin, 2014; Reis *et al.,* 2014; Rios, 2017; Rios *et al.,* 2018). Esses trabalhos melhoraram a compreensão geral dos fatores que controlam os processos de fragmentação da lava/magma, como a natureza do corpo ígneo (intrusivo ou subaéreo), composição química, condições e ambiente de colocação, granulometria dos sedimentos (grossa a fina), a consolidação e saturação em água dos sedimentos, e contrastes de densidade entre magma e sedimentos, e as variações espaciais desses fatores (Kokelaar, 1982; Busby-Spera & White, 1987; Goto & McPhie, 1996; Dadd & Van Waggoner, 2002; Jerram & Stollhofen, 2002; Skilling *et al.,* 2002; Squire & McPhie, 2002; Zimanowski & Büttner, 2002; Petry *et al.,* 2007; Waichel *et al.,* 2007; Hole *et al.,* 2013). A maioria dos exemplos são formados a partir de interações entre lava/magma de composição máfica a intermediária e sedimento insaturado a saturado em água; exemplos derivados de lava félsica que fluíram sobre um substrato sedimentar são menos comuns (Tuffen *et al.,* 2001; Donaire *et al,* 2002; Branney *et al.,* 2008; McLean *et al.,* 2016; Rawcliffe, 2016; Gihm & Kwon, 2017; Kwon & Gihm, 2017).

O volume e geometria das brechas vulcânicas de matriz sedimentar, sua relação espacial com a intrusão ou com o derrame vulcânico que a originou, sua estrutura interna e variações espaciais na textura são as principais características que permitem sua discriminação de outras rochas vulcanoclásticas semelhantes. O seu domínio de ocorrência varia em volume, de poucos m^3, ao longo dos contatos entre os sedimentos e intrusões, para exemplos de vários km^3, ao longo do contato entre sedimentos e derrames vulcânicos (Figura 6). Os domínios de ocorrência das brechas vulcânicas de matriz sedimentar são tipicamente sem estratificação e altamente discordantes do acamamento. A estratificação original no sedimento é normalmente destruída (Snyder & Fraser, 1963; Busby-Spera & White, 1987; Hanson & Wilson 1993; Brooks, 1995; Doyle, 2000; White *et al.*, 2000; Skilling *et al.*, 2002; Brown & Bell, 2007).

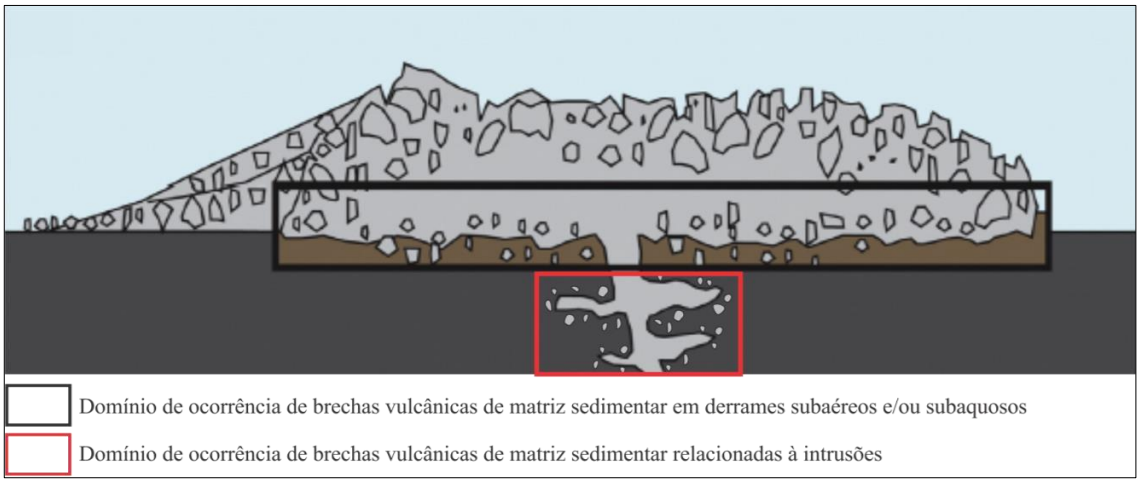

Figura 6: Domínio de ocorrência de brechas vulcânicas de matriz sedimentar em derrames e em intrusões (Modificado de Rosa *et al.*, 2016).

Há ocorrências de brechas vulcânicas de matriz sedimentar como resultado da relação lava-sedimento ao longo do contato entre as Formações Botucatu e Serra Geral, Bacia do Paraná, como foi exposto por Petry (2006), Petry *et al.* (2007), Waichel *et al.* (2007, 2008), Reis (2013), Luchetti *et al.* (2014), Michelin (2014), Rios (2017), Rios *et al.* (2018).

Waichel *et al.* (2007) sugeriu que os peperitos teriam sido originadas pela interação entre os derrames e sedimentos úmidos (silte e argila) depositados em ambiente lacustre, sugerindo que uma mudança climática provavelmente ocorreu entre o ambiente desértico e os primeiros derrames da Formação Serra Geral.

Petry (2006) e Petry *et al.* (2007), observaram que a formação de autobrechas de derrame representaria, também, um importante processo na geração dos peperitos.

Mizusaki, (1986), Reis (2013), Michelin (2014), Rios (2017) e Rios *et al.* (2018) discutem que os sedimentos saturados em água fazem com que as interações ocorram de forma concomitante ao evento magmático, onde o contraste de temperatura da lava com o sedimento saturado permite que os processos de fluidização/vaporização se iniciem, possibilitando a gênese do depósito vulcanoclástico.

2.3.1 Processos de formação da brecha vulcânica de matriz sedimentar

A lava/magma se fragmenta e se desintegra ao entrar em contato com o sedimento não consolidado formando fragmentos vulcânicos de morfologias variadas, que se misturam em diferentes proporções com o sedimento. Estes clastos apresentam variações em suas morfologias, desde formas em blocos a fluidais, que refletem os diferentes processos de fragmentação (rúptil e dúctil) que ocorrem durante a formação da brecha vulcânica de matriz sedimentar (Figuras 7 A, B). Além do mais, essas diferentes morfologias dos clastos vulcânicos estão também atreladas ao tempo de resfriamento da lava e seu aumento de viscosidade. Brechas vulcânicas de matriz sedimentar com clastos em formas de blocos têm sido identificadas em associação com sedimentos inconsolidados e secos, por exemplo, ambientes eólicos (Brooks *et.al.*,1982; Goto & McPhie, 1996; Doyle, 2000; Jerram & Stollhofen, 2002; Skilling *et al.*, 2002; Squire & McPhie, 2002).

A fragmentação do magma e a mistura do material vulcânico com o sedimentar provavelmente são simultâneas. A junção dos componentes vulcânicos e sedimentares é favorecida quando a densidade e a viscosidade da lava são semelhantes às do sedimento, pelo menos no momento da interação (Zimanowski & Büttner, 2002). Vários fatores podem influenciar as texturas resultantes, incluindo: reologia de magma, composição, conteúdo de voláteis, velocidade de fluxo, reologia do sedimento, tamanho do grão, seleção, razão da mistura lava/água, volume total da mistura lava-sedimento, proporção da mistura lava-sedimento, volume total de água aquecida nos poros, pressão confinante e a natureza dos aspectos locais e regionais. A maioria desses fatores variam espacialmente e temporalmente durante a formação das brechas vulcânicas de matriz sedimentar (Brooks *et al.*, 1982; Kokelaar 1982; Busby-Spera & White, 1987; Kano,

1989; Hanson, 1991; Hanson & Wilson, 1993; McPhie *et al.*, 1993; Rawlings, 1993; Goto & McPhie, 1996; Hanson & Hargrove, 1999; Dadd & Van Waggoner, 2002; Hunns & McPhie, 1999; Doyle, 2000; Gifkins *et al.*, 2002).

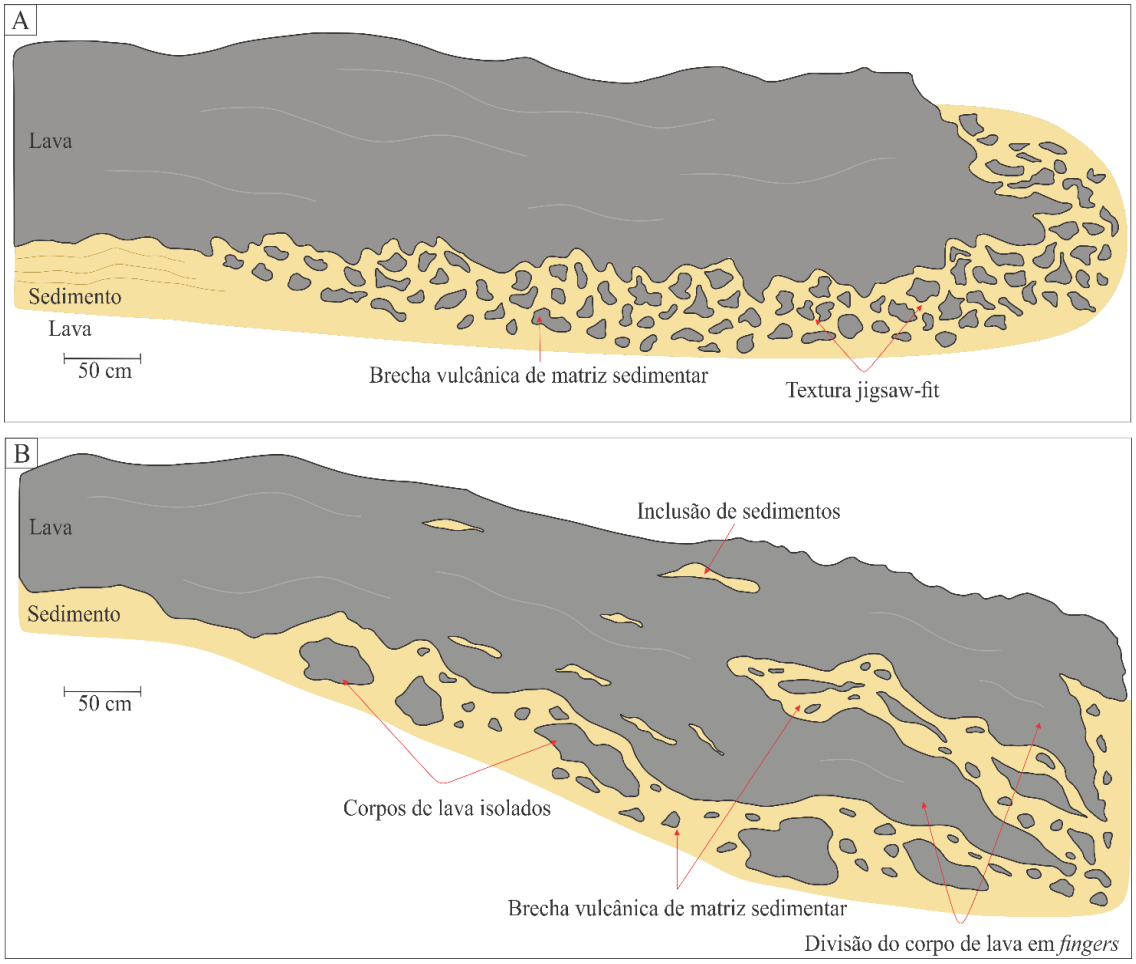

Figura 7: Diferenças de brechas vulcânicas de matriz sedimentar com base na morfologia dos clastos vulcânicos: A) brechas vulcânicas de matriz sedimentar com clastos em blocos; B) brechas vulcânicas de matriz sedimentar com clastos fluidais. Modificado de Rawcliffe (2016).

Clastos com morfologia em bloco são subédricos, com formas poliédricas a tabulares, comumente exibem textura *jigsaw-fit*, característica da fragmentação *in situ*. Enquanto que os clastos com aspecto fluidal possuem morfologias globulares, caracterizada por contornos irregulares, que variam em formas: ameboides, *tendrils-like* e *wispy-like* (Lorenz, 1984; Busby-Spera & White, 1987; Skilling *et al.*, 2002) (Figura 8) Entretanto, combinações de diferentes morfologias dos clastos podem ser observadas dentro do mesmo depósito vulcanoclástico, deduzindo uma combinação de processos de fragmentação rúptil e dúctil, sugerindo uma fragmentação em multiestágio, no qual as

populações de clastos se formariam sob condições térmicas e mecânicas distintas (Skilling *et al.*, 2002).

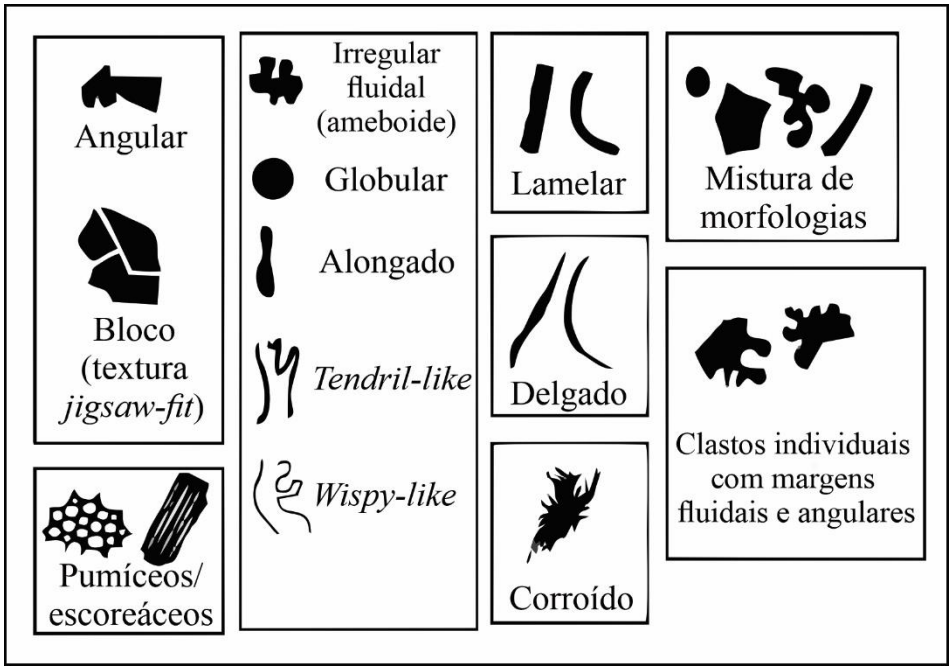

Figura 8: Diferentes morfologias dos fragmentos vulcânicos em brechas vulcânicas de matriz sedimentar. Modificado e traduzido de Skilling *et al.* (2002).

Em relação as características dos sedimentos, diversas variáveis afetam a formação das brechas vulcânicas de matriz sedimentar, que incluem: tamanho do grão, composição, seleção, coesão, porosidade e permeabilidade (Lorenz, 1984; Busby-Spera & White, 1987; Squire & McPhie, 2002; Skilling *et al.*, 2002).

2.4 FEIÇÕES E DEPÓSITOS EPICLÁSTICOS

Em terrenos com sedimentação e vulcanismo ativos, todos os depósitos de superfície, sejam eles de origem vulcânica ou sedimentar, estão sujeitos aos agentes e processos de transporte, relacionados ao ambiente sedimentar em questão (McPhie *et al.*, 1993). Situam-se nas porções superiores dos derrames e possuem origem relacionada a processos intempéricos e erosivos, são agrupadas junto às rochas epiclásticas (Fischer,1960; Cas & Wright, 1987) (Figura 9).

São formados por misturas de sedimentos de origem vulcânica e sedimentar que estavam sujeitos ao retrabalhamento significativo antes da deposição final, e/ou que foram redepositados muito tempo após a erupção. As marcas de transporte,

retrabalhamento e ressedimentação pós-erupção são modificações nas formas dos fragmentos vulcânicos, especialmente arredondamento, misturas de partículas não vulcânicas, misturas de partículas vulcânicas de composição amplamente diferente, partículas que mostram os efeitos do intemperismo e/ou alteração diagenética parcial e associação com fácies sedimentares não vulcânicas. Os sedimentos de origem vulcânica são mais conhecidos em terrenos vulcânicos subaéreos, onde intemperismo e erosão são vigorosamente ativos durante e após as erupções - sistemas desérticos, fluviais, aluviais, lacustres, litorâneos (McPhie et al.,1993).

Após o evento vulcânico cessar há o resfriamento da porção superficial das lavas formando diaclases na superfície do derrame. Com o retorno da sedimentação sobre o substrato vulcânico inicia-se o processo de preenchimento dessas fissuras pelos sedimentos que estão sendo transportados, formando assim as fraturas preenchidas por sedimentos. A intensificação dos processos intempéricos e erosivos sobre o substrato vulcânico faz com que haja a desagregação de fragmentos do mesmo. Estes litoclastos são transportados e depositados juntamente com os demais sedimentos disponíveis no ambiente, dando origem aos depósitos epiclásticos, caracterizados por brechas sedimentares ou conglomerados intrabacinais (Reis, 2013; Michelin, 2014; Rios, 2017; Rios *et al.,* 2018).

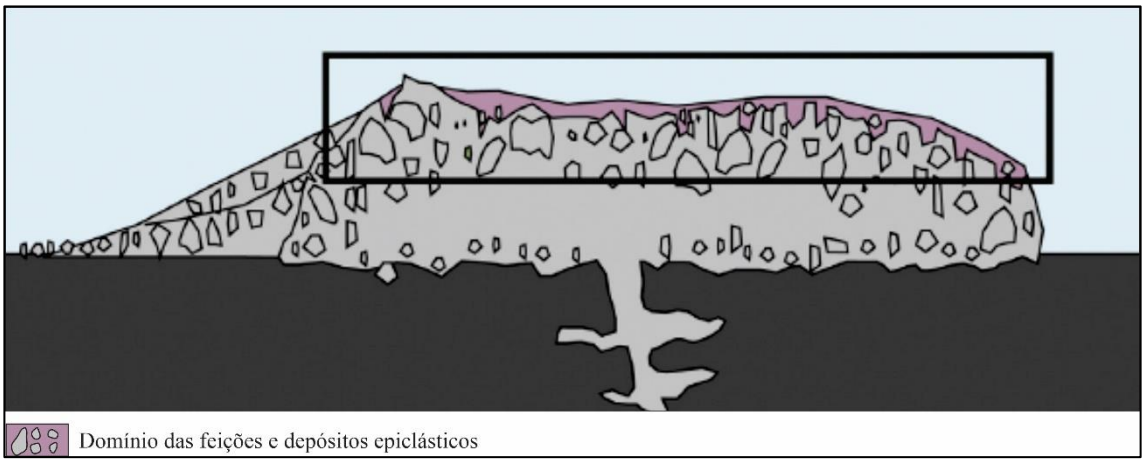

Figura 9: Modo de ocorrência das feições e depósitos epiclásticos (Modificado de Rosa *et al.,* 2016).

CAPÍTULO 3 - METODOLOGIA

3. METODOLOGIAS

As metodologias utilizadas neste trabalho foram divididas em três etapas principais: levantamento bibliográfico, atividades de campo, análises laboratoriais - petrografia, difração de raios X (DRX), além do tratamento dos dados e confecção da tese.

3.1 LEVANTAMENTO BIBLIOGRÁFICO

A obtenção de dados envolveu a consecução de artigos publicados e uma revisão bibliográfica referente ao tema a ser abordado na pesquisa. Conjuntamente foram analisadas imagens de satélite do Google Earth, cartas topográficas e fotografias aéreas das áreas próximas a borda sudeste atual da Bacia do Paraná (RS). Objetivando identificar pontos estratégicos onde as feições de interação lava-sedimento pudessem ser visualizadas, descritas e amostradas.

3.2 ATIVIDADES DE CAMPO

Na segunda etapa foram realizados os trabalhos de campo nas áreas previamente selecionadas ao longo da borda sudeste atual da Bacia do Paraná, no estado do Rio Grande do Sul, Brasil. Nesta situação, as rochas em contexto de interação vulcano-sedimentar afloram ao longo de escarpas que cortam a porção central do estado. As localidades identificadas para o estudo foram escolhidas em lugares onde as escarpas são cortadas por estradas, pedreiras, rios e parques estaduais. Foram escolhidas seis áreas chaves (Figuras 10A, B).

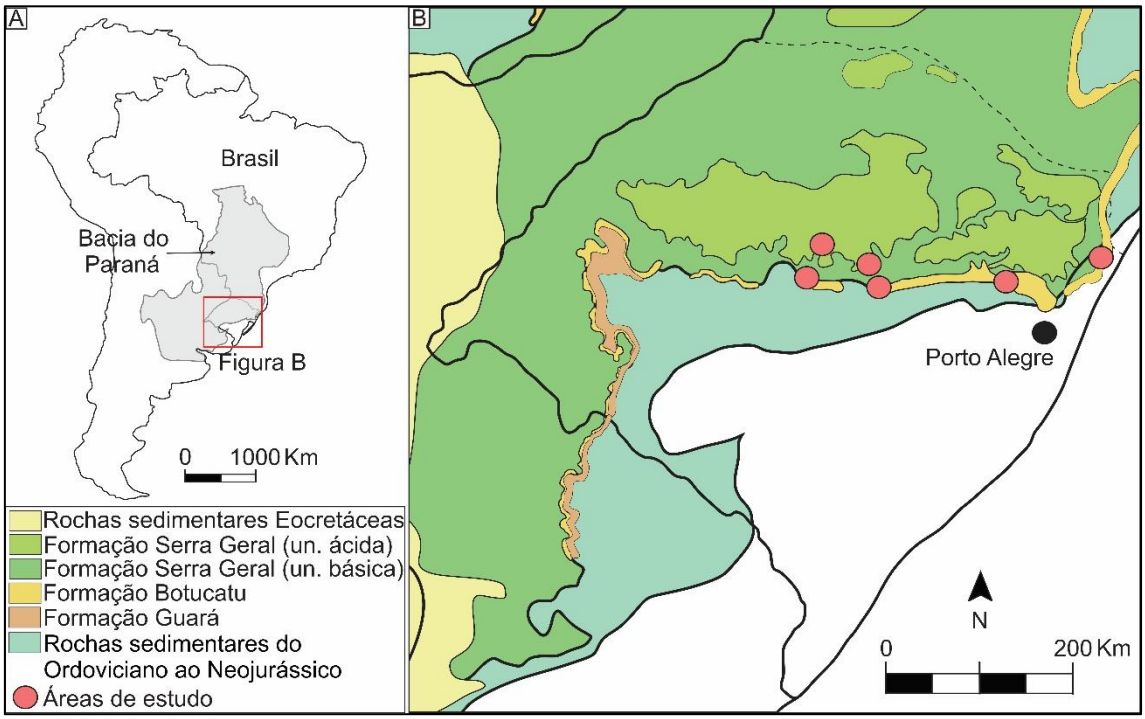

Figura 10: A) Localização da Bacia do Paraná na Plataforma Sul-Americana. B) Localização das áreas estudadas ao longo da borda sudeste atual da Bacia do Paraná (RS) (Modificado de Janasi *et al.*, 2011; Reis *et al.*, 2019).

Nos levantamentos de campo se priorizou as descrições das rochas sedimentares, vulcânicas, das estruturas e depósitos de interação entre elas, além da coleta de amostras para análises futuras. Os afloramentos selecionados foram descritos e fotografados em detalhe. Nesse estágio a confecção de perfis estratigráficos colunares na escala de 1:50 e de croquis foi fundamental para um melhor entendimento das geometrias, arquiteturas e escalas das feições vulcano-sedimentares. Foram descritas fácies, associação de fácies, elementos arquiteturais, identificações de superfícies e coleta de medidas de paleocorrentes.

Foram adotadas as técnicas de modelamento de fácies propostas por Walker & James (1992) que incluem: 1) Individualização e descrição das fácies (composição, geometria, texturas, estruturas sedimentares) e padrões de paleocorrentes; 2) Compreensão dos processos sedimentares; e 3) Associação de fácies, refletindo os diferentes ambientes e sistemas deposicionais.

3.3 PETROGRAFIA

A descrição de 112 lâminas delgadas, preparadas a partir de amostras extraídas de afloramentos em contexto de interação vulcano-sedimentar, foi inicialmente feita por métodos de petrografia convencional. Posteriormente, 30 lâminas delgadas foram selecionadas para petrografia quantitativa, essas amostras são referentes a matriz das brechas vulcânicas (depósitos vulcanoclásticos) e conglomerados intrabacinais (depósitos epiclásticos). A petrografia foi executada no Laboratório de Petrologia Sedimentar no Departamento de Mineralogia e Petrologia da Universidade Federal do Rio Grande do Sul com uso de microscópios de luz polarizada e do software Petroledge® (De Ros & Goldberg, 2007). A análise petrográfica sistemática visa o reconhecimento das principais feições texturais, composicionais, diagenéticas e de porosidade. Foram registrados os teores, hábitos, localizações, bem como as distribuições e relações entre os constituintes primários e diagenéticos. As lâminas foram preparadas a partir de amostras impregnadas com resina azul, afim de facilitar a observação de poros e constituintes. Durante as descrições as lâminas foram tingidas com alizarina e ferrocianeto de potássio, a fim de identificar os constituintes carbonáticos.

A quantificação das amostras foi executada por análise modal, através da contagem de 300 pontos por lâmina, dispostos segundo transectas perpendiculares à estrutura principal da rocha A descrição com o software Petroledge® segue uma ordem sistemática. Inicialmente ocorre a identificação da amostra quanto a sua localização e um resumo das principais feições encontradas na lâmina. Segue-se a análise das feições estruturais, granulometria, arredondamento, esfericidade e seleção assim como a orientação, sustentação e empacotamento da fábrica. Os constituintes primários, diagenéticos e poros são descritos e quantificados com respeito a seus tipos, hábitos, localização e relações paragenéticas. A quantificação dos constituintes primários, diagenéticos e de porosidade foi realizada com base no método Gazzi-Dickinson (Zuffa, 1985).

Por meio de fotomicrografias foram registradas as principais feições texturais, composicionais, diagenéticas e de porosidade das lâminas. As fotomicrografias foram tiradas com um microscópio Zeiss AXIO Imager A2 com câmera Zeiss AXIO cam e utilizando o software ZEN™ 2011, já com escalas adequadas para cada lente utilizada no microscópio.

3.4 DIFRAÇÃO DE RAIOS-X (DRX)

As amostras das lâminas delgadas selecionadas para a petrografia quantitativa foram submetidas a análises de DRX em rocha total (Método do Pó) para refinar a composição dos argilominerais presentes no arcabouço das rochas.

O equipamento utilizado foi um difratômetro X Siemens (BRUKER AXS) D-5000 com goniômetro θ-θ e a radiação de Kα em tubo de cobre nas condições de 40kV e 30 mA (radiação Cu Kalpha =1,54178 Angstrom) com monocromador curvado de grafite no feixe secundário. (radiação Cu Kalpha = 1,54178 Angstrom). O intervalo angular analisado foi de 5 a 75° 2theta. As amostras foram analisadas a 0,05°/1s com fendas de divergência e anti-espalhamento de 1° e fenda de recepção de 0,2 mm e os resultados foram aplicados ao software DIFFRACplus tendo como resultado alguns difratogramas. As análises foram sucedidas no Laboratório de Difração de Raios X do Centro de Estudos em Petrologia e Geoquímica (CPGq) do IGEO-UFRGS.

CAPÍTULO 4 - CONTEXTO GEOLÓGICO

4. BACIA DO PARANÁ - SUPERSEQUÊNCIA GONDWANA III

A Bacia do Paraná é uma bacia Paleozoica da Plataforma Sul-Americana cujo depocentro estima-se aproximadamente 7.000 m de rochas sedimentares e vulcânicas com idades do Ordoviciano ao Cretáceo (Zalán *et al.*, 1987, 1990) (Figuras 11A, B). Recobre uma área de 1.400. 000 km^2 abrangendo o Brasil, Paraguai, Uruguai e Argentina (Milani et al., 2007)

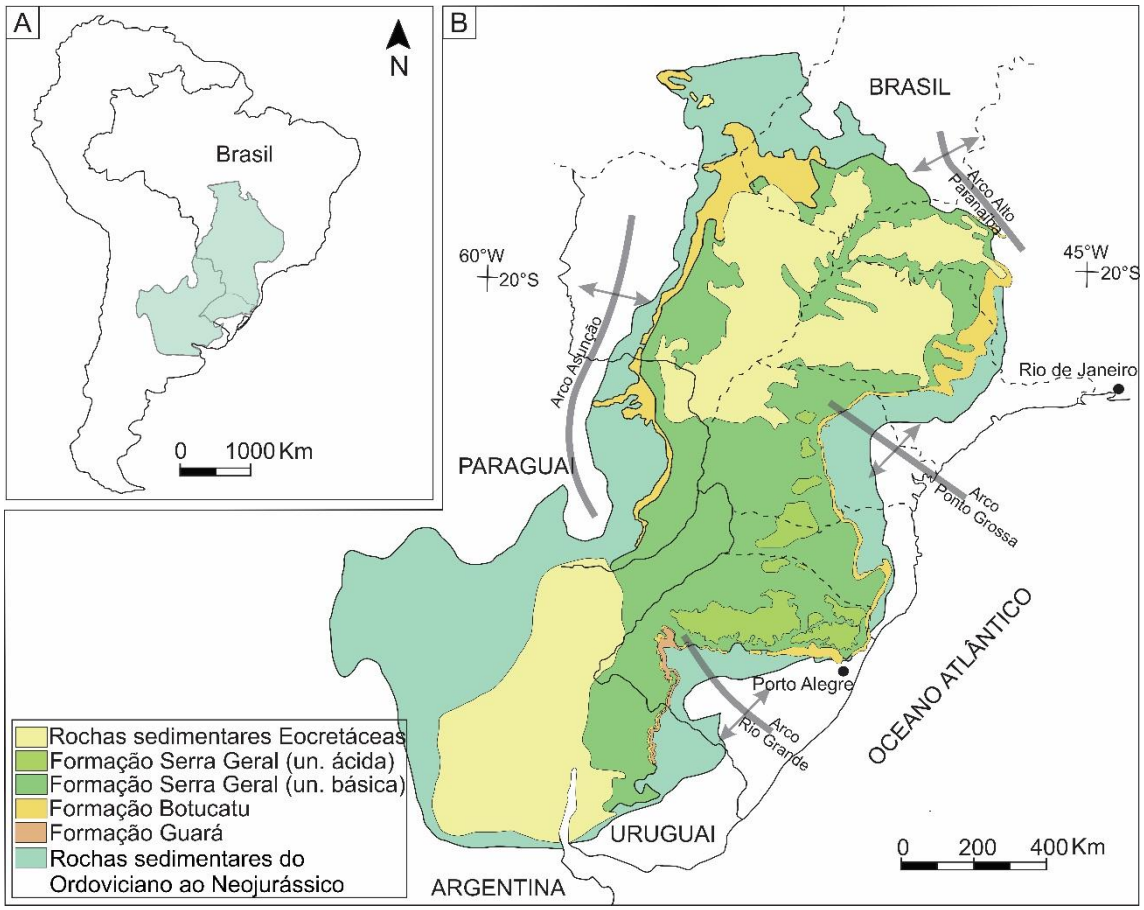

Figura 11: A) e B) Mapa geológico simplificado da Bacia do Paraná na Plataforma Sul Americana. Observar as ocorrências das Formações Guará, Botucatu e Serra Geral (Modificado de Janasi *et al.*, 2011; Rossetti *et al.*, 2018; Reis *et al.*, 2019).

O registro vulcano-sedimentar da Bacia do Paraná é dividido em seis Supersequências, da base para o topo segundo Milani (1997): Rio Ivaí (Neo-Ordoviciano ao Eo-Siluriano), Paraná (Devoniano), Gondwana I (Neo-Carbonífero ao Eo-Triássico), Gondwana II (Meso-Triássico ao NeoTriássico), Gondwana III (Neo-Jurássico ao Eo-

Cretáceo) e Bauru (Eo-Cretáceo ao Neocretáceo) (Figura 12). O pacote vulcano-sedimentar que compreende a Supersequência Gondwana III, Jurássico Superior ao Cretáceo Inferior, é o alvo desse trabalho e compreende as Formações Botucatu e Serra Geral (Figura 12).

A Formação Botucatu representa um imenso *erg*, caracterizado por estratos cruzados de grande porte (1-30m) e é interpretada como depósitos residuais de dunas eólicas. Sua espessura é bastante variável, provavelmente devido à preservação do paleo-relevo de dunas, podendo atingir até 100 m de espessura. Há predomínio de arenitos quartzosos, rosados, bem selecionados, granulometria fina a média e grãos arredondados que associados com estratificações cruzadas de grande porte indicam depósitos residuais de dunas eólicas. (Scherer, 1998, 2000, 2002). É limitada na base por uma discordância regional que se estende por toda a bacia onde há registros de conglomerados e arenitos conglomeráticos, relacionados a canais efêmeros (Almeida, 1954; Bigarella & Salamuni, 1961, 1967; Soares, 1975; Bigarella, 1979; Almeida & Melo, 1981; Milani 1997; Milani *et al.,* 1998; Scherer, 2000). A idade Cretáceo Inferior da Formação Botucatu inclui vestígios de invertebrados, vertebrados e coníferas silicificadas (Brito, 1979; Suguio & Coimbra, 1972; Fernandes *et al.,* 1990, 2004; Leonardi & Oliveira, 1990; Fernandes & Carvalho, 2008; Pires *et al.,* 2011). Os sedimentos da Formação Botucatu foram recobertos pelas lavas da Formação Serra Geral. No entanto, o ambiente sedimentar eólico permaneceu atuante durante o início do vulcanismo e essas relações de contato evidenciam uma idade relativa para seu início e também para o término da sedimentação (Milani et al., 1998; Scherer, 2002; Milani *et al.*, 2007).

A Formação Serra Geral representa um intenso magmatismo com até 1,800 m de espessura de lavas subaéreas de afinidade toleítica (Piccirillo & Melfi, 1988). No Brasil as rochas vulcânicas da Formação Serra Geral recobrem uma área de 917.000 km^2 sendo o volume mínimo estimado de 450.000 km^3 (Frank *et al.,* 2009). Petrologicamente, as rochas vulcânicas da Formação Serra Geral são dominadas por basaltos toleíticos (90%), seguido por andesitos toleíticos (7%) e em menores proporções riolitos e riodacitos (3%) especialmente nas porções mais superiores (Melfi *et al.,* 1988; Piccirillo & Melfi, 1988; Peate *et al.,* 1992). Em termos geoquímicos, ocorre uma diferenciação destas rochas ao longo da bacia com relação ao conteúdo de TiO_2 (Bellieni *et al.,* 1984) e de elementos-traços, especialmente Y e Yb (Peate, 1989). Datações isotópicas sugerem que a maior parte do magmatismo ocorreu em um intervalo relativamente curto (<4 Ma) e com idades

de aproximadamente 134 Ma (Cretáceo Inferior) (Renne *et al.,* 1992; Thiede & Vasconcellos, 2010; Janasi *et al.,* 2011; Baksi, 2018; Rocha *et al.,* 2020).

Entretanto, foi observado no levantamento de campo do presente trabalho a ocorrência de uma unidade sedimentar com características distintas da Formação Botucatu e que também ocorre entre os derrames vulcânicos da Formação Serra Geral. Essa unidade possui características litológicas e faciológicas semelhantes às da Formação Guará e foi reconhecida na área estudada (Zerfass *et al.*, 2007; Godoy *et al.,* 2011, 2016, 2018).

A Formação Guará, na Bacia do Paraná (Scherer & Lavina, 2005, 2006; Zerfass *et al.,* 2007; Godoy *et al.,* 2011, 2016, 2018; Reis, 2016, 2020; Reis *et al.,* 2019), e o Membro Batoví, porção inferior da Formação Tacuarembó, no Uruguai (Perea *et al.*, 2009; Amarante *et al.,* 2019) possuem uma associação fossilífera (répteis, peixes, conchostráceos e moluscos) que indica uma idade relativa para Jurássico Superior (Perea *et al,* 2009; Soto & Perea, 2010; Francischini *et al.,* 2015). No oeste do estado do Rio Grande do Sul, foi definida uma distribuição lateral de associações de fácies para a Formação Guará como sendo constituídas por canais fluviais entrelaçados perenes e canais fluviais entrelaçados efêmeros. Já na porção norte do estado, canais fluviais fracamente canalizados que intercalam com depósitos de dunas eólicas e, na porção sul do estado, por lençóis de areia eólicos (Sherer & Lavina, 2005, 2006). Os depósitos fluviais apresentam padrão de paleocorrentes para SSW, enquanto que as dunas eólicas possuem paleocorrentes para NE (Scherer & Lavina, 2005). Esta unidade é limitada na base e topo por desconformidades com as Formações Sanga do Cabral e Botucatu, respectivamente (Scherer & Lavina, 1997; Scherer, 2000).

Entretanto, os dados de campo na região central do Rio Grande do Sul (Figuras 13 A, B), limite sudeste atual da borda da Bacia do Paraná, mostraram que essa unidade é limitada na base por uma desconformidade com a Formação Caturrita (Triássico Superior) e seu topo encontra-se em contato com as vulcânicas da Formação Serra Geral, além de ocorrências de depósitos fluviais entre os derrames. Por essa razão, a idade do topo dessa unidade, na área de estudo, foi considerada como pertencente ao Cretáceo Inferior (Zerfass *et al.*, 2007). A Formação Caturrita é representada por um conjunto de camadas lenticulares, tabulares e sigmoidais de arenitos finos a conglomerados que ocorrem intercalados com pelitos. Esses depósitos são relacionados a um ambiente flúvio-deltaico (Andreis *et al.,* 1980; Zerfass *et al.,* 2007; Godoy *et al.,* 2018).

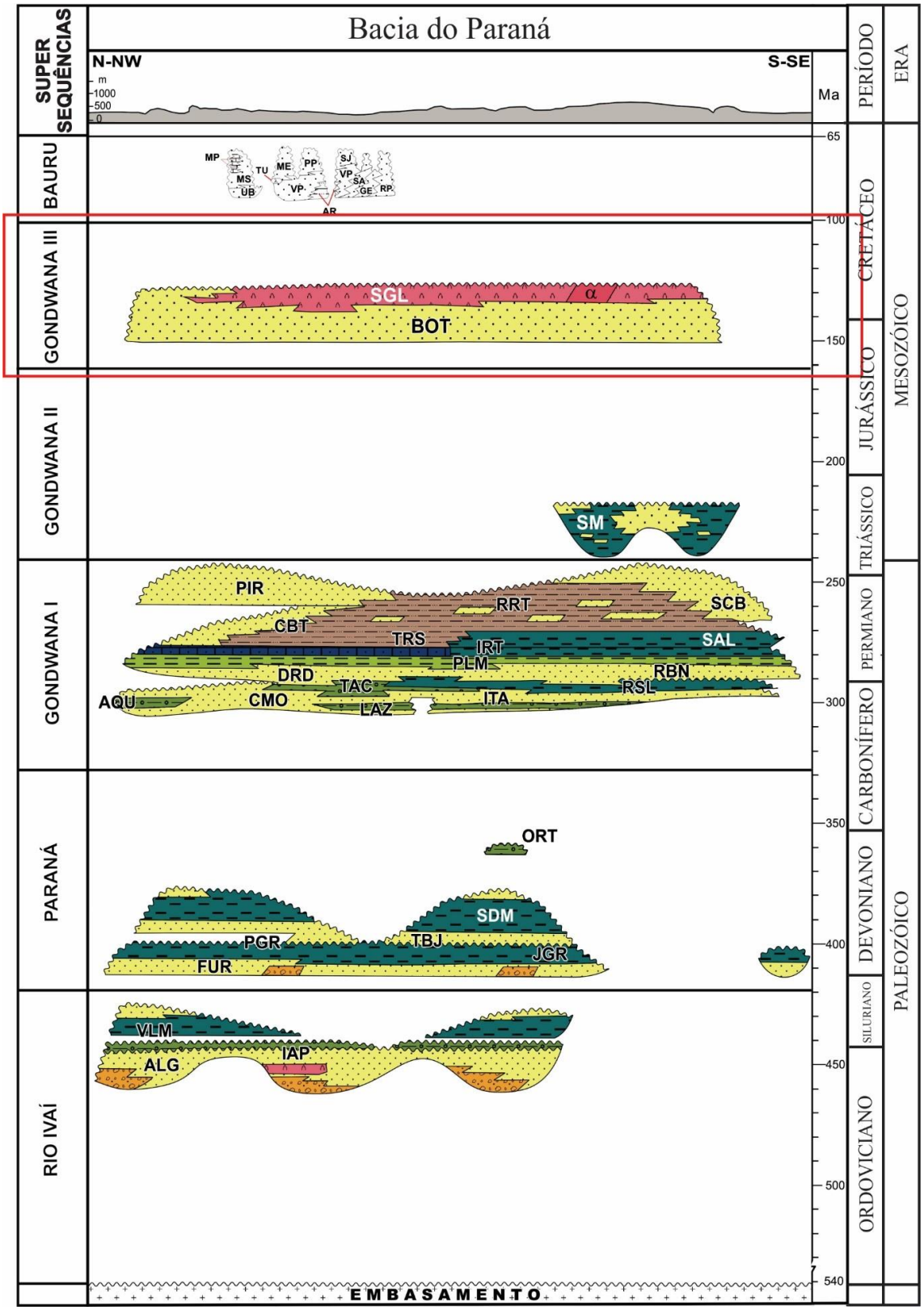

Figura 12: Coluna estratigráfica proposta para a Bacia do Paraná (em destaque a Supersequência Gondwana III) (Modificado de Milani *et al.*, 2007).

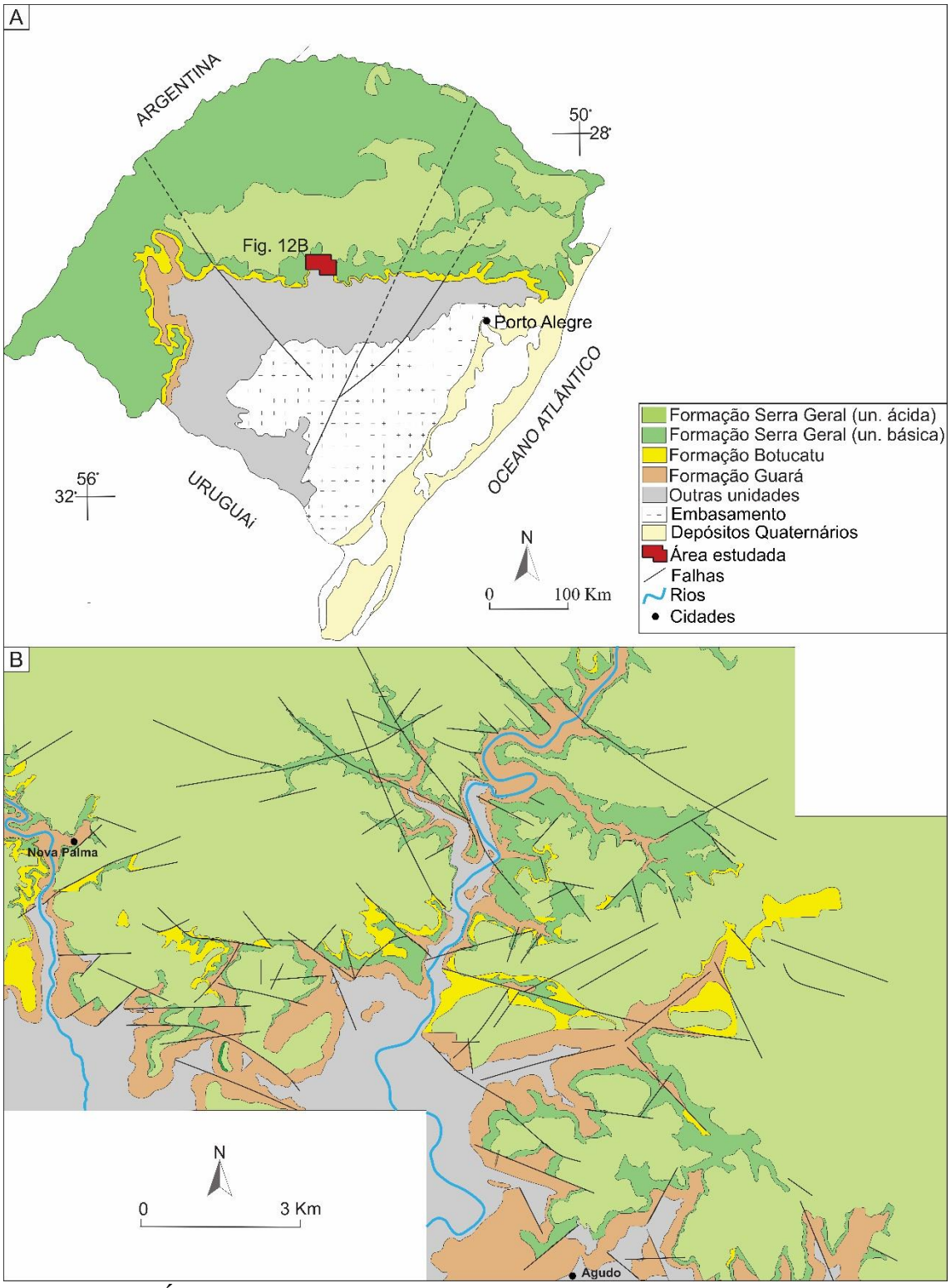

Figura 13: A) Área de estudo na borda sudeste atual da Bacia do Paraná, estado do Rio Grande do Sul (Modificado de Scherer, 2002; Janasi *et al*., 2011; Reis, 2016; Rios *et al.*, 2018). B) Detalhe da área de estudo no intervalo Jurássico Superior - Cretáceo Inferior (Modificado de Zerfass *et al.*, 2007; Godoy *et al.*, 2011).

Com relação à tectônica da Bacia do Paraná, dois estilos estruturais principais são destacados: deformações associadas a intrusões ígneas e deformações associadas a

reativações de elementos tectônicos lineares, predominantemente com direções NE e NW (Reis, 2013). No entanto, os lineamentos NE são relativamente mais abundantes e com maior densidade, enquanto que os lineamentos NW possuem relativamente menor densidade, porém com predomínio de estruturas regionais (Betiollo, 2006). Secundariamente, lineamentos E-W são observados principalmente na porção mais ao sul da Bacia (Zalán, 1986; Artur & Soares, 2002).

As orientações NW e NE são consideradas mais antigas pois foram originadas a partir da reativação, durante o Fanerozoico, de potenciais zonas de fraqueza do embasamento cratônico da bacia. Essas zonas de fraqueza influenciaram fortemente a paleogeografia, sedimentação e distribuição das fácies em toda a bacia, bem como o desenvolvimento de estruturas tectonosedimentares. Já os lineamentos E-W desenvolveram-se a partir da separação do Gondwana, sendo considerados ativos a partir do Triássico (Zalán *et al.*, 1987, 1990, 1991). As estruturas de orientação NW foram reativadas no Eocretáceo e estão associadas a diques de diabásio (Strugale *et al.*, 2007).

CAPÍTULO 5 - RESULTADOS OBTIDOS

5. SÍNTESE INTEGRATIVA DOS ARTIGOS

A Bacia do Paraná, na Plataforma Sul-Americana, registrou um evento vulcânico de ampla magnitude no Cretáceo Inferior, relacionado com a quebra do Gondwana e a formação do Oceano Atlântico Sul. É a denominada Formação Serra Geral, caracterizada por um enorme volume de lavas e intrusões associadas que recobriram e interagiram com um extenso sistema eólico ativo, a Formação Botucatu, formando depósitos e feições vulcano-sedimentares. Os derrames vulcânicos do Serra Geral recobriram unidades contemporâneas e regionalmente dispersas, a Formação Guará. A sincronicidade dessas unidades sedimentares e vulcânicas produziu diversas feições vulcano-sedimentares ao longa da interface lava-sedimento. Portanto, os artigos propostos abordam principalmente a gênese das interações vulcano-sedimentares, visando a verificação e proposição de modelos paleoambientais a partir das mesmas. Além da discussão estratigráfica e diagenética que são fundamentais para uma melhor compreensão do arcabouço estratigráfico da bacia durante o Jurássico Superior e Cretáceo Inferior.

O primeiro manuscrito intitulado “Volcano-sedimentary interactions - a key to understand Cretaceous paleoenvironments in the Paraná Basin (southern Brazil)” de autoria de Fernando Rodrigues Rios, Ana Maria Pimentel Mizusaki, Cassiana Roberta Lizzoni Michelin e Isaque Conceição Rodrigues da Silva foi submetido no Journal of Volcanoglogy and Geothermal Research. O artigo propõe o reconhecimento e a verificação paleoambiental a partir de modelos existentes para o Cretáceo por meio de 6 afloramentos no limite sudeste da borda atual da Bacia do Paraná. Os depósitos e feições vulcano-sedimentares foram reconhecidos, mostrando a complexidade do ambiente e dos processos na associação lava-sedimento. Eles se originaram pela interação de sedimentos consolidados ou inconsolidados, saturados ou não em água, com derrames de composição basáltica ou dacítica. As feições e depósitos de interação foram classificadas como concomitantes ao vulcanismo formando feições e depósitos vulcanoclásticos, ou apenas feições de recobrimento com ausência de interações; e podem ser posteriores ou em intervalos de quiescência do vulcanismo e retorno da sedimentação (epiclásticas).

A partir de tais informações, e por meio de características distintivas dos processos de interação, entre as rochas vulcânicas com os sedimentos analisados, nas

feições e depósitos vulcano-sedimentares, a morfologia do ambiente eólico da Formação Botucatu pôde ser, por analogia, comparada aos ambientes eólicos atuais. De tal forma que o paleoambiente proposto indica um ambiente sedimentar com diferentes domínios, categorizados por sua saturação em água: 1) Domínio de campos de dunas – insaturado em água, mínimo de umidade nos poros; 2) Domínio de transição, insaturado a super saturado em água. 3) Domínio de lençóis de areia eólicos, saturado a super saturado em água, com sedimentos úmidos e/ou água nos poros. Os diferentes componentes siliciclásticos encontrados em cada domínio permitiram a formação de diferentes feições e depósitos vulcano-sedimentares.

O segundo manuscrito intitulado “Evolution of the Upper Jurassic and Lower Cretaceous vulcano-sedimentary register - southeast portion of Paraná Basin, Brazil” de autoria de Fernando Rodrigues Rios, Ana Maria Pimentel Mizusaki, Rualdo Menegat e Isaque Conceição Rodrigues da Silva foi submetido na Cretaceous Research. Mediante dados de 29 afloramento, 13 perfis verticais e 334 medidas de paleocorrente, na região central do Rio Grande do Sul, limite sudeste atual da borda da Bacia do Paraná, mostraram a ocorrência de depósitos flúvio-eólicos da Formação Guará em contato com as rochas vulcânicas da Formação Serra Geral.

Através da análise de fácies e de elementos arquiteturais, a fim de reconstituir a evolução desse pacote vulcano-sedimentar, o trabalho chegou a um novo entendimento das relações temporais e espaciais dos sistemas flúvio-eólicos (Formação Guará), eólicos (Formação Botucatu) e vulcânicos (Formação Serra Geral) que se desenvolveram nesse intervalo temporal. As Formações Guará, Botucatu e Serra Geral são compostas por vinte e uma fácies agrupadas em cinco associações de fácies (canal fluvial entrelaçado, canal fluvial entrelaçado efêmero, lençóis de areia eólicos, dunas eólicas e planície vulcânica) com seus respectivos elementos arquiteturais. As ocorrências de contatos entre depósitos das Formações Guará e Botucatu e dessas com os derrames da Formação Serra Geral demonstram que esses ambientes sedimentares permaneceram ativos durante o início do vulcanismo, e que não houve hiato entre essas unidades.

O terceiro manuscrito intitulado “Volcanoclastic and epiclastic diagenesis of sandstones associated with volcano-sedimentary deposits from the Upper Jurassic, Lower Cretaceous, Paraná Basin, southern Brazil” de autoria de Fernando Rodrigues Rios, Ana Maria Pimentel Mizusaki, Cassiana Roberta Lizzoni Michelin e Isaque Conceição Rodrigues da Silva foi submetido no Journal of South American Earth Sciences. Por meio

da petrografia quantitativa, amostras da matriz arenosa dos depósitos vulcanoclásticos e epiclasticos foram analisadas, a fim de discutir a paragênese das interações vulcano-sedimentares. Processos diagenéticos normais de soterramento foram discutidos para os arenitos epiclásticos e de diagênese de contato para os arenitos vulcanoclásticos. A composição original dos arenitos vulcanoclásticos e epiclásticos analisados é heterogênea, sendo a principal distinção entre eles é a presença de indicativos texturais de fluidização encontradas nos arenitos vulcanoclásticos, ao longo da interface lava-sedimento. Tais evidências texturais apontam para sedimentos inconsolidados e que se encontravam provavelmente úmidos ou saturados em água no momento da interação com o derrame vulcânico. Os arenitos epiclásticos possuem como principal constituinte diagenético as argilas infiltradas e esmectitas neoformadas, já os arenitos vulcanoclásticos são cimentados principalmente por calcedônia e secundariamente zeólita. O volume intergranular ocupado pelos cimentos nos arenitos vulcanoclásticos ao longo da interface lava-sedimento, apontam para condições de formação precoces, próximas a superfície e são indicativas da diagênese de contato.

CAPÍTULO 6 - ARTIGOS

6.1 VOLCANO-SEDIMENTARY INTERACTIONS - A KEY TO UNDERSTAND CRETACEOUS PALEOENVIRONMENTS IN THE PARANÁ BASIN (SOUTHERN BRAZIL)

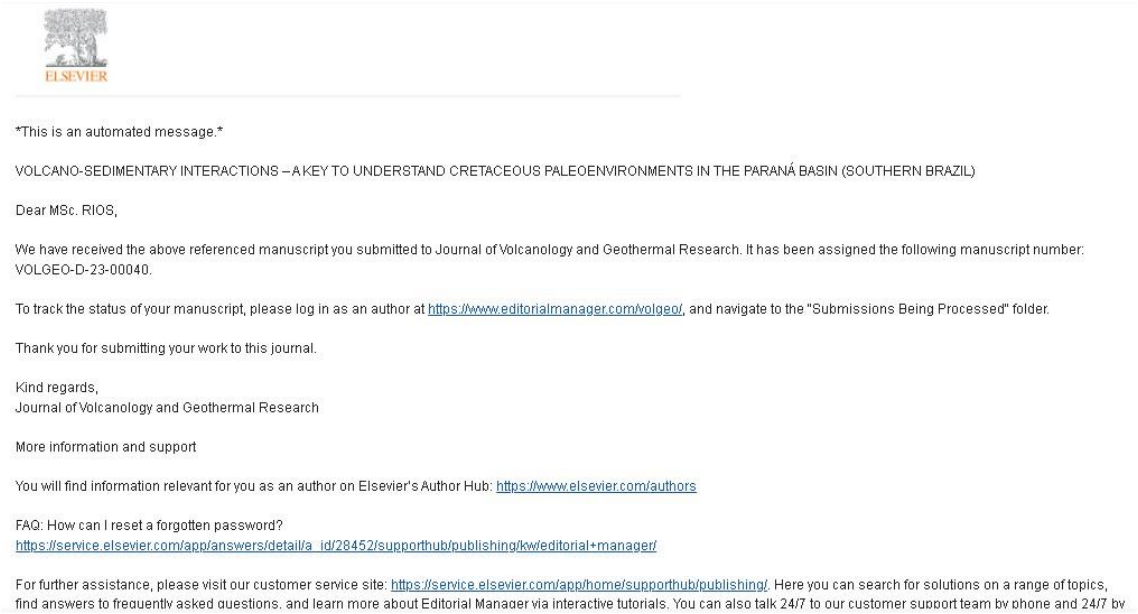

This is an automated message.

VOLCANO-SEDIMENTARY INTERACTIONS – A KEY TO UNDERSTAND CRETACEOUS PALEOENVIRONMENTS IN THE PARANÁ BASIN (SOUTHERN BRAZIL)

Dear MSc. RIOS,

We have received the above referenced manuscript you submitted to Journal of Volcanology and Geothermal Research. It has been assigned the following manuscript number: VOLGEO-D-23-00040.

To track the status of your manuscript, please log in as an author at https://www.editorialmanager.com/volgeo/, and navigate to the "Submissions Being Processed" folder.

Thank you for submitting your work to this journal.

Kind regards,
Journal of Volcanology and Geothermal Research

More information and support

You will find information relevant for you as an author on Elsevier's Author Hub: https://www.elsevier.com/authors

FAQ: How can I reset a forgotten password?
https://service.elsevier.com/app/answers/detail/a_id/28452/supporthub/publishing/kw/editorial+manager/

For further assistance, please visit our customer service site: https://service.elsevier.com/app/home/supporthub/publishing/. Here you can search for solutions on a range of topics, find answers to frequently asked questions, and learn more about Editorial Manager via interactive tutorials. You can also talk 24/7 to our customer support team by phone and 24/7 by

VOLCANO-SEDIMENTARY INTERACTIONS – A KEY TO UNDERSTAND CRETACEOUS PALEOENVIRONMENTS IN THE PARANÁ BASIN (SOUTHERN BRAZIL)

Fernando Rodrigues RIOS[a*], Ana Maria Pimentel MIZUSAKI[a], Cassiana Roberta Lizzoni MICHELIN[b], Isaque Conceição RODRIGUES da Silva[a]

[a]UFRGS, Instituto de Geociências, Programa de Pós-Graduação em Geociências, Campus do Vale – Porto Alegre (RS).
[b]UFRGS, Instituto de Geociências, Departamento de Mineralogia e Petrologia, Campus do Vale – Porto Alegre (RS).

ABSTRACT The Lower Cretaceous in the Paraná Basin registers an immense volcanism (Serra Geral Formation) that covered an active sedimentary system (Botucatu Formation) that precedes the fragmentation of the southern Gondwana. So, the fluvial-aeolian deposits underlying aeolian deposits of residual dunes, were gradually covered by volcanic flows. Intense basic and minor acidic magmatism covered an extensive continental aeolian environment. The interface between the two units shows an aeolian environment during the early stages of volcanism forming deposits and volcano-sedimentary features overlying and underlying the flows. In six outcrops on the southern portion of the current border of Paraná Basin, in Rio Grande do Sul state, these deposits and features were recognized, showing the complexity of the environment and the processes associated with lava flows and sediments. They were formed by the interaction of consolidated or unconsolidated sediments, saturated or not in the water, with basaltic or dacitic flows. Interaction features and deposits synchronous to volcanism (volcanoclastic), later or in intervals between volcanic events (epiclastic) and only cover, with absence of interactions, were identified. Through the distinctive characteristics of the interaction processes between the volcanic rocks and the sediments analyzed in the volcanic-sedimentary features and deposits, the morphology of the aeolian environment of Botucatu Formation could be, by analogy, compared to the current aeolian environments. The proposed paleoenvironment indicates a sedimentary environment with different domains, categorized by their water saturation. The different siliciclastic components found in each domain allowed the generation of different features and volcanic-sedimentary deposits evidencing aspects related to the presence or absence of water among the proposed domains.
Keywords: Volcano-sedimentary interaction, Volcanoclastic, Breccia, Botucatu Formation, Serra Geral Formation.

1. INTRODUCTION

The end of the Jurassic and the beginning of Cretaceous in Paraná Basin located in the South American platform are marked by aeolian deposits and basic to acid lava flows (Fig. 1A) (Milani et al., 1998; Scherer et al., 2021). Aeolian sediments covered by lava flows originate features and rocks along the contact between them are known as lava-sediment interactions. Both consolidated and unconsolidated sediments, the presence of

fluids, especially water, and the contemporaneity between sedimentation and magmatism contribute to the complexity presented by volcano-sedimentary interactions. Volcano-sedimentary interactions are fundamental in paleoenvironmental reconstructions and important stratigraphic markers. Due to the fact they provide a relative age, sedimentation and magmatism are contemporary events and must be analyzed together (Macdonald, 1939, Branney and Suthren, 1988; Allen, 1992; Boulter, 1993; McPhie et al., 1993; Rios et. al., 2018).

Both igneous and sedimentary conditions control the rocks and features generation through the volcano-sedimentary interaction, such as emplacement, type of lava, temperature, degree of crystallization, granulometry, composition, consolidation, and degree of water saturation in sediments. However, the processes and products from interactions are still not fully understood. Regarding lavas, processes can occur still at high temperatures when molten or when fully crystallized, at room temperature of how lava/magma interacts with consolidated or unconsolidated sediments with or without the presence of water. The interaction between volcanic rocks and sediments can occur concomitantly with extrusions (probable intrusions are also included) or later, due to weathering, erosion, and sedimentation (Kokelaar, 1982; Lorenz, 1984; Busby-Spera and White, 1987; McPhie et al., 1993; Hanson and Hargrove, 1999; Dadd and Van Wagoner, 2002; Jerram and Stollhofen, 2002; Lorenz et al., 2002; Skilling et al., 2002; Squire and McPhie, 2002; Zimanowski and Büttner, 2002; McLean et. al., 2016; Rawcliffe, 2016; Gihm and Kwon, 2017; Kwon and Gihm, 2017; Rios et. al., 2018; Nogueira et al., 2021; Jeon and Sohn, 2022)

In Paraná Basin, the transition from aeolian sedimentation of Botucatu Formation to the predominant volcanism of Serra Geral Formation is remarkable. The thick successions of basic and acidic flows show at the base intercalations of aeolian sediments that originate frequent volcanic-sedimentary features in many portions of the basin. Lava-sediment interactions are documented in literature and there are descriptive models of lava aspects of the generation of different lithologies and features. However, the understanding of these processes, the resulting rocks, and the environments involved require additional explanation (Petry et al., 2007; Waichel et al., 2008; Michelin, 2014; Reis et al., 2014; Rios et al., 2018).

Thus, this work aims to recognize these deposits and features searching for the mechanisms that influence the processes of volcano-sedimentary interaction from

igneous and sedimentary perspectives. Furthermore, the present study attempts to verify the existence of water or humidity for the existing paleoenvironmental models for the Cretaceous of Paraná Basin through the distinctive characteristics of interaction processes between the volcanic rocks and the analyzed siliciclastic sediments.

2. GEOLOGICAL SETTING

The Paraná Basin, in the southeast of South American Platform, records successive processes of subsidence, uplift, sedimentation, and magmatism from the Ordovician to the Cretaceous (Zalán et al., 1990; Milani, 1997; Milani et al., 1998, 2007). The basin holds approximately 7,000 m of volcanic-sedimentary sedimentation in the basin's depocenter subdivided into six Supersequences: Rio Ivaí, Paraná, Gondwana I, Gondwana II, Gondwana III and Bauru (Milani, 1997). The Gondwana III Supersequence (Neo-Jurassic to Early Cretaceous) is important to the study since it comprises an aeolian sedimentation associated with the Botucatu Formation and an intense magmatism called Serra Geral, where volcano-sedimentary interactions can be observed (Figs. 1A, B).

Siliciclastic deposits from Botucatu Formation outcrop in the southeast limit of the Paraná basin (Fig. 1C). There is a predominance of quartz sandstones that are well selected, pinkish, fine to medium grain size and rounded grains, associated with large crossed stratification, indicate residual deposits of aeolian dunes. At the base of the formation, there are lenticular deposits of conglomerates and sandstones from coarse to conglomerate granulometry, associated with ephemeral channels in a fluvial-alluvial context (Almeida 1954; Bigarella and Salamuni, 1961, 1967, Soares, 1975; Bigarella, 1979; Almeida and Melo, 1981; Scherer, 2000). The base of the formation (attributed to the Upper Jurassic - Lower Cretaceous) is marked by a regional unconformity and interactions with the Serra Geral volcanics in the upper portion. The Serra Geral Formation is a succession of up to 1,700 m with basic and, secondarily, acid flows of approximately 134 Ma (Lower Cretaceous - Renne et al., 1992; Thiede and Vasconcellos, 2010; Janasi et al., 2011; Baksi, 2018; Rocha et al., 2020).

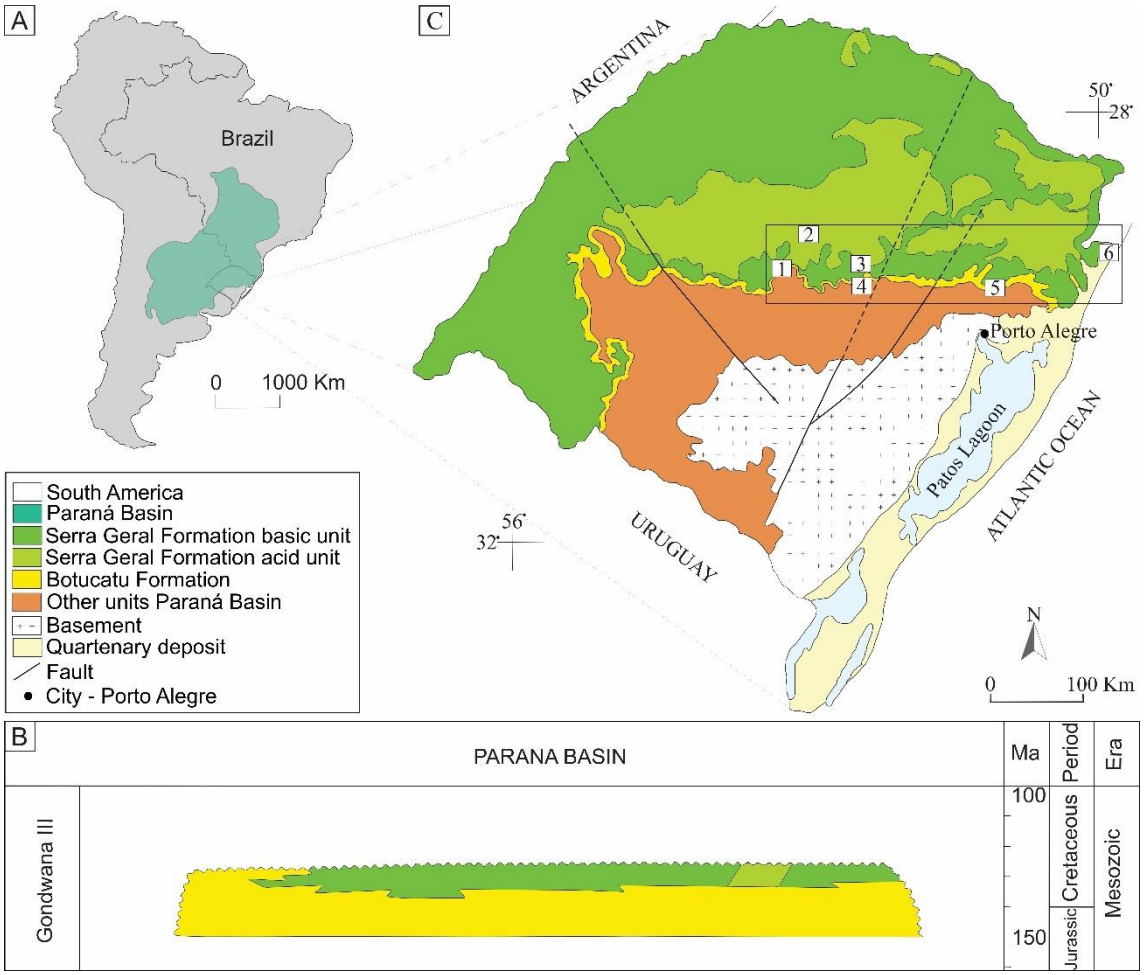

Figure 1: A) Paraná Basin in South America Platform. B) Gondwana III Supersequence, characterized by Botucatu and Serra Geral Formations (modified from Milani et al., 2007). C) Studied areas along the current edge of the Paraná Basin, Rio Grande do Sul state. Profile (1) 29°28'55" S/ 53°28'33" W; (2) 29°06'05" S/ 53°13'49" W; (3) 29°30'12" S/ 52°39'00" W; (4) 29°41'30" S/ 52°23'23" W; (5) 29°37'54" S/ 51°08'49" W; (6) 29°21'27" S/ 49°44'02" W (modified from Scherer, 2002; Janasi et al., 2011; Rios et al., 2018).

Botucatu Formation was gradually covered by the Serra Geral Formation lava flows, but the aeolian environment was still active during the initial stages of volcanism. This sedimentary content embraces sandstone layers from a few centimeters to several meters thick named *intertraps* (Milani et al., 1998; Scherer, 2002; Petry et al., 2007; Waichel et al., 2008; Michelin, 2014; Reis et al., 2014; Rios et al., 2018)

The study area is in the current southeast boundary of Paraná Basin where Botucatu and Serra Geral Formations preferentially outcrop along E–W escarpments (Fig. 2). Analysis of aerial photos and previous research information allowed the selection of six regions with interaction sediments and lava flows (Fig. 1).

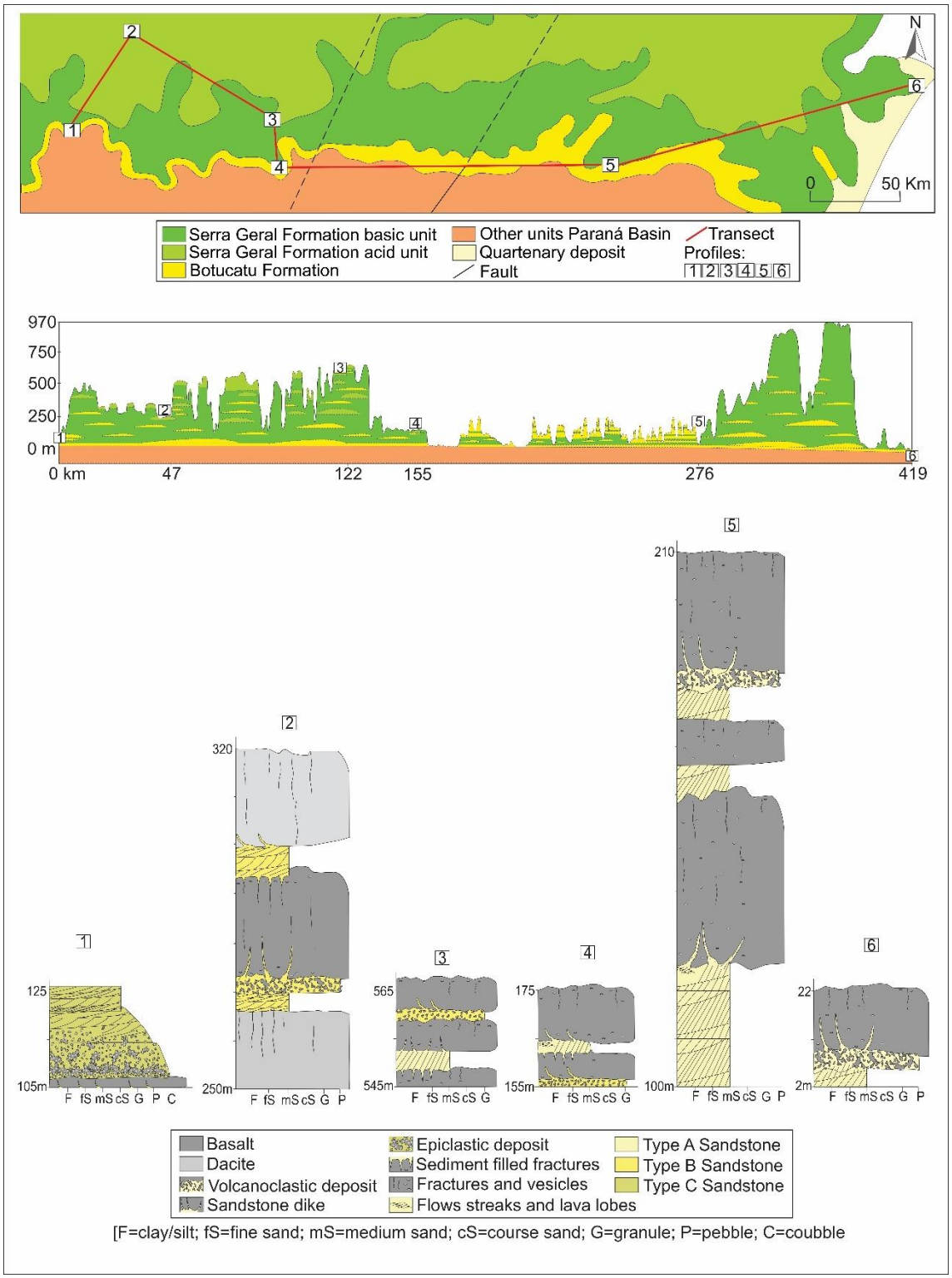

Figure 2: Location of the study areas (see Fig. 1C), the topographic profile that composes the transect, location and representation of the vertical profiles in Paraná Basin.

3. MATERIALS AND METHODS

Six vertical profiles were made allied to the characterization of sedimentary and volcanic rocks, structures, and products associated with the lava-sediment interaction. The transects were made using the topographic position of the outcrops according to the software *Google Earth* (Fig. 2).

The collected samples were macroscopically described, photographed and selected for petrography. Ninety-two samples were analyzed by conventional petrography and complemented by X-ray diffraction analysis (XRD).

Analyzes of X-ray diffraction using whole rock and fine fraction (<4μm), were performed at the X-Ray Diffraction Laboratory of the Institute of Geosciences of the Federal University of Rio Grande do Sul. The diffractometer used was a Siemens D5000 Diffraktometer under K α Cu radiation conditions, 40 kV, 30 mA of filament current and range from 2 to 72° (2θ).

4. RESULTS

The rocks and products of the interaction between volcanic and sediments were identified and described in the columnar profiles (Fig. 2; Tab. 1). For a better understanding, we will separately describe the volcanic and sedimentary lithotypes found. (Fig. 3A, B, C, D) are grouped in tables 2 and 3.

Profile	Flow streak and lava lobe	Preserved dune	Volcanoclastic deposit	Sandstone dike	Sediment-filled fractures	Epiclastic deposit
1				X		X
2			X	X	X	
3			X	X	X	
4	X		X	X	X	
5	X	X	X	X		
6		X	X	X		

Table 1: Volcano-sedimentary features and deposits observed in the different profiles (modified from Rios et al., 2018).

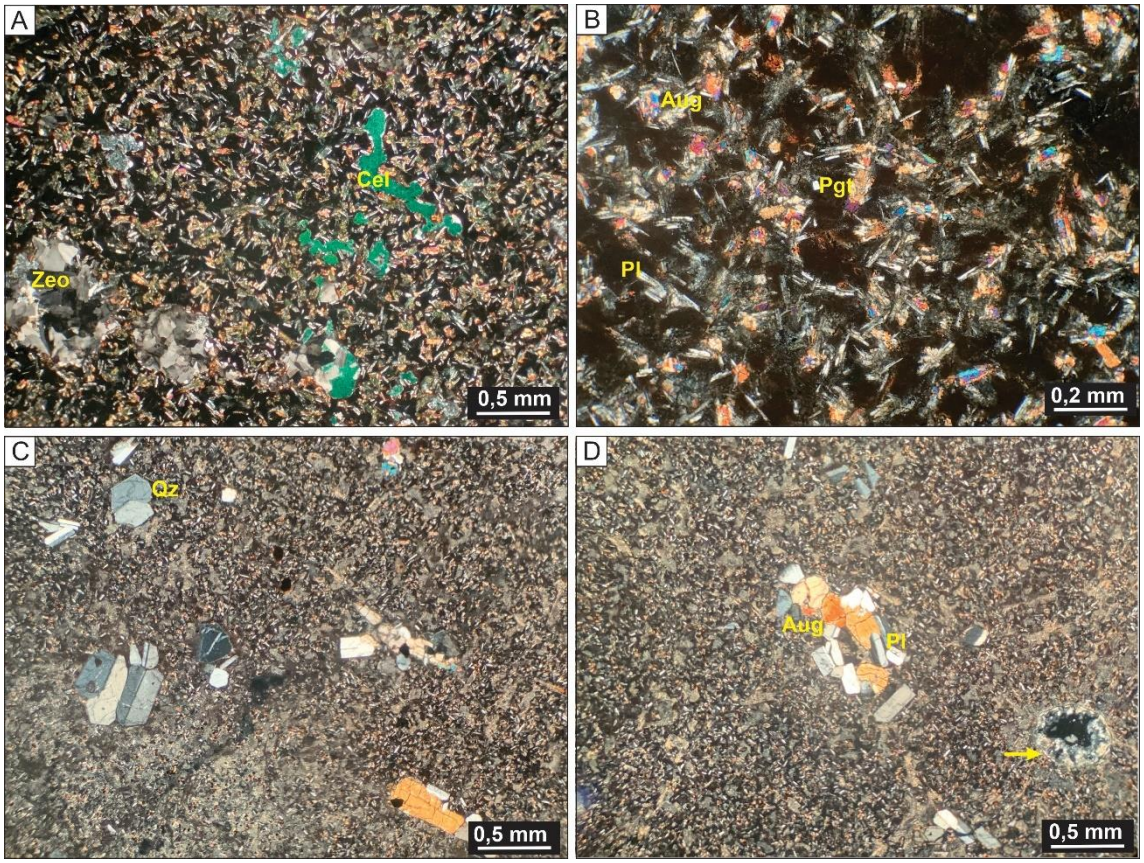

Figure 3: A) Basalt with vesicles filled with zeolite (Zeo) and celadonite (Cel), (crossed polarizers, XP). B) Basalt with glomeroporphyritic texture and plagioclase (Pl), augite (Aug) and pigeonite (Pgt) phenocrysts in a glassy matrix (XP). C) and D) Dacite with fine texture and glomeroporphyres of plagioclase, quartz (Qz) and augite; and vesicles filled with microcrystalline quartz (yellow arrow) (XP).

	Basic (Basalt)	Acid (Dacite)
Main characteristics	Flows, horizontal and vertical disjunction, intense fracturing. Eventually geodes are observed. Color is dark grey, hypocrystalline textures, fine inequigranular, idiomorphic to allotriomorphic crystals. Vesicles filled with microcrystalline quartz, agate, chalcedony, zeolite, celadonite and calcite (Fig. 3A).	Flows, horizontal disjunction, some fractures. Color is reddish brown, fine and glomeroporphyritic texture with phenocrysts. Vesicles filled with microcrystalline quartz.
Mineralogy	Plagioclase phenocrysts, secondarily augite and pigeonite in a glassy matrix, partially devitrified, without preferential orientation (Fig. 3B).	Glomeroporphyres of plagioclase, quartz and K-feldspar, and augite phenocrysts may occur (Fig. 3C and D).
Occurrence profile (see Fig. 2)	Profiles 1, 3, 4 e 5.	Profile 2.

Table 2: Main characteristics, composition, and occurrence profiles of volcanic rocks.

	Sandstone A	Sandstone B	Sandstone C

Classification (Folk, 1968)	Subarkose	Litharenites and sub-litharenites	Litharenites
Main characteristics	Pink, high textural maturity, fine to medium sand granulometry, sub-rounded to rounded grains.	Pink to brown, low to moderate textural maturity, clay to coarse sand granulometry, angular to rounded grains, interbedded silt-clay sheets.	Reddish to brownish, low textural maturity, fine sand to coarse sand granulometry, subangular to rounded grains.
Detrital composition and cement	Monocrystalline and polycrystalline quartz, predominantly, and K feldspar, secondarily. Tourmaline, zircon, apatite, and garnet as accessories.	Monocrystalline and polycrystalline quartz, detrital clay, volcanic fragments and feldspar. Opaque, muscovite, tourmaline and zircon as accessories.	Mono and polycrystalline quartz, volcanic fragments, feldspar, and sandstone fragments.
Diagenetic aspects	Cementation of microcrystalline quartz, chalcedony, opal, celadonite and calcite.	Presence of infiltrated clays. Cementation by microcrystalline quartz, chalcedony, zeolite, illite-smectite, Ti oxide, hematite, celadonite and calcite.	Presence of infiltrated clays. Cementation of microcrystalline quartz, smectite and zeolite.
Occurrence profile (see Fig. 2)	Profiles 3, 4, 5 and 6.	Profiles 1, 2, 3 e 4	Profile 1

Table 3: Classification, and characteristics of sandstones.

Interaction features and deposits can be concomitant with volcanism (volcanoclastic), after the volcanic event (epiclastic) or only covering by the flows, with the absence of interactions.

Flow streaks and lava lobes are features in which lava covers sediments with no evidence of disturbance or mixing. They occur at the lava-sediment interface (Figs. 4 A, B and C) or the top of the *intertraps* (Profiles 4 and 5, see Fig. 2). Figure 4D represents a structure indicating a pinkish paleodune, subarkose (Sandstone A – Table 3), large scale trough cross-stratification, inverse gradation in the strata and it was covered and preserved by lava (Profiles 5 and 6, see Fig. 2). When covered by the volcanic flow, the eolic dunes can completely preserve the morphology of the desert paleotopography (Waichel et al., 2008). Forming a duneiform (wavy) contact (Fig. 4D) with the volcanic flow that was superimposed. The print of lava lobes in the subarkose were observed in profile 4 (Fig. 4 C).

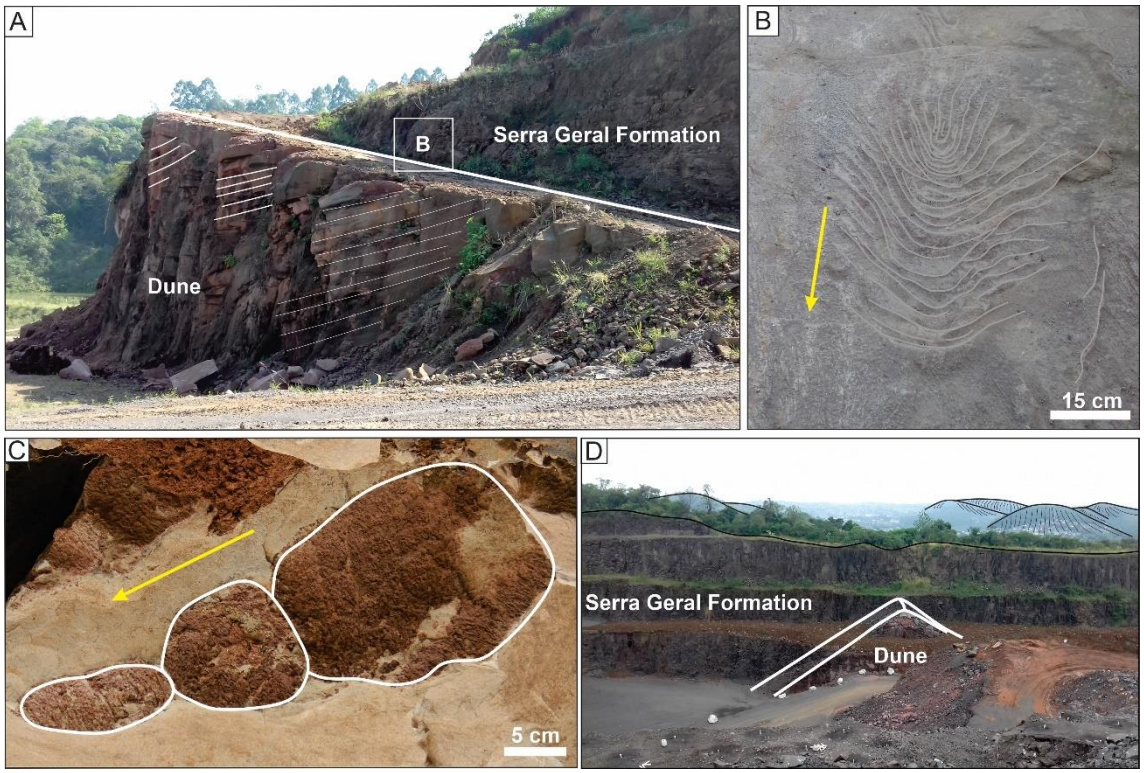

Figure 4: Details of the covering features in subarkose (Sandstone A). A) 10 meters thick dune, the base of profile 5 (modified from Rios et al., 2018). B) Detail of figure A, flow streaks over the dune (profile 5, see Fig. 2), the yellow arrow indicates lava flow. C) Prints of lava lobes on subarkose (profile 4, Fig. 2), yellow arrow indicates lava flow. D) Preserved dune beneath the volcanic flows of the Serra Geral formation, profile 5 (see Fig. 2).

In the contact between the lava flows and the sediments, volcanoclastic deposits with dimensions ranging from centimeters to meters are formed. They form at the lava-sediment interface - beneath volcanic flows, and may also occur with dyke morphology - discordant with bedding. The classification of volcanoclastic rocks can be based on the size and morphology of the volcanic clasts (angular, globular, fluidal and with a mixture of morphologies), on the type and mineralogical composition of the matrix sediments (Folk, 1968 – Table 3), and, when possible, on the genesis (McPhie et al., 1993; Lorenz 1984; Busby-Spera and White, 1987; Skilling et al., 2002).

This work named the volcanoclastic deposits in a more descriptive way using the term breccia associated with the compositions of volcanic clasts and sedimentary matrix (Rosa et al., 2016).

In columnar profiles 2, 3 and 4 (Fig. 2), the volcanoclastic deposits are defined as basaltic breccias of litharenite matrix (Sandstone B; Table 3). The occurrences have a lateral extension of up to 3 m and an average thickness of around 50 cm (Figs. 5A, B).

Volcanic clasts from 0.2 mm to 10 cm with angular, fluidal, and globular morphologies (Figs. 5D, E); eventually have some vesicles filled with sedimentary material. Primary sedimentary structures were not observed, but silty-clayey and sandy foliations forming planes along lava-sediment contact are common. (Figs. 5F, G). Poikilotopic zeolite, prismatic zeolite and prismatic quartz are common cements in the siliciclastic matrix (Figs. 5F, G).

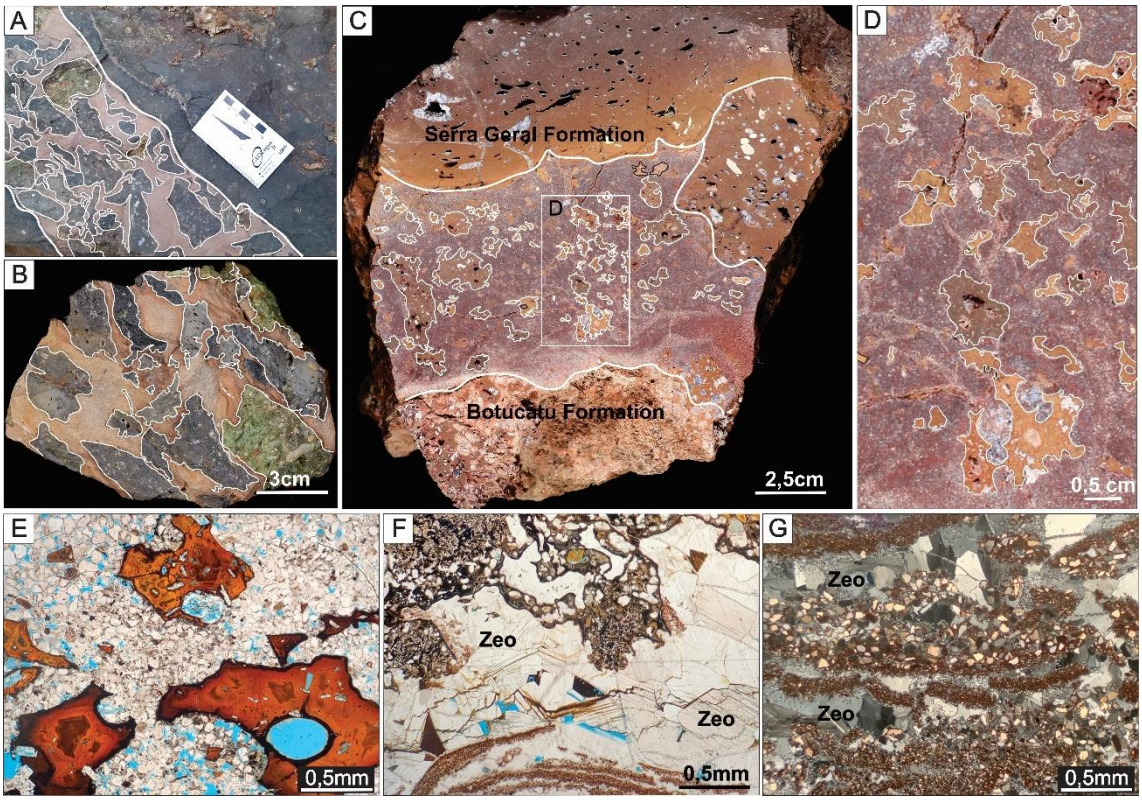

Figure 5: Details of the basaltic breccia of the litarenite matrix. A) and B) Deposit with dyke morphology and angular clasts (Profile 4, see Fig. 2). C) Formation of the basaltic breccia along the interface with the litarenite. D) Detail of figure C, destruction of sedimentary structures and volcanic clasts with angular and fluidal morphologies (Profile 3). E) Vitreous volcanic clasts with angular morphologies, indentations and vesicles (Profile 3, see Fig. 2) (uncrossed polarizers, //P). F) Basalt – litarenite interface (Sandstone B), destruction of the original sedimentary structures and cementation of the siliciclastic matrix by prismatic zeolite (Zeo) (Profile 4, see Fig. 2) (//P). G) Disruption of the foliations and cementation by zeolite (Profile 4, see Fig. 2) (crossed polarizers, XP).

Related to profiles 5 and 6 basaltic breccias of subarkose matrix (Sandstone A – Table 3) are common. The deposits are beneath the basaltic flow with extensions of up to 100 m and thicknesses of up to 4 m (Figs. 6A-D). Volcanic clasts from 0.2 mm to 40 cm, angular, globular, fluidal and clasts with mixed morphologies (Figs. 6B, D, E, G). Clasts

with sediment-filled vesicles are common (Fig. 6G). Large scale trough cross-stratification destroyed along the lava-sediment interface. The matrix is cemented by zeolite and calcite (Figs. 6 E-G).

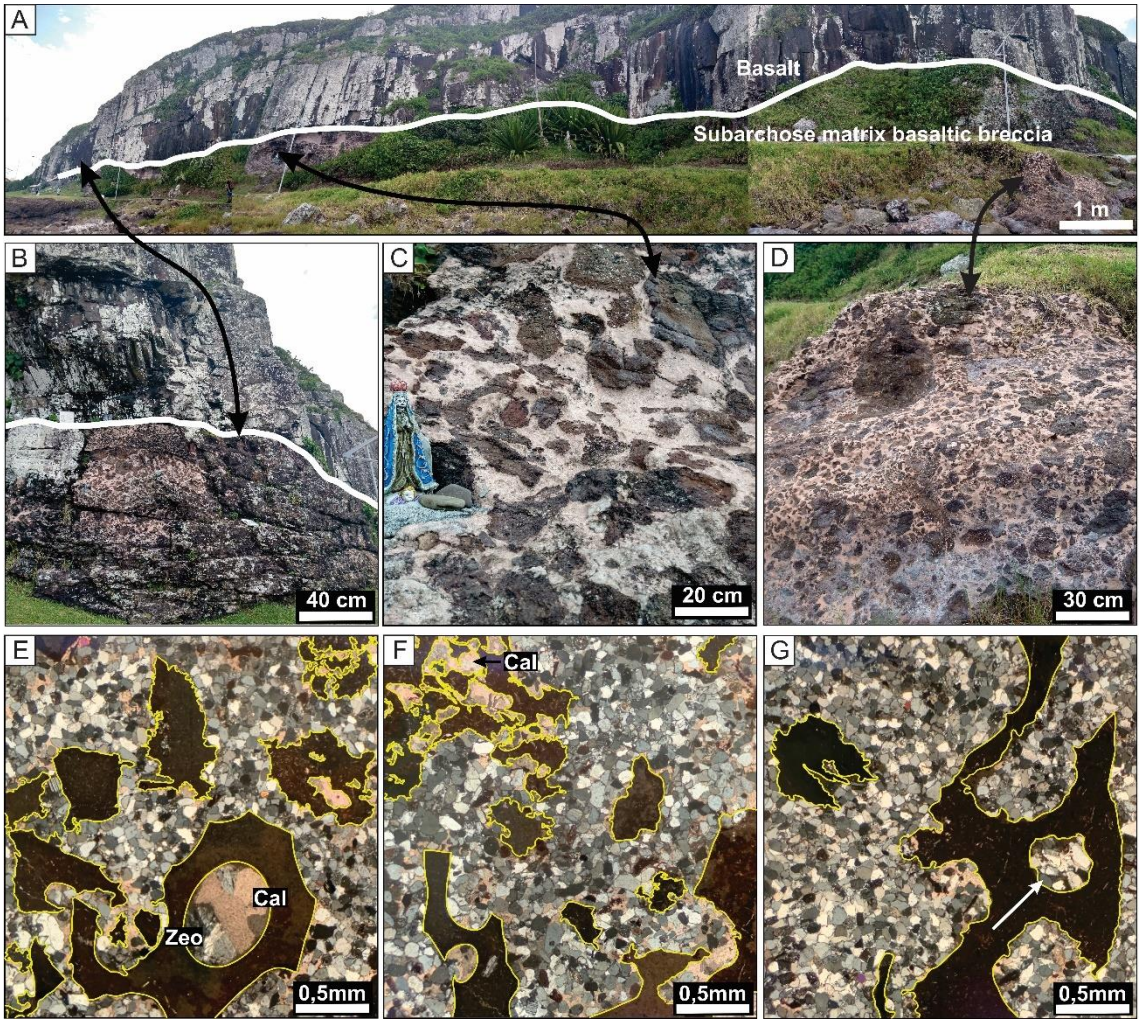

Figure 6: Details of the basaltic breccia of subarchose matrix (Profile 6, see Fig. 2). A) Photomosaic of the domain where the deposit occurs (Torres – RS). B) Contact between the basaltic breccia of subarchose matrix and basaltic flow. C) and D) Clasts from 5 to 30 cm with angular and globular morphologies, immersed in subarchose matrix. E) and F) Volcanic clasts with mixture of angular and fluidal morphologies, rounded edges, vesicles filled with calcite (Cal) and zeolite (Zeo) (crossed polarizers, XP). G) Vesicles filled with sediment (white arrow) (XP).

Associated with the breccias there are sandstone dykes (profiles 1 to 6, see Fig. 2) (Rios et al., 2018). These are fractures filled with sandstone, branched, with centimetric thicknesses (Fig. 7A), rectilinear (Fig. 7B), curved (Fig. 7C) or irregular limits (Figs. 7D-G). Reaction edges between the host rock (basalt) and the dyke, presence of volcanic clasts with fluidal to globular shapes are common (Figs. 7D-G).

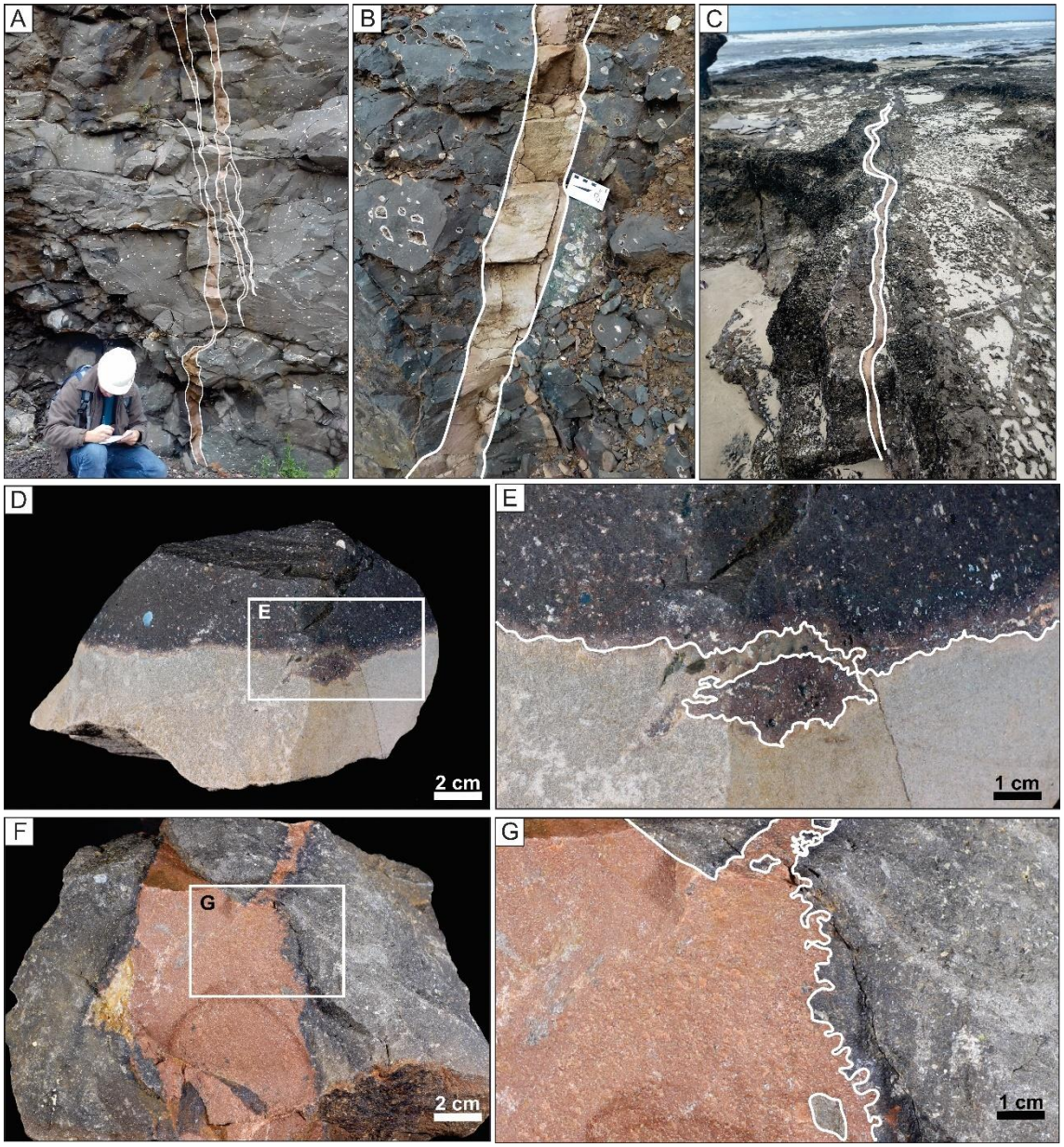

Figure 7: Details of the sandstone dykes. A) Branched sandstone dykes a few centimeters thick, profile 5 (see Fig. 2). B) Sandstone dykes with straight edges, profile 4. C) Sandstone dykes with curved edges, profile 6 (see Fig. 2). D) and E) Irregular edge and clast with fluidal morphology, profile 4 (see Fig. 2). F) e G) Irregular edge and clast with globular morphology, profile 4 (see Fig. 2).

The sandstone dykes in profiles 1, 2, 3 and 4 (see Fig. 2) are filled with sublitharenite (see Sandstone B; Table 3), with low textural maturity and detrital clay foliations. Sometimes, there is a decrease in the granulation of the volcanic rock (basalt or dacite) at the contact (Fig. 8A) and/or formation of detrital clay foliations parallel to the contact with the volcanic rock (Figs. 8A-C). The rupture and/or deformation of these foliations by the injection of sand is verified (Figs. 8D, E). Generally, near the edge of

the dykes, there are inclusions of sediments inside the volcanic rock and volcanic clasts with globular shapes in the sediments (Fig. 8F).

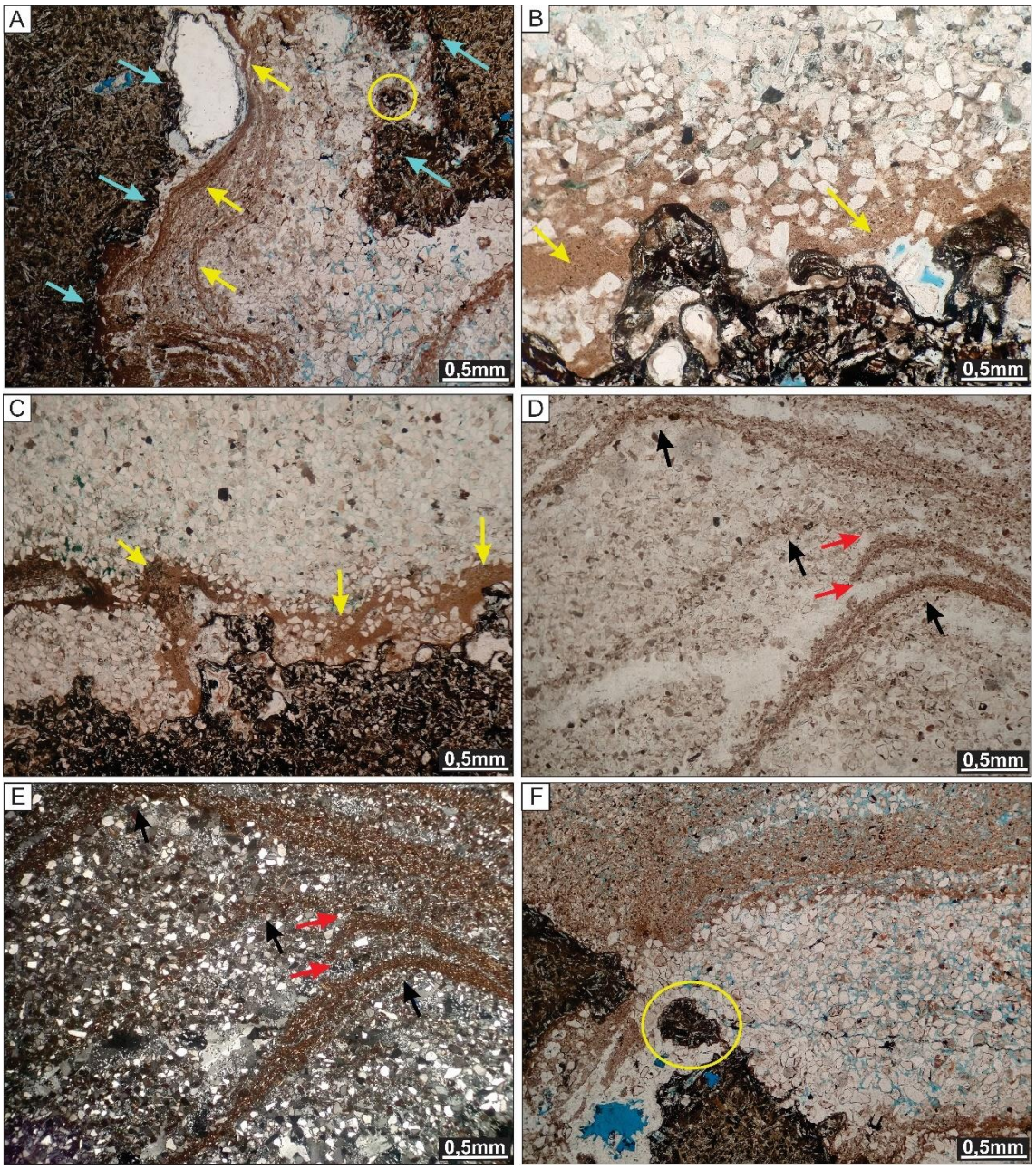

Figure 8: A) Contact of basalt with sublitharenite (Sandstone B), decrease in granulation (blue arrows). The formation of silty-clay foliations parallel to the contact (yellow arrows), (Profile 2, see Fig. 2), (uncrossed polarizers, //P). B) and C) Detrital clay segregation (yellow arrows) close to the contact with the basalt (Profile 4, see Fig. 2) (//P). D) (//P) and E) Deformation of the detrital clay foliations (black arrows) and their disruption by the injection of sand (red arrows), (Profile 2, see Fig. 2) (crossed polarizers, XP). F) Volcanic clast with globular morphology near the contact (Profile 2, see Fig. 2), (//P).

The sandstone dikes of profiles 3, 4, 5 and 6 (see Fig. 2) are filled with Sandstone A (see Table 3). The borders of the dyke are characterized by a decrease in basalt granulation (Figs. 9A-D). There are extensions of basaltic lava into the sediments (Figs. 9C, D). Volcanic clasts of fluidal and globular morphologies are observed (Figs. 9A and B)

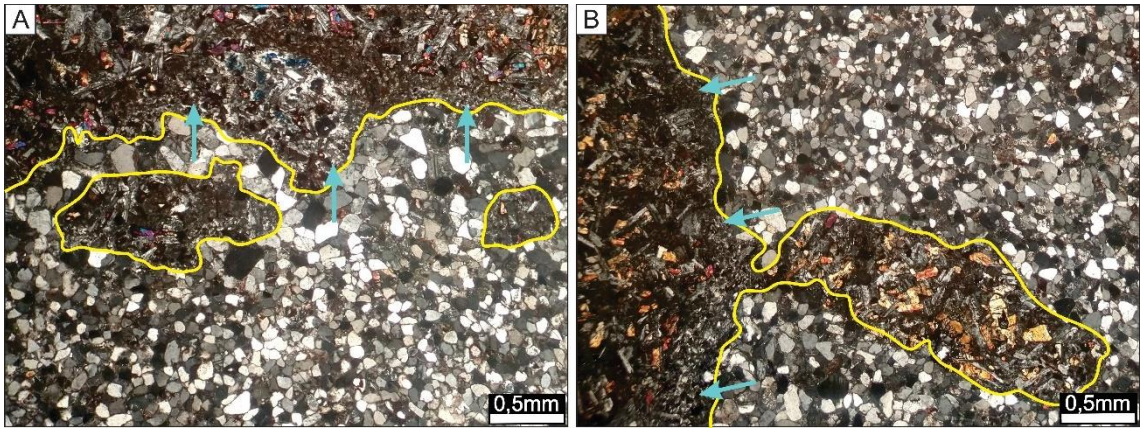

Figure 9: A) Granulation decreased (blue arrows) in contact between the basalt and the subarkose (Sandstone A). Volcanic clasts with fluidal morphologies, and globular (Profile 5, see Fig. 2), (crossed polarizers, XP). B) Elongations of basalt into the sediments and there is a decrease in basalt granulation (blue arrows), (Profile 5, see Fig. 2), (crossed polarizers, XP).

The other features described are epiclastic whereas occur after the partial or total cooling of the lavas and dominance of sedimentary processes.

Sediment-filled fractures, for example, were found in three profiles (2, 3 and 4; see Fig. 2) at the top of the basaltic flows. These features are associated with the presence of *intertraps* (Figs. 10A, B) and are filled with Sandstones A in profiles 3 and 4 and Sandstone B in profile 2 (Table 3, Fig 2).

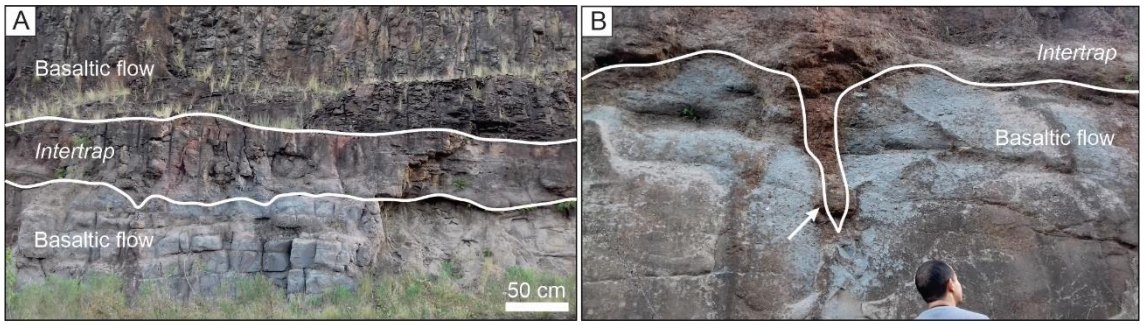

Figure 10: A) *Intertrap* between basaltic flows described in profile 3 (see Fig. 2). B) detail of sediment-filled fracture associated with the *intertrap* (Sandstone A) and top of basaltic flows, profile 3 (see Fig. 2) (modified from Rios et al., 2018).

The epiclastic deposit covers a basaltic flow and has a lenticular geometry as can be seen in profile 1 (see Fig. 2). It varies in length and thickness, 30 meters and 3 meters, respectively (Fig. 11A). The deposit was characterized based on its geometry, disposition (bottom and top), the texture of the intraclasts, "matrix," transport marks and effects of weathering on the intraclasts.

It is represented by a conglomerate, litharenite with clayey intraclasts. There is no preferential imbrication of intraclasts immersed in the lithoarenite "matrix" (Sandstone C – Table 3). The base of the deposit is in contact with the basalt flow through an erosive surface, has lenticular geometry, with intraclasts from 0.2 mm to 35 cm with irregular borders (Fig.11A, B). There is a transition evidenced by trough cross-satratification and a significant decrease in the amount and size of intraclasts at the top of the deposit (Figs. 11C-F). Intraclasts may have zeolite-filled vesicles (Figs. 11D, E). The top of the deposit has subangular to rounded grains, with punctual, linear, floating contacts, intragranular and intracrystalline porosity (Figs. 11G, H) and intergranular (Figs. 11 G - I).

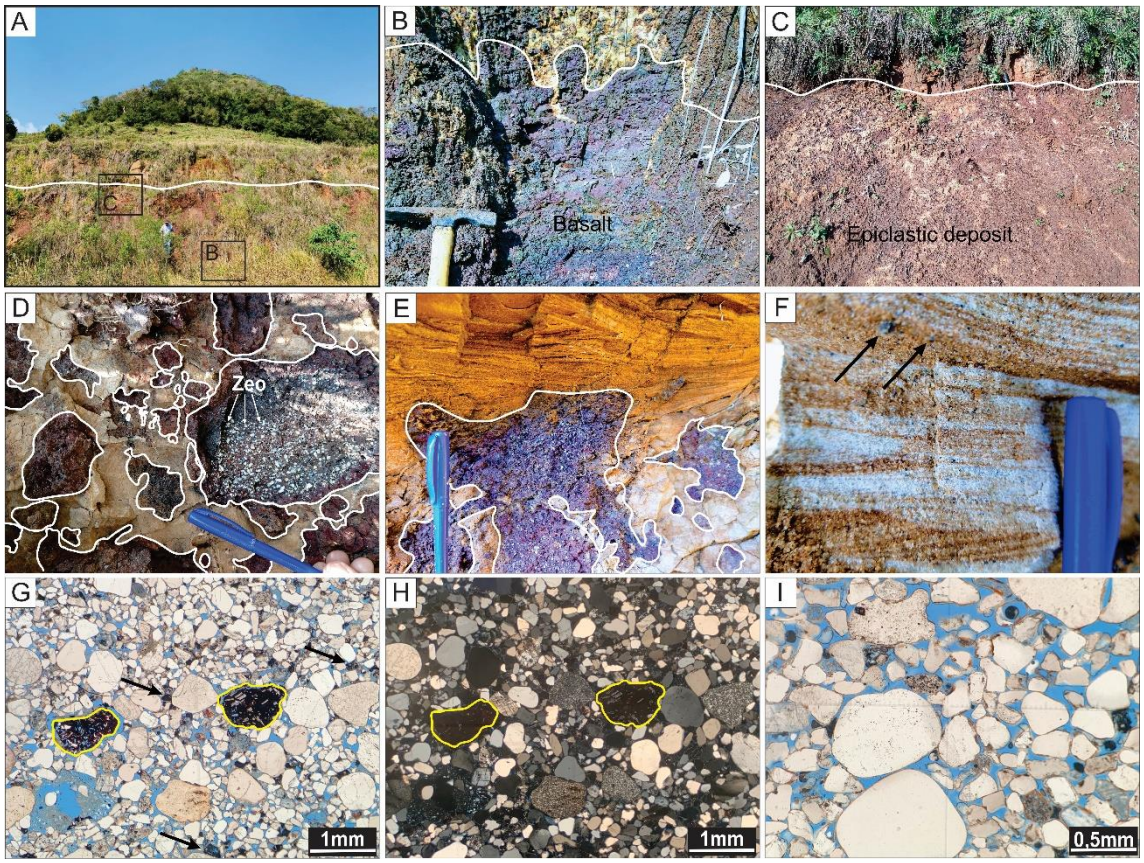

Figure 11: Details of the conglomerate, litharenite, with clayey intraclasts (Sandstone C) (Profile 1). A) Deposit of lenticular geometry, superimposed on a basaltic flow. B) Detail of Figure A, the base of the deposit in contact with the basaltic flow through an erosive surface. C) Detail of Figure A, top of the epiclastic deposit. D) and E) Irregular intraclasts

with vesicles filled with zeolite. F) Trough cross- stratification at the top of the deposit and small clayey fragments (black arrows). G) (uncrossed polarizers, //P) and H) Intragranular and intracrystalline porosity in clay fragments (in yellow) and small fragments (black arrows) (crossed polarizers, XP). I) Punctual, floating contacts and intergranular porosity (//P).

5. DISCUSSION

The recognition of volcanoclastic rocks, interaction features and covering between lava flows and sediments are requirements for the interpretation of the volcano-sedimentary paleoenvironment and sometimes a relative chronology. The identification and description of the features and volcanic-sedimentary deposits, the correlation, and the location of the profiles studied in the outcropping limit of the Juro-Cretaceous sequence of the Paraná Basin show the complexity of interactions of lava and sedimentary processes.

The Juro-Cretaceous Botucatu Formation, constitutes an aeolian continental desert environment where recurrent magmatic activity generates volcano-sedimentary interactions and covering features.

Sand sheets and dune fields (ergs) are a remarkable morphology of a current desert system, although ephemeral river plains, intermittent lakes (playas) and alluvial fans may also be associated (Giannini et al., 2008).

Ergs, the regions with aeolian dune fields in current deserts, occupy up to a maximum of 20% of the total area (Lancaster, 1995). Modern sand sheets, however, generally occur on the limits of dune fields (Kocurek and Nielson, 1986; Schwam, 1988). The development of these deposits is associated with: coarse-grained sediments (coarse sand to gravel), groundwater level close to the surface, frequent flooding and intense vegetation (Kocurek and Nielson, 1986).

Deserts are considered dynamic systems with active eolian sedimentation due to wind speed, low effective humidity and little vegetation covering (Lancaster, 1988; Kocurek and Lancaster, 1999).

In addition, it is essential to understand that changes in the properties of lava, sediments and transport processes in a desertic sedimentary environment affected by a volcanic event will result in different products of volcano-sedimentary interaction (Busby-Spera and White, 1987; McPhie et al., 1993; Dadd and Van Wagoner, 2002;

Jerram and Stollhofen, 2002; Skilling et al., 2002; Zimanowski and Büttner, 2002; Rios et al., 2018).

Consequently, the search for analogies with current desert environments makes it possible to propose a paleoenvironmental model (Fig. 12). The model presents a perspective of the events that formed the features and volcanic-sedimentary deposits according to the analyzed points. The model (Fig. 12) is mainly based on properties as: water saturation of the sediments - evaluated through the composition and granulometry of siliciclastic sediments (mainly the presence of silt-clay fractions and coarse sand fractions); degree of sediment consolidation; and textures and structures formed during the genesis of volcanic-sedimentary features and deposits (morphologies of volcanic fragments, formation of silt-clay foliations). The features and volcanoclastic deposits originated during volcanism through different sediment remobilization mechanisms, such as differences in temperature, fluidization, and sediment transport.

The proposed paleoenvironment indicates the existence of an active eolic sedimentary environment that differentiates laterally and temporally through different domains (Fig. 12A):

- Dune fields – essentially composed of Sandstone A (Table 3), unsaturated in water, minimal moisture in the pores (Profiles 5 and 6, see Fig.2);
- Aeolian sand sheets - Sandstones B and C (Table 3), saturated to supersaturated in water, with wet sediments and/or water in the pores (Profiles 1 and 2, see Fig.2).
- Transition – Sandstones A and B (Table 3), unsaturated to supersaturated in water (Profiles 3 and 4, see Fig.2).

Towards the west of the studied profiles on the current edge of the Paraná Basin as figure 12A indicates it is possible to recognize a decrease in the quantity deposits related to the composition of subarkose or Sandstone A (profiles 3, 4, 5 and 6, see Fig. 2). Concerning Profiles 5 and 6 (see Fig. 2) only Sandstone A is related to volcanoclastic features and deposits. In profiles 3 and 4 (see Fig. 2), sublitharenites and litharenites, Sandstone B, compose the features and volcanoclastic deposits but Sandstone A occurs as *intertraps*. Profile 2 (see Fig. 2) marks the predominance of Sandstone B and the absence of Sandstone A. In profile 1 (see Fig. 2), litharenite, Sandstone C, indicates a significant increase in the granulometry of siliciclastic constituents in the epiclastic deposit. Looking all these evidences it is possible to infer an increase in the presence of water and/or humidity towards the west profiles (Fig. 12A).

The contemporaneity of the processes of sedimentation and magmatism in an aeolian environment means that the sediments transported by the wind are sometimes deposited on a volcanic substrate. A sediment layer is formed and named *intertrap* when immediately recovered by a subsequent lava flow. As a result, in the domain of aeolian dune fields, sediment remobilization mechanisms may have been inhibited in certain locations. For example, where there is the complete preservation of aeolian dunes (Figs. 4D and 12B-1). It is a feature compositionally related to Sandstone A and is found exclusively in the dune field domain. The sediments, at the time of lava placement, probably had a minimum of water in the pores. Thus, the combination of sediment properties and low humidity possibly preserved the bedding and its internal structures and prevented lava fragmentation (Scherer, 2002; Waichel et al., 2008; Rios et al., 2018). Consequently, it inhibited the formation of volcanoclastic breccias and sandstone dykes (Fig. 12B-1).

Associated with the paleo relief there are flow streaks and lava lobes (Figs. 4B and C). Their genesis is related to the differences in density and temperature between the sedimentary and volcanic components. In such a way that, when flowing over the unconsolidated sediment, the lava deforms, also deforming the underlying sediment (Figs. 12B-1 and B-3) (Waichel et al., 2008). These features were found in dune domains and transition fields and are associated with Sandstone A.

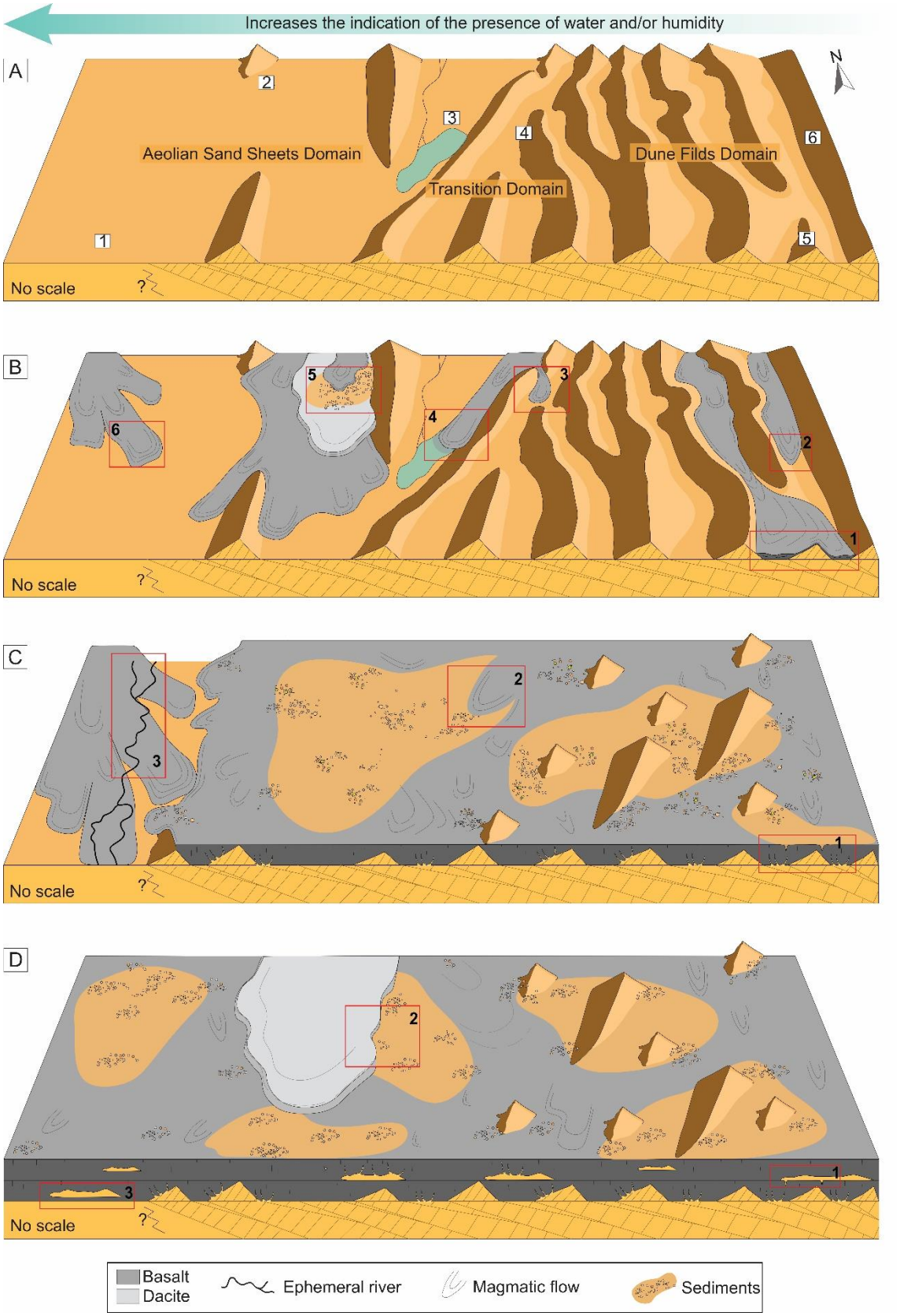

Figure 12: Proposition of a paleoenvironmental model, figures from A to D indicate succession in time. A) Different domains indicating an increase in the presence of water and/or humidity towards the west of the 6 profiles studied along the current edge of the Paraná Basin. B), C) and D) Volcano-sedimentary environment and the contemporaneity

of eolic sedimentation and magmatism forming volcanic-sedimentary features and deposits.

Volcanoclastic deposits characterized by basaltic breccias of litharenite matrix and basaltic breccias of subarkose matrix are formed by the fluidization process. They occur in all suggested domains, dune fields (Figs. 12B-2, C-1), transition fields (Figs. 12B-4, C-2) and aeolian sand sheets (Fig. 12B-5). These deposits were formed by the temperature contrast of the lava with the partially wet, humid, or water-saturated sediment responsible for the fluidization process. Water is vaporized and the former steam is trapped along the sediment-lava interface. Lava fragments when in contact with wet unconsolidated sediment, forming igneous clasts (Skilling et al., 2002; Squire and McPhie, 2002). The clasts have variations in their morphologies, which may be associated with the different domains of occurrence. Clasts with angular shapes (Figs. 5B, 6C and 6D) are more characteristic of the dune field domain, although they are found in the transitional domain. Clasts with fluidal and globular morphologies (Figs. 5F-H) were found more frequently in the aeolian and transitional sand sheets domains when compared to the dune fields domain. Clasts with mixed morphologies (Figs. 5E, 6E-G) are common across domains. Probably due to the different brittle and ductile fragmentation processes that occurred during the genesis of these deposits (Skilling et al., 2002; Squire and McPhie, 2002). Fluidization is responsible for the destruction of primary sedimentary structures; however, it promotes the development of silt-clay foliations at the lava-sediment interface (Figs. 5F-H) (Kokelaar, 1982; Branney and Suthren, 1988; McPhie et al., 1993; Doyle, 2000; Skilling et al., 2002; Brown and Bell, 2007).

Sandstone dykes are also formed through the fluidization process (Kokelaar, 1982). It is a feature found in all proposed domains, dune fields (Figs. 12B-2 and C-1), transition fields (Figs. 12B-3, B-4 and C-2) and aeolian sand sheets (Figs. 12B-5, B-6 and 12D-2). Humidity in unconsolidated sediments is converted into steam. It is pressurized, and confined at the base of volcanic flow. Fracturing, due to the rapid cooling of the magmatic body, reduces the pressure, with the injection of sediments along the pressure relief zone. The base of the flows is reworked by the steam flow, involving the “pull-out” and formation of clasts from the volcanic flow (Rios et al., 2018). Clastic dykes differ from one domain to another through their filling. Sandstone dykes filled by Sandstone A are associated with dune fields and transition domains. Sandstone dykes filled by Sandstone B are associated with aeolian and transition sand sheet domains. The textural

homogenization of the sediments and the consequent formation of silt-clay layers (Figs. 8A-C), parallel to the contact with the volcanic, probably originated from the fluidization of the sediments, as well as in the volcanoclastic deposits.

The fractures filled by sediments and the conglomerate, litharenite, with clayey intraclasts are features were defined as epiclastic as the result of the re-sedimentation of pre-existing rocks. It contains fragments derived from syn-eruptions and post-eruptions, through weathering and erosion processes (Fisher 1960; Cas & Wright 1987; McPhie et al., 1993).

The fractures filled by sediments also have morphology conditioned to the volcanic paleo relief and the condition of contemporaneity between the sedimentary and volcanic systems (Figs. 10A, B). In this study, sediment-filled fractures are associated with cooling fractures, common at the top of flows (Fig. 12C-1). These fractures are filled with sediments, probably the result of a return of sedimentation, the same that probably originated the *intertraps* (Fig. 12D-1) (Michelin, 2014; Rios et al., 2018). These features were found in the domains of aeolian and transitional sand sheets and are associated with Sandstones A and B.

The conglomerate, litharenite, with clayey intraclasts was formed in a time interval between volcanic events and associated with exposure, weathering and reworking (Fig. 12B-6). Ephemeral river channels have invaded the exposed and partially or fully cooled volcanic surface (Fig. 12C-3). The base of the deposit was formed after the erosion of the volcanic plain by the ephemeral channels that were installed mobilizing the volcanic fragments displaced (Fig. 12C-3). In water, in addition to the sudden cooling, the fragmentation of the lava also causes the exsolution of gases from the magma, which causes vesiculation. The clasts are heavily replaced by clay minerals, they exhibit irregular shapes and contours, common characteristics of glassy fragments (McPhie et al., 1993). In addition, they have many vesicles filled with zeolite (Fig. 11D), a mineral commonly associated with the alteration of volcanic glass (Tucker, 2001). At the top of the deposit, the amount of volcanic material available for transport decreased and trough crossbedding structures were formed by subaqueous tractive currents (Figs. 11E, F). In this way, the volcanic-sedimentary material was deposited, forming the poorly selected epiclastic deposit (Fig. 12D-3), with fragments of volcanic origin with a wide granulometric variation (medium sand to cobble). The active diagenetic process caused

the volcanic intraclasts to be partially or totally replaced by clay minerals and Fe oxides. It is a specific deposit of aeolian sand sheets.

6. CONCLUSIONS

Interaction features and deposits concomitant to volcanism (vulcanoclastic), later or in intervals between volcanic events (epiclastic) and only cover, with absence of interactions, were identified.

By comparing the morphology of the aeolian system of the Botucatu Formation to current aeolian environments, the proposed paleoenvironment indicates a sedimentary environment with different domains that allowed the formation of different features and volcanic-sedimentary deposits. The domains were defined in aeolian sand sheets (saturated to super saturated in water) occurring at the edge of dune fields (unsaturated in water) and, between them, the transition (unsaturated to super saturated in water).

By means of this analogy, an increase in the amount of water and/or humidity towards the west of the profiles studied in the current border of the Paraná Basin is proposed, not being possible to estimate the water contents (%) that were present.

This fact is confirmed by the appearance, towards the west of the profiles studied, of silt-clay fractions, as well as the increase in the granulometry of the sediments associated with the aeolian sand sheets, with evidence of ephemeral fluvial channels. In addition, the fragmentation of lava forming volcanic clasts with different morphologies and their mixture with the different siliciclastic components found in each domain points, mainly, to aspects related to differences in humidity between the proposed domains, evidenced by the fluidization in the genesis of the features and deposits volcanoclastic.

Acknowledgments

The first author is grateful to all who contributed to this work. Special thanks are due to the Conselho Nacional de Desenvolvimento Científico e Tecnológico (CNPq, grant number: 141345/2017-9) for the grant awarded at the period of this doctorate program.

7. BIBLIOGRAPHIC REFERENCES

Allen, R.L., 1992. Reconstruction of the tectonic, volcanic and sedimentary setting of strongly deformed Zn-Cu massive sulfide deposits at Benambra, Victoria, Australia. Econ. Geol. 87, 825-854. doi: https://doi.org/10.2113/gsecongeo.87.3.825.

Almeida, E.F.M., 1954. Botucatu, um deserto triássico da América do Sul. DNPM Div. Geo. Min., Notas Prel. E Estudos, 86.

Almeida, E.F.M., Melo, C., 1981. A Bacia do Paraná e o vulcanismo no Mesozóico. In: Bistrichi, C.A., Carneiro, C.D.R., Dantas, A.S.L., Ponçano, W.L. (Eds.), Mapa geológico do Estado de São Paulo, nota explicativa. Instituto de Pesquisas Tecnológicas, 1, 46-77.

Baksi, A.K., 2018. Paraná flood basalt volcanism primarily limited to ~ 1 Myr beginning at 135 Ma: New40Ar/39Ar ages for rocks from Rio Grande do Sul, and critical evaluation of published radiometric data. J. Volcanol. Geotherm. Res. 355, 66–77. doi:10.1016/j.jvolgeores.2017.02.016

Bigarella, J.J., 1979. Botucatu and Sambaiba sandstones of South America (Jurassic and Cretaceous); and Cave sandstone and similar sandstone of Southern Africa (Triassic). In: McKee, F.D. (Ed.), A Study of Global Sand Seas. U.S. Geological Survey Professional Paper, 1052, 233-238.

Bigarella, J.J., Salamuni, R., 1961. Early Mesozoic wind patterns as suggested by dune bedding in the Botucatu Sandstone of Brazil and Uruguai. Geol. Soc. Amer. Bull., 72, 1089-1106.

Bigarella, J.J., Salamuni, R., 1967. Botucatu Formation. In: Bigarella, J.J., Becker, R.D., Pinto, I.D. (Eds.), Problems in Brazilian Gondwana Geology, Curitiba, pp. 197–206.

Boulter, C.A., 1993. High-level peperitic sills at Rio Tinto, Spain: implications for stratigraphy and mineralization. Trans. Inst. Min. Metall. 102, B30-B38.

Branney, M., Suthren, R., 1988. High-level peperitic sills in the English Lake District: distinction from block lavas, and implications for Borrowdale Volcanic Group stratigraphy. Geol. J. 23, 171-187. doi: https://doi.org/10.1002/gj.3350230206.

Brown, D.J., Bell, B.R., 2007. How do you grade peperites? J. Volcanol. Geotherm. Res., 159, 409-420. doi: https://doi.org/10.1016/j.jvolgeores.2006.08.008.

Busby-Spera, C.J., White, J.D.L., 1987. Variation in peperite textures associated with differing host-sediment properties. Bull. Volcanol. 49, 765-775. doi: 10.1007/BF01079827.

Cas, R.F., Wright, J.V., 1987. Volcanic Succession: Modern and ancient: London, Allen & Unwin, 528 p.

Dadd, K.A., Van Wagoner, N.A., 2002. Magma composition and viscosity as controls on peperite texture: an example from Passamaquoddy Bay, southeastern Canada. In: Skilling, I.P., White, J.D.L., McPhie, J. (Eds.), Peperite: Processes and Products of Magma-Sediment Mingling. J. Volcanol. Geotherm. Res., 114, 63-80. doi: 10.1016/S0377-0273(01)00288-8.

Doyle, M.G., 2000. Clast shape and textural associations in peperite as a guide to hydromagmatic interactions: Upper Permian basaltic and basaltic andesite examples from Kiama, Australia. Aust. J. Earth Sci. 47, 167-177. doi: https://doi.org/10.1046/j.1440-0952.2000.00773.x

Fischer, R.V., 1960. Classification of volcanic breccias. Geologic Society American Bulletin, 71: 973-982. doi: https://doi.org/10.1130/0016-7606(1960)71[973:COVB]2.0.CO;2.

Folk, R.L., 1968. Petrology of Sedimentary Rocks. Hemphill, Austin, TX., pp.107.

Giannini, P.C.F., Assine, M.L., Sawakuchi, A.O. 2008. Ambientes Eólicos. In: Silva, A.J.C.L.P., Aragão, M.A.N.F., Magalhães, A.J.C. (org.). Ambientes de Sedimentação Siliciclástica do Brasil. 1 Edição, São Paulo, 2008, p. 72-101.

Gihm, Y.S., Kwon, C.W., 2017. Textural variations and fragmentation processes in peperite formed between felsic lava flow and wet substrate: An example from the Cretaceous Buan Volcanics, southwest Korea. J. Volcanol. Geotherm. Res. 331, 92–101. doi: https://doi.org/10.1016/j.jvolgeores.2017.01.001

Hanson, R.E., Hargrove, U.S., 1999. Processes of magma/wet sediment interaction in a large-scale Jurassic andesitic peperite complex, northern Sierra Nevada, California. Bull. Volcanol. 60, 610-626. doi: https://doi.org/10.1007/s004450050255.

Janasi, V.D.A., de Freitas, V.A., Heaman, L.H., 2011. The onset of flood basalt volcanism, Northern Paraná Basin, Brazil: a precise U-Pb baddeleyite/zircon age for a Chapecó-type dacite. Earth and Planetary Science Letters, 302(1), 147-153. doi: 10.1016/j.epsl.2010.12.005.

Jeon Y., Sohn, Y.K., 2022. Interactions of pāhoehoe and ‘a‘ā lavas and fluvial sediments on an alluvial plain (the Cretaceous Gyeongsang Basin, Republic of Korea). J. Volcanol. Geotherm. Res.432, 107699. doi: https://doi.org/10.1016/j.jvolgeores.2022.107699.

Jerram, D., Stollhofen, H., 2002. Lava/sediment interaction in desert settings: are all peperite-like textures the result of magma-water interaction? In: Skilling, I.P., White, J.D.L., McPhie, J. (Eds.), Peperite: Processes and Products of Magma-Sediment Mingling. J. Volcanol. Geotherm. Res. 114, 231-249. doi: 10.1016/S0377-0273(01)00279-7.

Kobayashi, T., Matsuda, A., Kamichika, M., Sato, T., 1986. Studies of the dry surface layer in a sand dune field. (1) Modeling of the dry surface layer of sand under isothermal steady conditions. Journal of Agricultural Meteorology, 42(2), 113–118. https://doi.org/10.2480/agrmet.42.113.

Kocurek, G., Nielson, J. 1986. Conditions favourable for the formation of warm-climate aeolian sand sheets. Sedimentology, 33, 795-816. doi: https://doi.org/10.1111/j.1365-3091.1986.tb00983.x.

Kocurek, G., Lancaster, N., 1999. Aeolian system sediment state: Theory and Mojave Desert Kelso dune field example. Sedimentology, 46, 505-515. doi: https://doi.org/10.1046/j.1365-3091.1999.00227.x

Kokelaar, B.P., 1982. Fluidization of wet sediments during the emplacement and cooling of various igneous bodies. J. Geol. Soc. London 139, 21-33. doi: https://doi.org/10.1144/gsjgs.139.1.0021.

Kwon, C.W., Gihm, Y.S., 2017. Fluidization of host sediments and its impacts on peperitos forming processes, the Cretaceous Buan Volcanics, Korea. J. Volcanol. Geotherm Res. 341: 84–93. doi: https://doi.org/10.1016/j.jvolgeores.2017.05.019.

Lancaster, N. 1988. Development of Linear Dunes in the Southwestern Kalahari, Southern-Africa. Journal of Arid Environments, 14, 233-244. doi: https://doi.org/10.1016/S0140-1963(18)31070-X.

Lancaster, N., 1995. The Geomorphology of Desert Dunes. London, Routledge, 312p.

Lorenz, B.E., 1984. Mud-magma interactions in the Dunnage Mélange, Newfoundland. In: Kokelaar, B.P., Howells, M. (Eds.), Volcanic and Associated Sedimentary and Tectonic Processes in Modern and Ancient Marginal Basins, Geol. Soc.

London. Spec. Publ. 16, pp. 271-277. doi: https://doi.org/10.1144/GSL.SP.1984.016.01.20

Lorenz, V., Zimanowski, B., Büttner, R., 2002. On the formation of deep-seated subterranean peperite-like magma–sediment mixtures. J. Volcanol. Geotherm Res., 114 (12). doi: 107–118. 10.1016/s0377-0273(01)00293-1.

Macdonald, G.A., 1939. An intrusive peperite at San Pedro Hill, California. Calif. Univ. Publ. Dept. Geol. Sci. Bull. 24, 329-338.

McLean, C.E., Brown, D.J., Rawcliffe, H.J., 2016. Extensive soft-sediment deformation and peperite formation at the base of a rhyolite lava: Owyhee Mountains, SW Idaho, USA.Bull Volcanol. 78, 42. doi: https://doi.org/10.1007/s00445-016-1035-2.

McPhie, J., Doyle, M.G., Allen, R.L., 1993. Volcanic Textures: A Guide to the Interpretation of Textures in Volcanic Rocks. Centre for Ore Deposit and Exploration Studies, University of Tasmania, Hobart (198 p.).

Michelin, C.R.L. 2014. Ágata do Distrito Mineiro de Salto do Jacuí (Rio Grande do Sul, Brasil) - uma caracterização com base em técnicas estratigráficas, petrográficas, geoquímicas e isotópicas. PhD Thesis, Programa de Pós-Graduação em Geociências, Instituto de Geociências, Universidade Federal do Rio Grande do Sul.

Milani, E.J., 1997. Evolução tectono-estratigráfica da Bacia do Paraná e seu relacionamento com a geodinâmica fanerozóica do Gondwana sul-ocidental. PhD Thesis, Programa de Pós-Graduação em Geociências, Instituto de Geociências, Universidade Federal do Rio Grande do Sul.

Milani, E.J., Faccini, U.F., Scherer, C.M., Araújo, L.M., Cupertino, J.A., 1998. Sequences and Stratigraphic Hierarchy of the Paraná Basin (Ordovician to Cretaceous), Southern Brazil. BoI. IG USP, Série Científica, 29, 125-173. doi: http://dx.doi.org/10.11606/issn.2316-8986.v29i0p125-173

Milani, E.J., Melo, J.H.G., Souza, P.A., Fernandes, L.A., França, A.B., 2007. Bacia do Paraná. Boletim de Geociências da Petrobras, 15(2): 265-287. doi: https://www.researchgate.net/publication/279547262_Parana_basin.

Nogueira, A. C. R., Rabelo, C. E. N., Góes, A. N., Cardoso, A. R., Bandeira, J., Rezende, G. L., dos Santos, R. F. S., Truckenbrodt, W., 2021. Evolution of Jurassic intertrap deposits in the Parnaíba Basin, northern Brazil: The last sediment-lava

interaction linked to the CAMP in West Gondwana, Palaeogeography, Palaeoclimatology, Palaeoecology. 572, 110370. doi: https://doi.org/10.1016/j.palaeo.2021.110370.

Petry, K., Jerram, D.A., Almeida, D.P.M., Zerfass, H., 2007. Volcanic-sedimentary features in the Serra Geral Fm., Paraná Basin, southern Brazil: Examples of dynamic lava-sediment interactions in an arid setting. J. Volcanol. Geotherm. Res., 159: 313–325. doi: https://doi.org/10.1016/j.jvolgeores.2006.06.017.

Rawcliffe, H. J., 2016. Lava-water-sediment interaction: processes, products and petroleum systems. PhD Thesis, School of Geographical and Earth Sciences, College of Science and Engineering, University of Glasgow.

Reis, G.S., Mizusaki, A.M.P., Roisenberg, A., Rubert, R.R., 2014. Formação Serra Geral (Cretáceo da Bacia do Paraná): um análogo para os reservatórios ígneo-básicos da margem continental brasileira. Pesquisas em Geociências, 41(2), 155-168. doi: https://doi.org/10.22456/1807-9806.78093.

Renne, P.R., Ernesto, M., Pacca, I.G., Coe, R.S., Glen, J.M.G., Prevot, M., Perrin, M., 1992. The Age of Parana Flood Volcanism, Rifting of Gondwanaland, and the Jurassic-Cretaceous Boundary. Science (80-.). 258, 975–979. doi:10.1126/science.258.5084.975

Rios, F.R., Mizusaki, A.M.P., Michelin, C.R.L., 2018. Feições de interação vulcano-sedimentares – exemplos na Bacia do Paraná (RS). UNESP, Geociências, 37(3), 483-495. doi: https://doi.org/10.5016/geociencias.v37i3.12172.

Rocha, B.C., Davies, J.H.F.L., Janasi, V.A., Schaltegger, U., Nardy, A.J.R., Greber, N.D., Lucchetti, A.C.F., Polo, L.A., 2020. Rapid eruption of silicic magmas from the Paraná magmatic province (Brazil) did not trigger the Valanginian event. Geology, 48(12): 1174-1178. doi: https://doi.org/10.1130/G47766.1

Rosa, C.J.P., McPhie, J., Relvas, J.M.R.S., 2016. Distinguishing peperite from other sediment-matrix igneous breccias: Lessons from the Iberian Pyrite Belt. J. Volcanol. Geotherm. Res. 315, 28–39. doi: https://doi.org/10.1016/j.jvolgeores.2016.02.007

Scherer, C.M.S. 2000. Eolian dunes of the Botucatu Formation (Cretaceous) in Southernmost Brazil: morphology and origin. Sedimentary Geology, 137: 63–84. doi: 10.1016/S0037-0738(00)00135-4

Scherer, C.M.S. 2002. Preservation of aeolian genetic units by lava flows in the Lower Cretaceous of the Paraná Basin, southern Brazil. Sedimentology, 49, 97-116. doi: 10.1046/j.1365-3091.2002.00434.x.

Scherer, C. M. D. S., Lavina, E. L. C., Reis, A. D. D., Horn, B. L. D., 2021. Estratigrafia da sucessão sedimentar mesozoica da Bacia do Paraná no Rio Grande do Sul. In: Jelinek, A. R., Sommer C. A. (Eds.), Contribuições à Geologia do Rio Grande do Sul e Santa Catarina, Compasso Lugar-Cultura, pp. 289-304. doi: https://rigeo.cprm.gov.br/handle/doc/22504.

Schwam, J., 1988. The structure and genesis of Weichselian to Early Holocene aeolian sand sheets in western Europe. Sedimentary Geology, 55(3/4),197-232. doi: https://doi.org/10.1016/0037-0738(88)90132-7.

Skilling, I.P., White, J.D.L., McPhie, J., 2002. Peperite: a review of magma–sediment mingling. J. Volcanol. Geotherm. Res. 114, 1–17. doi: https://doi.org/10.1016/S0377-0273(01)00278-5

Soares, P.C., 1975. Divisão estratigráfica no Mesozóico no Estado de São Paulo. Ver. Bras. Geoc., 5, 251-267.

Squire, R.J., McPhie, J., 2002. Characteristics and origin of peperite involving coarse-grained host sediment. In: Skilling, I.P., White, J.D.L., McPhie, J. (Eds.), Peperite: Processes and Products of Magma-Sediment Mingling. J. Volcanol. Geotherm. Res. 114, 45-61. doi: https://doi.org/10.1016/S0377-0273(01)00289-X.

Tucker, M. E., 2001. Sedimentary Petrology, Third Edition: Oxford, UK, Blackwell Science Ltd., 262 p.

Thiede, D.S., Vasconcelos, P.M., 2010. Paraná flood basalts: rapid extrusion hypothesis confirmed by new 40Ar/39Ar results. Geology, 38, 747-750. doi: https://doi.org/10.1130/G30919.1.

Waichel, B.L., Scherer, C.M.S., Frank, H.T., 2008. Basaltic lavas covering active Aeolian dunes in the Paraná Basin in Southern Brazil: features and emplacement aspects. J. Volcanol. Geotherm. Res. 169, 59–72. doi: https://doi.org/10.1016/j.jvolgeores.2007.11.004

Zalán, P.V., Wolff, S., Astolfi, M.A.M., Vieira, I.S., Conceição, J.C.J., Appi, V.T., Neto, E.V.S., Cerqueira, J.R., Marques, A., 1990. The Paraná Basin, Brazil. Tulsa: AAPG Memoir, 51: 681- 708.

Zimanowski, B., Büttner, R., 2002. Dynamic mingling of magma and liquefied sediments. In: Skilling, I.P., White, J.D.L., McPhie, J. (Eds.), Peperite: Processes and Products of Magma-Sediment Mingling. J. Volcanol. Geotherm. Res. 37-44. doi: https://doi.org/10.1016/S0377-0273(01)00281-5.

6.2 EVOLUTION OF THE UPPER JURASSIC AND LOWER CRETACEOUS VULCANO-SEDIMENTARY REGISTER - SOUTHEAST PORTION OF PARANÁ BASIN, BRAZIL

This is an automated message.

EVOLUTION OF THE UPPER JURASSIC AND LOWER CRETACEOUS VULCANO-SEDIMENTARY REGISTER - SOUTHEAST PORTION OF PARANÁ BASIN, BRAZIL

Dear MSc. Rios,

We have received the above referenced manuscript you submitted to Cretaceous Research. It has been assigned the following manuscript number: YCRES-D-23-00053.

To track the status of your manuscript, please log in as an author at https://www.editorialmanager.com/ycres/, and navigate to the "Submissions Being Processed" folder.

Thank you for submitting your work to this journal.

Kind regards,
Cretaceous Research

More information and support

You will find information relevant for you as an author on Elsevier's Author Hub: https://www.elsevier.com/authors

FAQ: How can I reset a forgotten password?
https://service.elsevier.com/app/answers/detail/a_id/28452/supporthub/publishing/
For further assistance, please visit our customer service site: https://service.elsevier.com/app/home/supporthub/publishing/
Here you can search for solutions on a range of topics, find answers to frequently asked questions, and learn more about Editorial Manager via interactive tutorials. You can also talk 24/7 to our customer support team by phone and 24/7 by live chat and email

EVOLUTION OF THE UPPER JURASSIC AND LOWER CRETACEOUS VULCANO-SEDIMENTARY REGISTER - SOUTHEAST PORTION OF PARANÁ BASIN, BRAZIL

Fernando Rodrigues RIOS[a*], Ana Maria Pimentel MIZUSAKI[a,b], Rualdo MENEGAT [b], Isaque Conceição RODRIGUES da Silva[a]

[a]UFRGS, Instituto de Geociências, Programa de Pós-Graduação em Geociências, Campus do Vale – Porto Alegre (RS). [b]Universidade Federal do Rio Grande do Sul, Instituto de Geociências, Departamento de Paleontologia e Estratigrafia - Caixa Postal 15.001, CEP 91509-900, Porto Alegre, RS, Brasil.

ABSTRACT The period between Upper Jurassic and Lower Cretaceous on the southern border of Paraná Basin was characterized by the accumulation of the aeolian system from Botucatu Formation which was entirely preserved by the volcanic flows of Serra Geral Formation. Intense basic and acid magmatism to a lesser extent, covered an extensive aeolian continental environment. However, data from 29 outcrops, 13 vertical stratigraphic profiles and 334 paleocurrent measurements, in the central region of Rio Grande do Sul state, the current southeast limit of the Paraná Basin's border, exposed fluvial-eolian deposits of Guará Formation in contact with volcanic rocks of Serra Geral Formation. This work considers a new temporal and spatial relationships understanding between the fluvio-aeolic, aeolian and volcanic systems that developed in this temporal range. For this purpose, facies analysis and architectural elements were used to reconstruct the evolution of this volcanic-sedimentary register. It is evident that Guará, Botucatu and Serra Geral Formations are composed of twenty-one facies grouped into five facies associations (braided fluvial channel, ephemeral braided fluvial channel, aeolian sand sheets, aeolian dunes, and volcanic plain) according to their architectural elements. The contacts between the deposits of Guará and Botucatu Formations and their contacts between Serra Geral Formation flows demonstrate that these sedimentary environments remained active during the volcanism onset, and there was no hiatus between these units. Therefore, Guará and Botucatu Formations present ages between Upper Jurassic and Lower Cretaceous.

Keywords: Botucatu Formation; Serra Geral Formation; Guará Formation; Fluvio-eolian systems; aeolian systems.

1. INTRODUCTION

For a long time, the Jurassic-Cretaceous period of Paraná Basin was subdivided into three units: fluvial-eolian basal unit (Guará Formation); classic wind intermediate unit (Botucatu Formation); and an entire volcanic top unit (Serra Geral Formation) (Milani, 1997; Milani et al., 1998; Scherer, 2002; Scherer and Lavina, 2005, 2006; Reis, 2016, 2020; Amarante et al., 2019; Reis et al. al., 2019). Recently, literature has demonstrated the intercalation of sandstones on the bottom of Serra Geral Formation, which were commonly considered of minor expression and called intertraps (Waichel et al., 2008; Michelin, 2014; Reis et al., 2014; Rios et al., 2018). Because of this, these

researches indicated Botucatu Formation as continuous with Serra Geral Formation, positioning Guará Formation as a separate unit and prior to the other two ones.

The work herein aims to investigate the possibilities of these three systems being contemporary based on a detailed study of their faciological evolutions and the contact surfaces that constraint them. The main hypothesis is that these systems can be contemporary and regionally dispersed in a sectoral way, showing different predominance among the units (Zerfass et al., 2007). The synchronism of the three systems concluded when the volcanic flows of Serra Geral Formation covered all the sedimentary systems.

2. GEOLOGICAL SETTING

Paraná Basin is a paleozoic basin in South American Platform (Fig. 1A) and its depositional history occurred in pulses separated by erosive and non-depositional phases, recorded by successive processes of subsidence, uplift, sedimentation and magmatism (Zalán et al., 1990; Milani, 1997; Milani et al., 1998, 2007). Each of the six volcano-sedimentary successions corresponds to a Supersequence, composing a stratigraphic record that developed from Ordovician to Cretaceous, defined according to Milani (1997), from the bottom to the top as: Rio Ivaí, Paraná, Gondwana I, Gondwana II, Gondwana III and Bauru. The volcano-sedimentary successions comprise the Gondwana III Supersequence, Upper Jurassic to Lower Cretaceous, which is the focus of the work and include Botucatu and Serra Geral Formations.

Botucatu Formation has been characterized in literature as being composed of aeolian dunes residual deposits formed by medium subarkose sandstones, with high compositional and textural maturity, and large cross-stratifications. It is limited on the bottom by a regional unconformity that extends throughout the basin and it is covered by volcanic rocks of Serra Geral (Milani Formation 1997; Milani et al., 1998). On its bottom there are records of conglomerates and conglomeratic sandstones, related to ephemeral channels (Almeida 1954; Bigarella and Salamuni, 1961, 1967, Soares, 1975; Bigarella, 1979; Almeida and Melo, 1981; Scherer, 2000). The Botucatu Formation Lower Cretaceous age includes traces of invertebrates, vertebrates and silicified conifers (Brito, 1979; Suguio and Coimbra, 1972; Fernandes et al., 1990, 2004; Leonardi and Oliveira, 1990; Fernandes and Carvalho, 2008; Pires et al., 2011).

The Botucatu Formation sediments are covered by the lava flows of Serra Geral Formation. Nevertheless, the aeolian sedimentary environment remained active during the volcanism onset and these contact relationships show a relative age for its onset and also for the end of sedimentation (Milani et al., 1998; Scherer, 2002). Serra Geral Formation represents an intense magmatism up to 1,700 m thick, predominantly basic and, secondarily, acidic of approximately 134 Ma (Lower Cretaceous) (Renne et al., 1992; Thiede and Vasconcellos, 2010; Janasi et al., 2011; Baksi, 2018; Rocha et al., 2020).

However, it was observed during fieldwork a sedimentary unit with distinct characteristics from Botucatu Formation and which also appears among the volcanic flows of Serra Geral Formation. This unit has similar lithological and faciological characteristics to those of Guará Formation and it was recognized in the studied area (Zerfass et al., 2007; Godoy et al., 2011, 2016, 2018).

Guará Formation, in Paraná Basin (Scherer and Lavina, 2005, 2006; Zerfass et al., 2007; Godoy et al., 2011, 2016, 2018; Reis, 2016, 2020; Reis et al., 2019), and Batoví Member, lower portion of Tacuarembó Formation, in Uruguay (Perea et al., 2009; Amarante et al., 2019) hold a fossiliferous association that indicates a relative age of Late Jurassic (Perea et al., 2009; Soto and Perea, 2010; Francischini et al., 2015). In the west of Rio Grande do Sul state, a lateral distribution of facies associations of Guará Formation was defined as perennial braided fluvial channels and ephemeral braided fluvial channels. In northern portion of the state, weakly formed fluvial channels that intertwine with deposits of aeolian dunes and, in the southern portion of the state, with aeolian sand sheets (Sherer and Lavina, 2005, 2006). The fluvial deposits show a paleocurrent pattern to SSW, while the aeolian dunes show paleocurrent to NE (Scherer and Lavina, 2005). This unit is limited at the bottom and top by nonconformities with Sanga do Cabral and Botucatu Formations, respectively (Scherer and Lavina, 1997; Scherer et al., 2000).

Nonetheless, field data from central region of Rio Grande do Sul state (Fig. 1B and C), southeastern limit of Paraná Basin's current border, showed that this unit is limited at the bottom by an unconformity with Caturrita Formation (Upper Triassic) and its top is in contact with the volcanic rocks of Serra Geral Formation, as well as fluvial deposits between lava flows. Therefore, the age on the top of this unit, in the study area, was considered Lower Cretaceous (Zerfass et al., 2007) (Fig. 2). Caturrita Formation is represented by a set of lenticular, tabular and sigmoidal layers from fine to conglomerate

sandstones that occur interspersed with pelites. These deposits are related to a fluvio-deltaic environment (Andreis et al., 1980; Zerfass et al., 2007; Godoy et al., 2018).

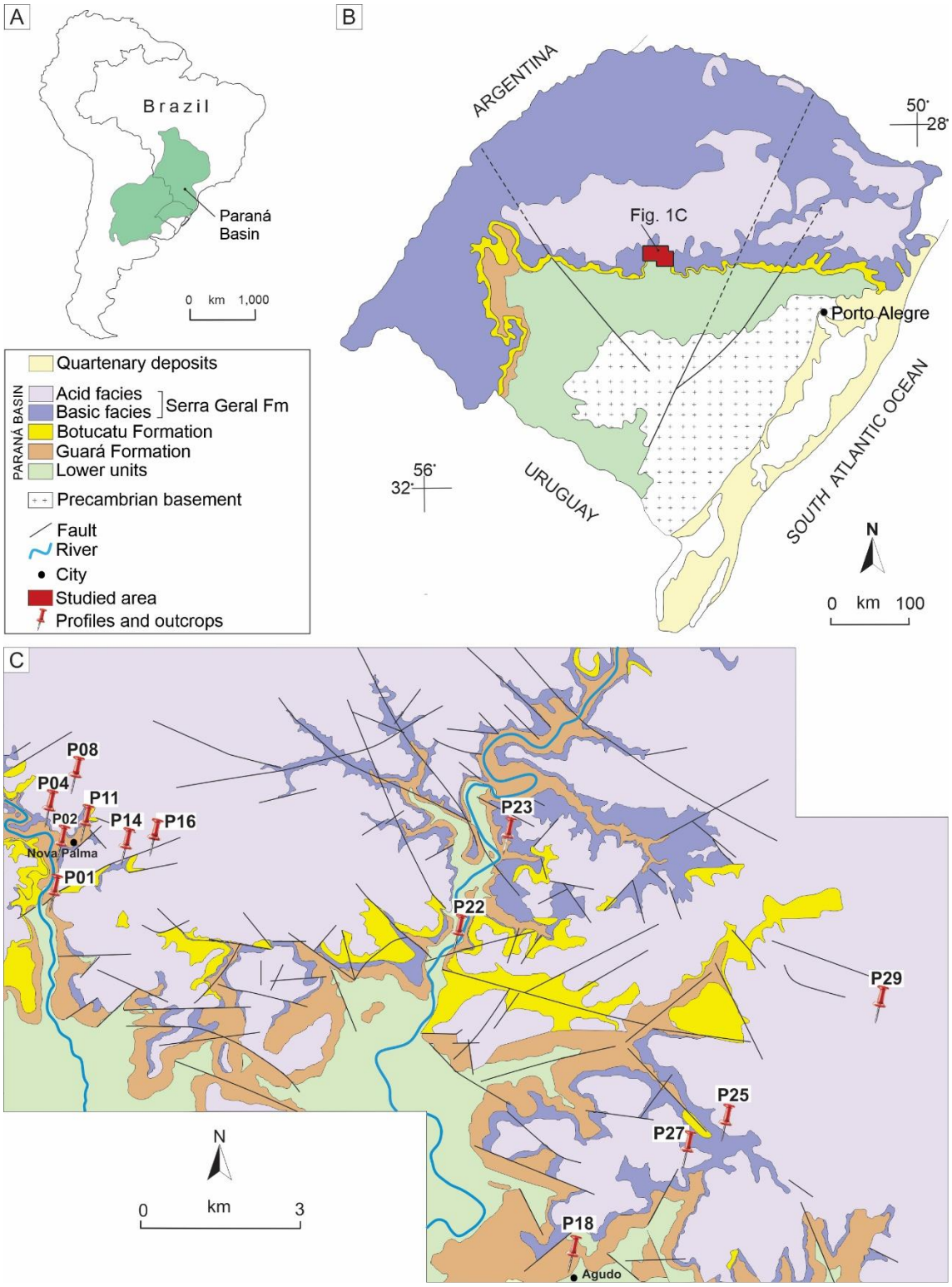

Figure 1: A) Paraná Basin in South American Platform. B) Study area on the current border of Paraná Basin, Rio Grande do Sul state (modified from Scherer, 2002; Janasi et

al., 2011; Reis, 2016; Rios et al., 2018). C) Studied points location in Upper Jurassic - Lower Cretaceous (modified from Zerfass et al., 2007; Godoy et al., 2011).

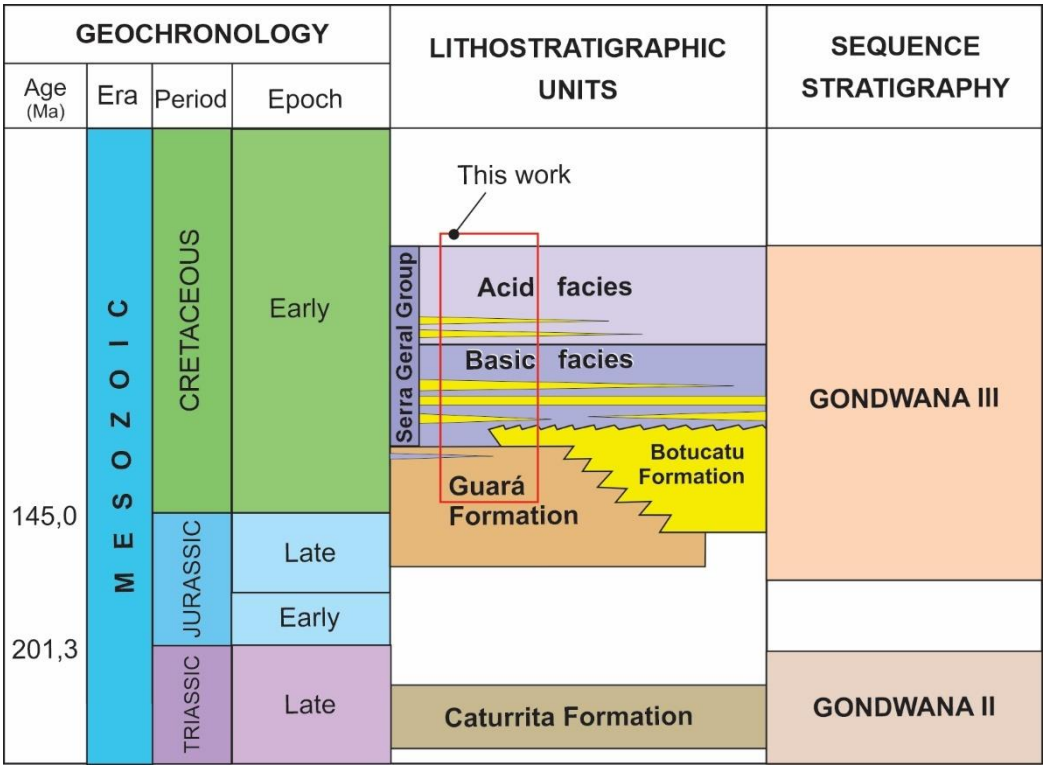

Figure 2: Lithostratigraphic chart studied area (modified from Zerfass et al., 2007).

3. MATERIALS AND METHODS

The investigation of an area with Upper Jurassic-Lower Cretaceous age was carried out by literature research, analysis of aerial, satellite images and topographic maps of the current border of Paraná Basin, Rio Grande do Sul state.

During the sampling, twenty-nine outcrops were examined and thirteen columnar stratigraphic profiles (Figs. 3 and 4) were surveyed at 1:50 scale using facies analysis techniques, identification of lithostratigraphic units, contact relationships, geometries and features of volcano-sedimentary deposits. The twenty-nine outcrops analyzed appear throughout escarpments, roads, rivers and quarries of the region (Fig. 1C). The outcropping units were described in detail and 334 paleocurrent measurements were taken from medium to large structures of facies interpreted as fluvial-aeolic and aeolian systems. Vertical analysis of stratigraphic units was based on the topographic position of columnar profiles distant from each other by hundreds of meters to few kilometers (Figs. 3 and 4). Due to the large number of faults, discontinuous outcrops and vegetation

covering in the region, it was difficult to establish a precise lateral correlation between the analyzed columnar profiles.

The facies analysis techniques considered the assumptions and methods proposed by Walker and James (1992), Brookfield and Silvestro, (2010) through the individualization and description of facies through distinctive attributes such as composition, geometry, textures, sedimentary structures and paleocurrents measurements. The facies follow the patterns proposed by Miall (1996). The first capital letter refers to the grain size and the second lowercase letter to the sediment structure. The letter (a) was added to indicate wind processes. The same logic was used for volcanic rocks, where the first capital letter represents the lithological composition, and the second lowercase letter, indicate the main volcanic structure observed.

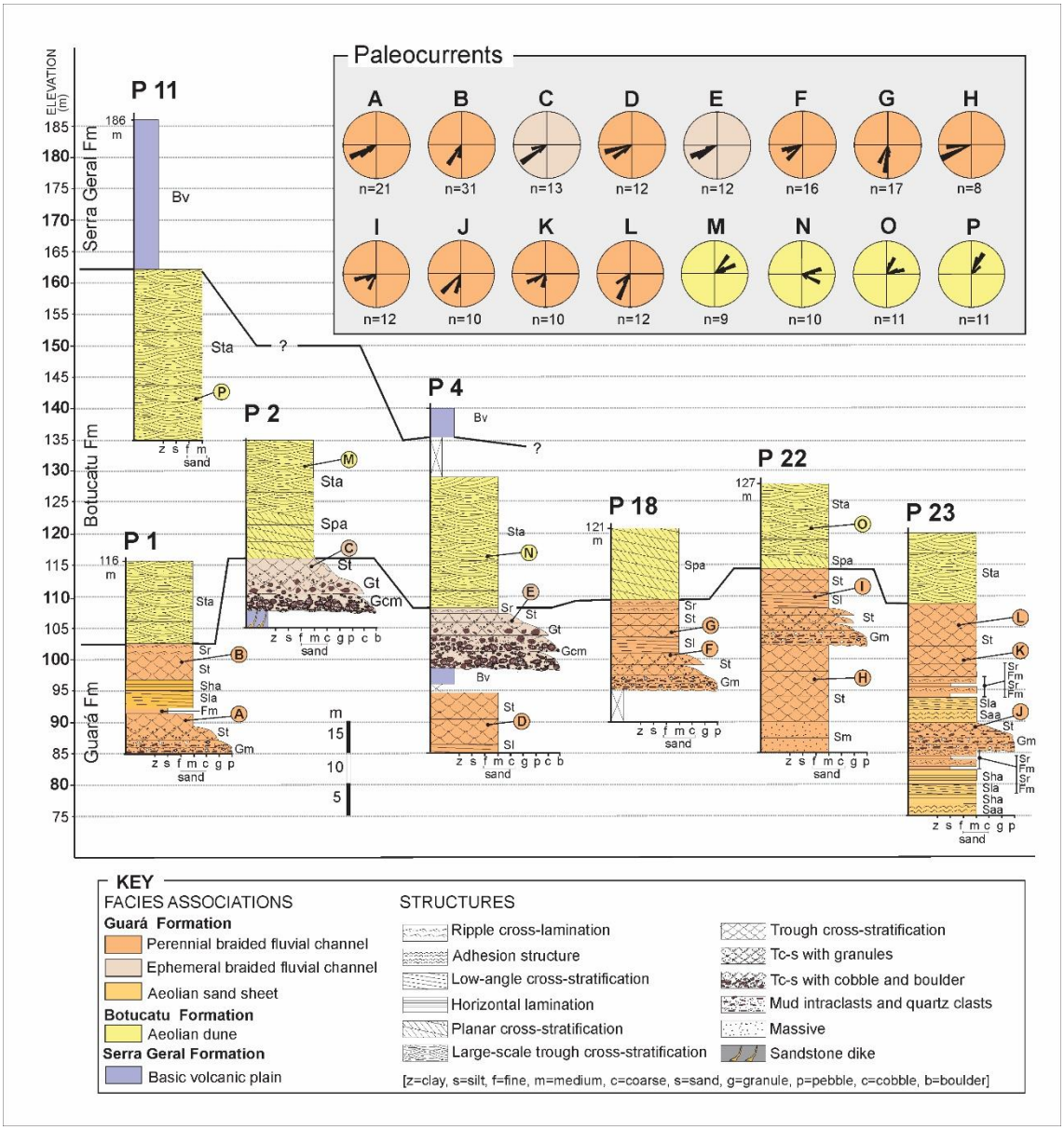

Figure 3: Columnar stratigraphic profiles of Guará, Botucatu and Serra Geral Formations and respective facies, facies associations and paleocurrent measurements. See Fig. 1 for the location of profiles and Tab. 1 for the facies code.

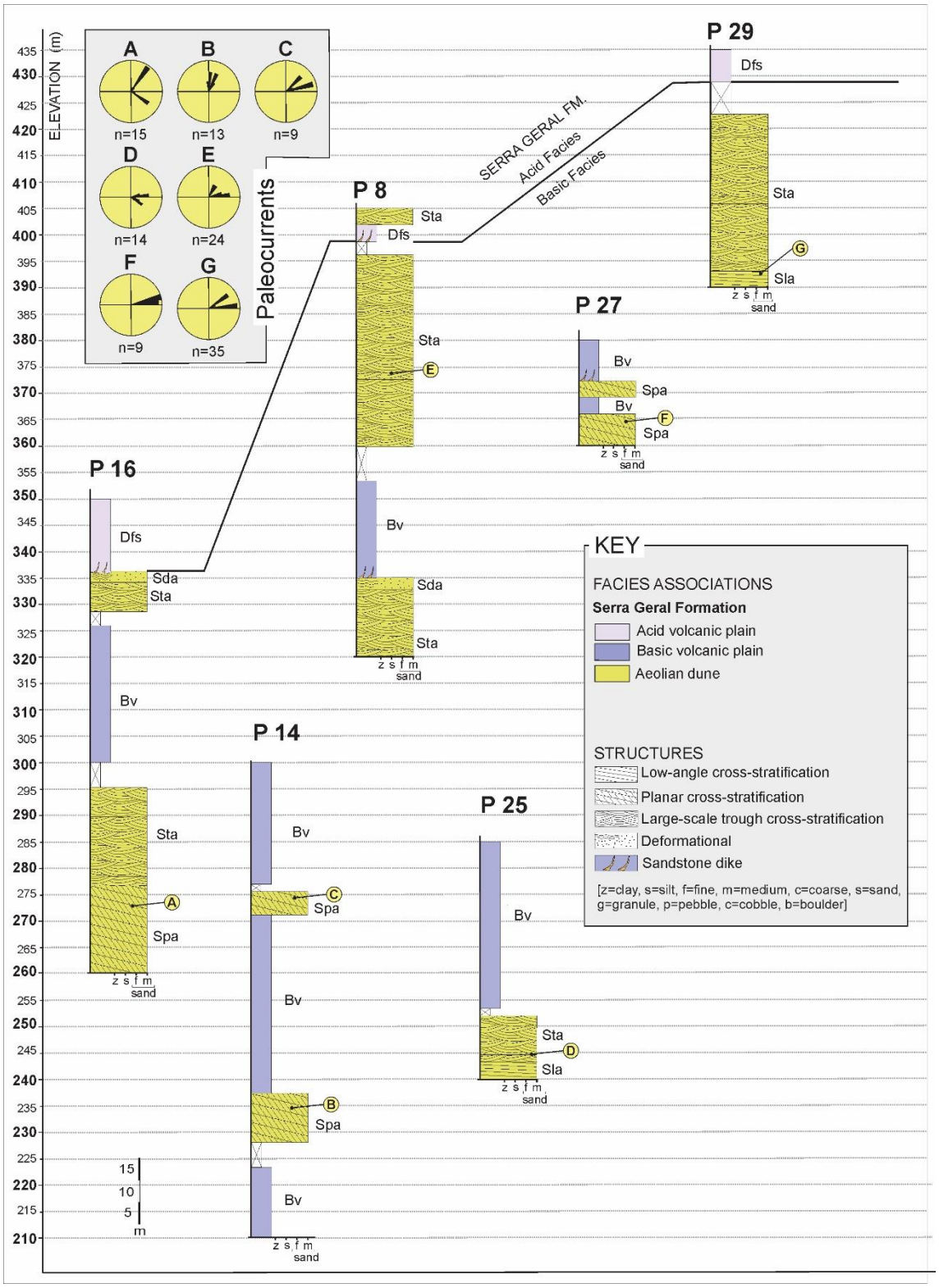

Figure 4: Columnar stratigraphic profiles of Serra Geral Formation and the respective facies, facies associations, and paleocurrent measurements. See Fig. 1 for location of profiles and Tab. 1 for the facies code.

4. RESULTS AND DISCUSSIONS

4.1 Facies and facies associations

In the Upper Jurassic and Lower Cretaceous volcano-sedimentary succession of Paraná Basin twenty-one facies were identified and grouped into five facies association with their respective architectural elements, as shown in Table 1. The facies association represent groups of facies from depositional processes derived from perennial and ephemeral braided river systems, dune fields aeolian system, sand sheets, and, finally, volcanic plains.

The braided fluvial facies association (BFFA) reunite facies of three architectural elements of: a) channel (CH), constituted by amalgamated lenticular register of sand-conglomeratic facies with normal gradation and trough cross-stratification deposited by traction processes and forms of bedding 3D; b) downstream accretion (DA) comprises rocks of medium sandy facies, with low-angle cross-stratification that migrates to trough cross-stratification and climbing ripple on the top, with paleocurrents coinciding with the fluvial flow; c) foodplain fines (FF) consisting of tabular geometries, massive pelites and medium sandstones with climbing ripples.

The association of ephemeral braided fluvial facies (EBFFA) is essentially formed by architectural elements of proximal and medium channel constituted by massive conglomeratic facies and stratified at the bottom that grades to sandy-conglomeratic and sandy with trough cross-stratification and medium sand with climbing cross-stratification.

The aeolian dune facies association (ADFA) are well selected medium sandstones, with large trough cross-stratification that record migration and subcritical climbing. The aeolian sand sheet facies association (ASSFA) comprises tabular medium sandstones with horizontal lamination and adhesion structures. Finally, volcanic plain facies association (VPFA) comprises vesicular basalt facies (Bv) with tabular and columnar disjunctions, and dacites with flow structures and vesicular levels (Dfs) filling valleys of the aeolian paleotopography.

An ideal composite columnar profile with a thickness of 360 m correlated to 13 profiles surveyed in the area, reunite facies succession, facies association, depositional cycles of the depositional systems, as well as the lithostratigraphic units (Fig. 5).

FACIES ASSOCIATION	FACIES CODE	FACIES DESCRIPTION	ARCHITECTURAL ELEMENT	GEOMETRY/ INTERNAL RELATIONSHIP	INTERPRETATION
Perennial braided Fluvial Channel	Fm	Massive pelite, reddish brown.	Foodplain fines Channel and Downstream accretion	Amalgamated bodies, with a thickness of 0.3 to 1.5 m, moderate lateral continuity, erosive or concave base and flat or concave top, erosive surfaces at the bottom or disconformity in contact with Caturrita Formation.	Middle to proximal longitudinal bars with reworking of fluvio-eolian deposits
	Sr	Medium-grained sandstone, moderately selected, with ripple lamination.			
	Sl	Medium-grained sandstone, moderately selected, with low-angle cross-stratification.			
	St	Gravelly medium to very coarse-grained sandstone, poorly- to moderately-sorted, with trough cross-stratification.			
	Sm	Medium-grained sandstone, moderately sorted, massive.			
	Gm	Massive sandy conglomerate with muddy intraclasts and pebble-sized quartz clasts.			
Ephemeral Braided Fluvial Channel	Sr	Medium-grained sandstone, moderately- to well- sorted, with ripple lamination.	Channel	Amalgamated bodies, limited by concave erosive surfaces, 0,5 to 3 m thick, moderate lateral continuity (< 30 m).	Reworking of the volcanic plain, hyperpycnal unidirectional flow associated with flashflood
	St	Medium to very coarse-grained gravelly sandstone, poorly- to moderately-sorted, with trough cross-stratification.			
	Gt	Conglomerate with trough cross-stratification, intraclasts with zeolite-filled vesicles, with granular to cobble sized intraclasts			
	Gcm	Massive conglomerate, intraclasts with zeolite-filled vesicles, intraclasts size from pebbles to boulders			
Aeolian Sand Sheet	Sha	Medium-grained sandstone, well sorted, with horizontal lamination.	Laminated sand sheets.	Restricted lateral extension, packages of tabular geometry, thickness of 0,5 to 1 m, top and base flat.	Arid and wet plain with low availability of sediment.
	Sla	Medium-grained sandstone, well sorted, with low-angle cross-stratification, foresets with inverse grading.			
	Saa	Medium-grained sandstone, well sorted, with adhesion structure.			
Aeolian Dune	Sta	Medium-grained sandstone, well sorted, with medium scale trough cross-stratification, foresets with inverse grading.		Packages with wide lateral continuity (and restricted in intertrap), flat-concordant top and flat-concave basis, reactivation surfaces, thickness of 3 to 30 m.	Erg
	Spa	Medium-grained sandstone, well sorted, with planar cross-stratification, foresets with inverse grading.			
	Sla	Medium-grained sandstone, well sorted, with low-angle cross-stratification, foresets with inverse grading.			
	Sda	Medium-grained sandstone, moderately selected, with deformed undefined stratification.			
Volcanic Plain	Bv	Vesicular basalt with tabular and columnar disjunction with sandstone dikes.		Tabular to subhorizontal volcanic flow, flow structures (dacite), 3 to 25 m thick. Lavas fill paleo topography valleys.	Advance of volcanic flows over active fluvio-aeolian and aeolian systems.
	Dfs	Dacite with flow structures, vesicular levels, tabular disjunction, sandstone dikes.			

Table 1: Facies, facies association, architectural elements, respective geometries and interpretation.

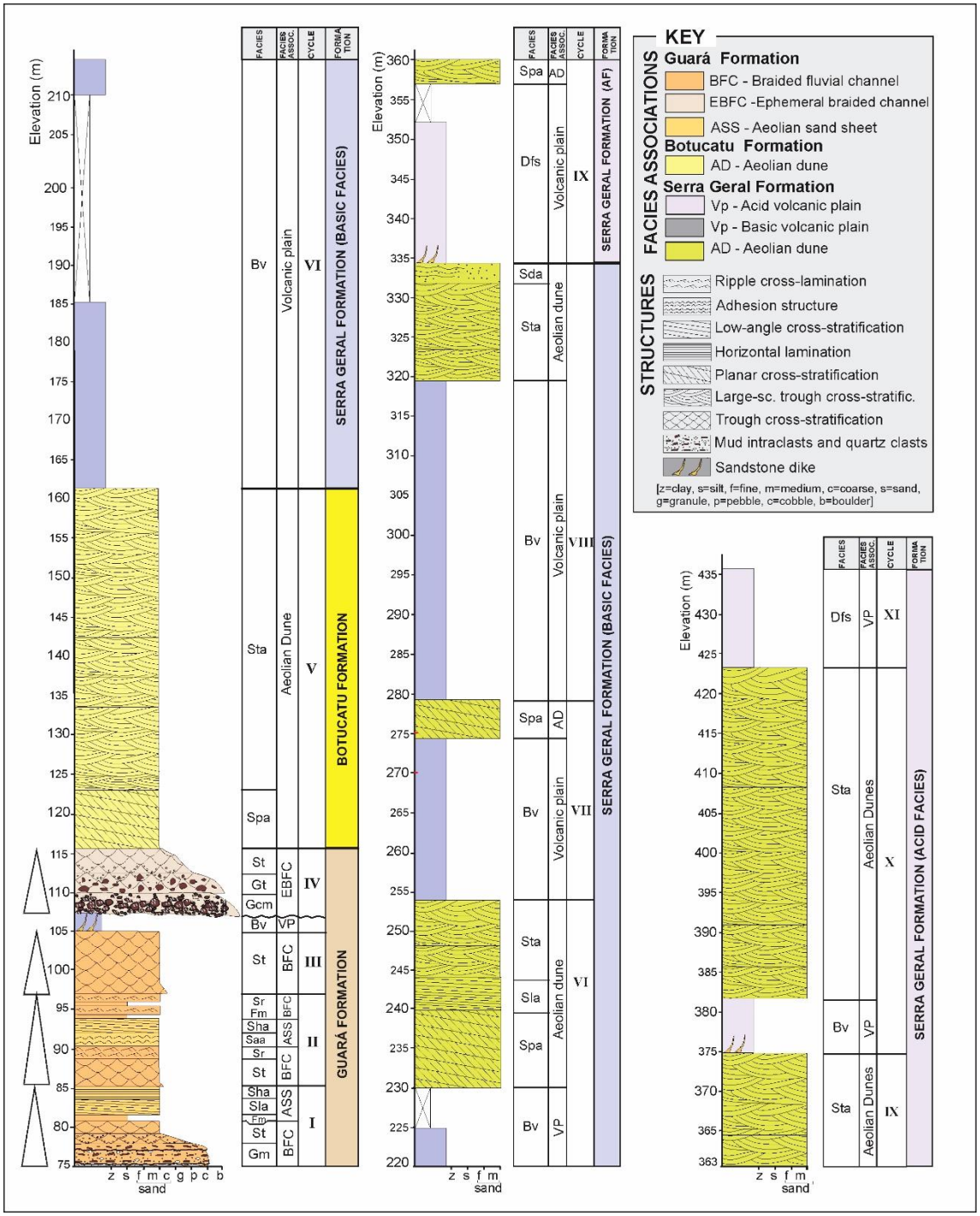

Figure 5: Ideal composite columnar section and respective facies, facies association and depositional cycles of the lithostratigraphic units of Upper Jurassic - Lower Cretaceous period, in the study area.

4.2 Cycles (depositional successions), facies associations and interpretations of the Guará Formation

Guará Formation (40 m thick) is bordered on the bottom by Caturrita Formation, through an unconformity, and on the top by Botucatu Formation, through an abrupt and flat surface, and comprises four cycles of facies association. The three bottom cycles, of up to 30 m in thickness, intercalate PBFFA and ASSFA and are superimposed by a thin 3.0 m flow of VPFA followed by an intermediate cycle of 7 m in thickness from EBFFA. (Table 1; Figs. 3 and 5).

Bottom cycles I, II and III, identified by fining upward sequences that culminate in humid aeolian sandstone successions, are distinct. In turn, cycle I starts with conglomeratic facies (Gm) whose lower limit occurs through erosive surfaces that concentrate levels of intraclasts and quartz clasts. Cycles II and III start with sandstone facies (St). The ASS facies occur only in cycles I and II. In the first, as an alternation of Sla and Sha, and in the second, as Saa and Sha. Cycle II also shows the occurrence of fine facies (Sr) both under and superimposed on wet aeolian facies. (Fig. 6B).

The bottom portions of these cycles represent underwater 3D dunes characterized by channel architectural elements (CH) and downstream accretion (DA) and flood plain fine (FF) typical of perennial river channel associations (Miall, 1996; Allen et al., 2013). Downstream accretion elements (DA), represented by sets of simple cross-stratification or compound cross-stratification bounded by surfaces inclined downstream (Miall, 1988) (Fig. 6D). The common presence of middle channel bars with bedding migrating along their dorsum and front face, and the absence of lateral accretion elements suggest a river system with bed load and low sinuosity (Schumm, 1972; Bristow, 1987; Miall, 1996). The small number of fine deposits (Fm), (only in profiles 1 and 23; Figs. 3 and 6C) associated with the fine foodplain (FF), together with the mud intraclasts found above the erosive surfaces (Gm), demonstrate that the channel eroded margin deposits. This suggests that this is a fluvial perennial braided system with variable discharge, with a SW paleocurrent pattern (Fig. 3) and in a situation of low rate of accommodation space and high rate of degradation.

Tabular successions of aeolian sand sheets (ASSFA) represent areas covered by aeolian sands where there are no developed dunes (Fryberger et al, 1979; Kocurek and Nielson, 1986). They exhibit medium-grained sandstones with low-angle cross-lamination (Sla), horizontal (Sha) and adhesion structures (Saa), representing facies

characteristic of aeolian deposits (Kocurek and Nielson, 1986; Scherer and Lavina, 2005) (Figs 6D, E and F). The deposits are well selected and formed by inverse grading lamination (Fig. 6E). The wind ripple lamination from low angle (Sla) to horizontal (Sha) was formed due to the unavailability of dry sand for the aeolian dunes development. Adhesion structures were generated by the adhesion of sand grains to a wet surface, indicating a hydrated substrate (Kocurek and Fielder, 1982). It is possible to observe a vertical change of adhesion structures to dry aeolian features, indicating a probable change in depositional surface characteristics associated with variation in the position of the water table (Chakraborty and Chaudhuri, 1993) (Profile 23, Figs. 3 and 5). As these aeolian deposits occur associated and interspersed with perennial fluvial deposits (Profiles 1 and 23, Fig. 3 and 5), the interference of fluvial system in the aeolian system seems to be a control mechanism for the dry sand supply (Kocurek and Nielson, 1986). Consequently, the incorporation of this wind record in a saturated zone (Kocurek and Havholm, 1993) indicates a situation of increased rate of accommodation space and decreased degradation. However, the occurrence of humid aeolian deposits in a fluvial system indicates a possible establishment of more arid conditions regionally.

The thin flow combined between cycles III and IV consists of vesicular basalt with sandstone dikes at the bottom and distinguish the first occurrence of lava in this area. Above cycle IV a fining upward succession of EBFA (Table 1; Figs. 3 and 5). On the bottom, marked by an erosion surface (Fig 7A and B), there are conglomeratic facies from boulders to pebbles exclusively volcanic, massive and stratified (Gcm, Gt) that grade to sandy facies (St, Sr) limited by erosive or concave surfaces. They indicate deposition by tractive bed loads with unidirectional paleocurrents. The extensive erosion surface (< 30 m) over the volcanic plain (Profiles 2 and 4; Fig. 3 and 5) indicates a wide channel while the recurrence of erosion surfaces evidences a by-pass zone (Fig 7C). Conglomerates with cross-stratification (Gt) specify small channels filling (Miall, 1996) (Fig. 7D). The presence of medium to very coarse-grained gravel sandstones (St), also made up of volcanic fragments, and a posterior medium-grained sandstones (Sr), reveal that there was significant segregation of conglomerate load (Miall, 1996) (Fig. 7E). The EBFA is interpreted as an ephemeral fluvial system record of high energy and low sinuosity with multiepisodic deposition of the channel bed and paleocurrent pattern to SW (Fig. 3). They are deposited in a situation of low rate of accommodation space and high rate of degradation, typical of the bypass zone.

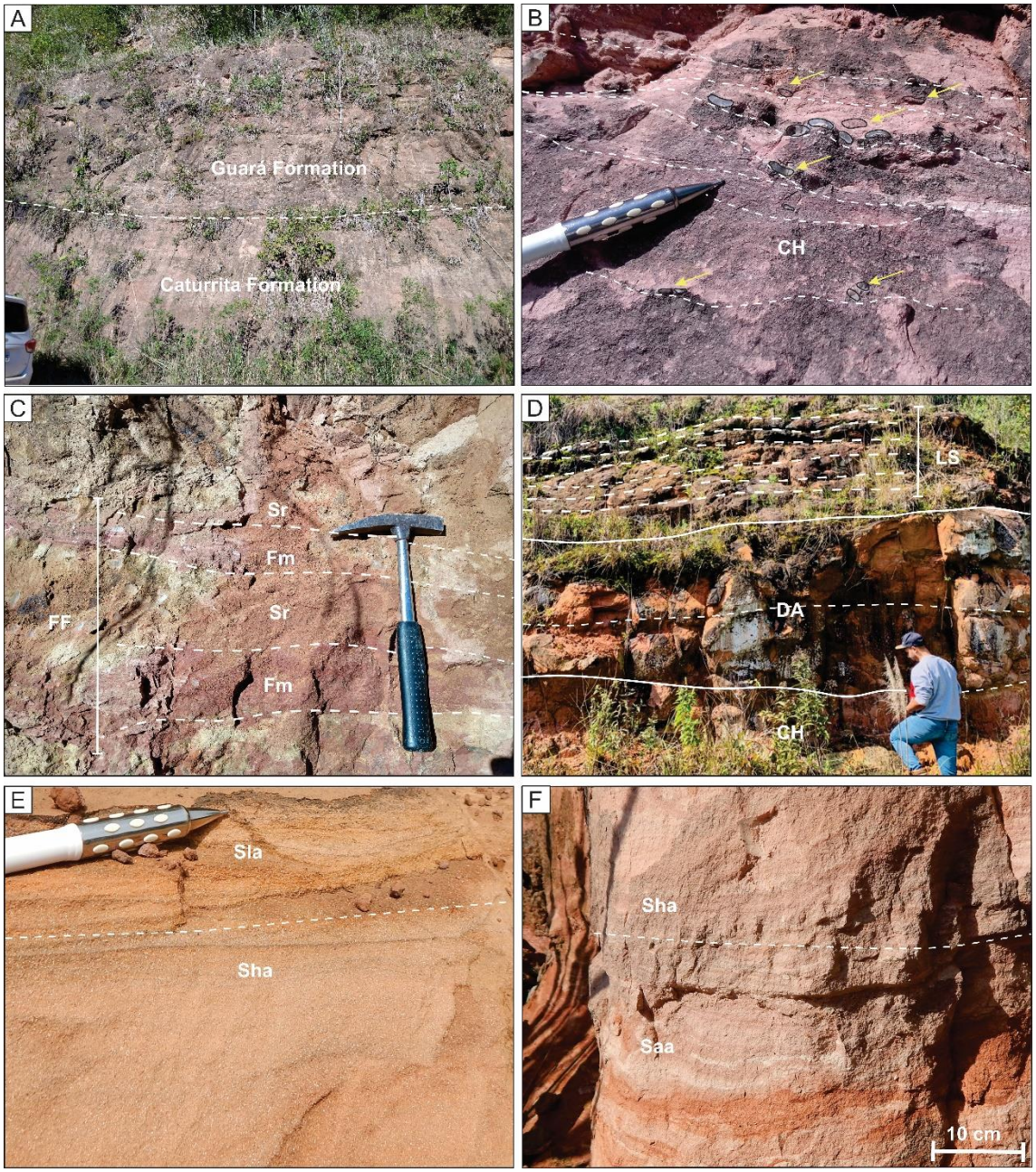

Figure 6: Facies and facies associations of the bottom portion of the composite columnar profile (Fig.5). A) Unconformity surface between the Caturrita and Guará formations. B) Detail of the facies of massive conglomerates deposited on erosive surfaces at channel bed. C) Massive pelites interspersed with fines foodplain (FF) ripples. D) Architectural elements of channel (CH) and downstream accretion (DA), at the bottom, and aeolian sand sheet facies association (ASSFA), at the top. E) Detail of slightly horizontal (Sha) and low angle (Sla) aeolian cross laminations. F) Aeolian facies laminations with adhesion structures (Saa) and horizontal stratification (Sha).

4.3 Facies and facies associations of Botucatu Formation

Botucatu Formation (50 m thick) borders Guará Formation at the bottom through an abrupt and flat contact. Aeolian facies associations cover the sedimentary successions

of cycles III (Profiles 1, 18, 22 and 23) and IV (Profiles 2 and 4) indicating increased aridity in the basin (Fig. 3). The tabular aeolian dune register is composed of well selected medium-grained sandstones, organized in sets of large wind ripples with cross-stratification (Hunter, 1977; Kocurek, 1981, 1991) (Fig. 7F). The deposits are formed by tractive depositional processes of wind ripples (Sta and Spa) where truncation surfaces are common, separating sets of cross laminations (Kocurek, 1981) with paleocurrents with a predominant NE pattern.

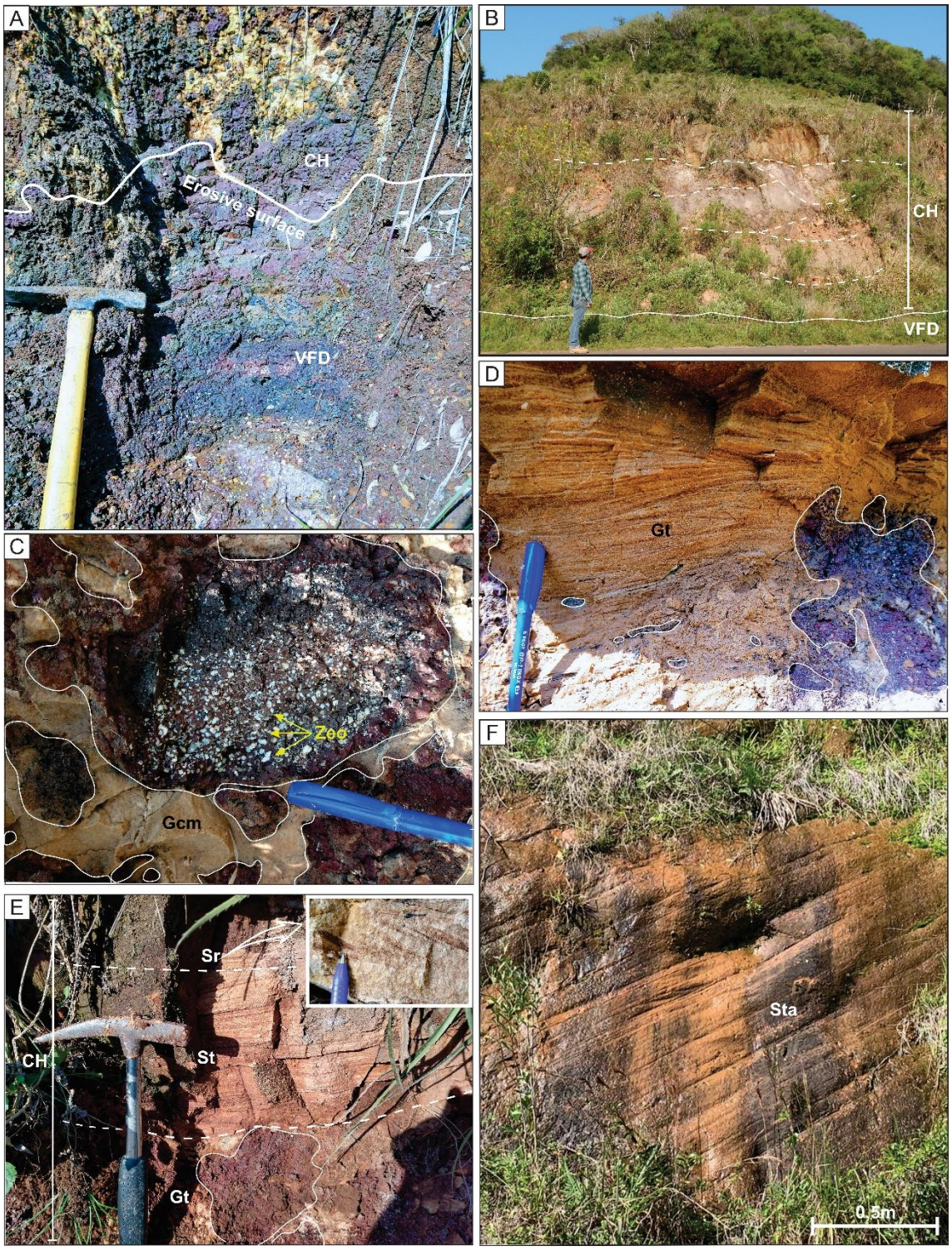

Figure 7: Facies and facies association of the medium portion of the columnar profile (Fig.5). A) Erosive surface over volcanic flood deposits (VFD) with massive conglomerates (Gcm) at the channel bottom (CH). B) Architectural elements of volcanic flood deposits (VFD) and amalgamated channel complex (CH). C) Massive conglomerate (Gcm) and intraclasts as vesicles filled with zeolite (Zeo). D) Conglomerate with trough cross-stratification (Gt). E) Stratified conglomerate (Gt) grading upwards to sandstone with trough cross-stratification (St) and ripples (Sr). F) Aeolian sandstone with large cross-stratification (Sta).

4.4 Volcano-sedimentary cycles of Serra Geral Formation

Overlying the sedimentary rocks of Botucatu Formation, there are five cycles (265 m thick) related to Serra Geral Formation. The three bottom cycles, identified here as cycles VI, VII and VIII, with a total thickness of 174 m, comprehend a vesicular basalt facies (Bv) as tabular flows superimposed by succession of the association of aeolian dune facies (ADFA) (Figs. 3, 5 and 7A). The two top cycles, recognized as cycles IX and X, with a total thickness of 91 m, are constituted by flows of the vesicular dacite facies with flow structure (Dfs) followed by aeolian sandstones of the ADFA.

At the bottom of cycle VI, 67m thick of flows over sandstones of Botucatu Formation through a wavy surface (duniform) that partially preserved the geometry of the aeolian deposition bed. At the top of the cycle, there is a 25 m thick ADFA sandstone register. This same recurrence is maintained in cycles VII and VIII. Finally, the two top cycles (IX and X), whose volcanic terms are acidic, repeat the structure succession of volcanic-eolian rocks of the basic cycles.

Both vesicular basalt facies (Bv) and vesicular dacite with flow structure (Dfs) were considered constituents of the volcanic plain facies association (VPFA). Magmatism occurred simultaneously with the deposition of aeolian dune fields and, as the basalt (Bv) and, later, dacite flows (Dfs) of the association of volcanic plain facies advanced, they preserved the paleotopography of the erg (Waichel et al., 2008; Rios et al., 2018; Jerram et al., 2000) (Figs. 4, 5, 8A and B).

The ADFA overlies the volcanic plain association and it is made up of well-rounded and spherical medium sandstones, with high textural and mineralogical maturity, arranged in sets of large trough cross-stratification (Sta), with grain flow structures with inverse grading, indicating aeolian dune deposits (Hunter, 1977; Kocurek, 1981, 1991, 1996). Moreover, there are medium sandstones, with low-angle planar cross-stratification and horizontal lamination (Sla and Spa) (Figs. 4, 5, 8C and D). The horizontal and low-angle stratification characterize bottom deposits of aeolian dunes (Kocurek and Nielson, 1986) (Figs 4, 5 and 8 D). The unidirectional dip of the large cross-stratification, with a consistent paleocurrent pattern of NE, indicates aeolian crescent dunes with sinuous crests (Fig. 8C). Parallel cross-stratification, on the other hand, designates transverse dunes with straight crests (Brookfield and Silvestro, 2010; Reis et al., 2019).

The occurrence of deformed and undefined sedimentary structures (Sda) in the adjacent contacts with volcanic flows (Bv and Dfs) indicates the important role of

fluidization in terms of destruction, deformation of original sedimentary structures and formation of clastic dykes (McPhie, 1993; Dadd and Van Wagoner, 2002; Skilling et al., 2002). Deformation may also be associated with the difference in density between the overlying lava and the underlying unconsolidated sediment, so that the sediments deform along with its sedimentary structures (Waichel et al., 2008) (Fig. Figs. 4, 5, 8A and B). The contemporaneousness of aeolian sedimentation with volcanism (basic and acid), evidenced in the sandstones between flows of about 265 m thick, indicates that the arid conditions prevailed since Botucatu Formation continued and the quiescence of lava flow controlled the wind activity.

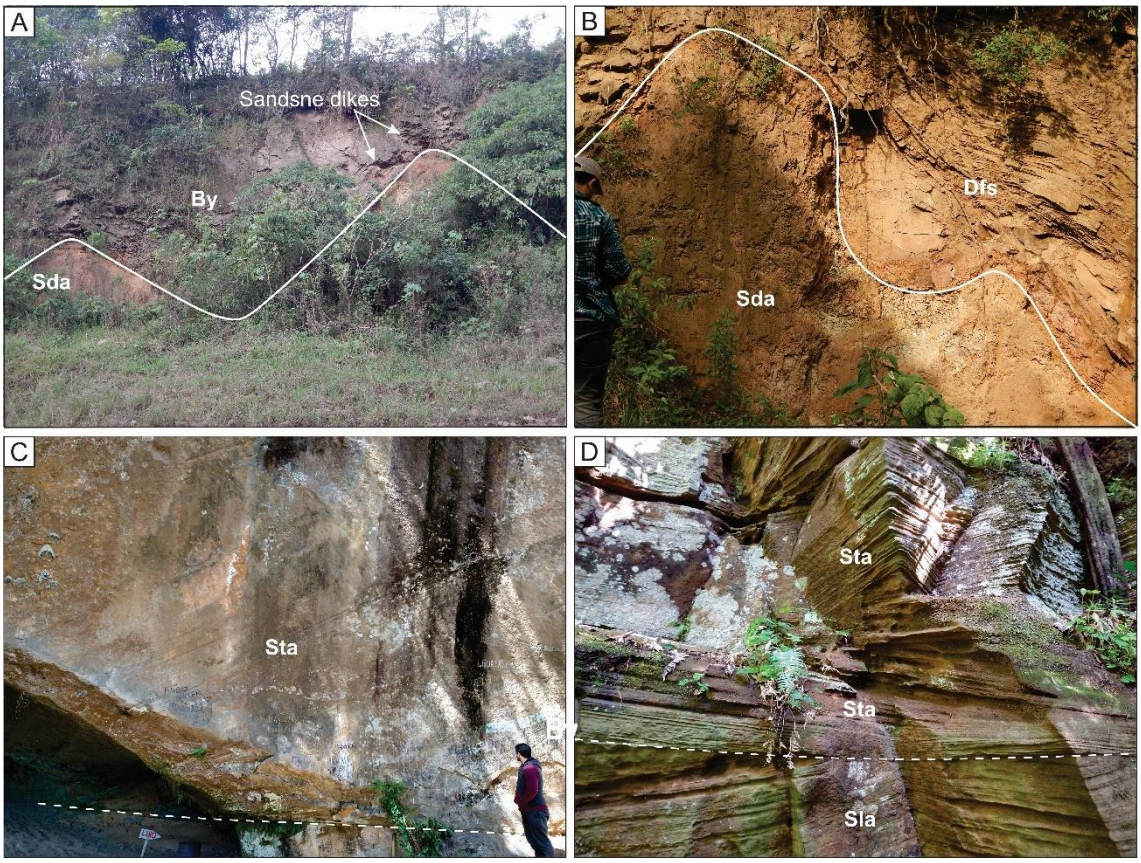

Figure 8: Facies and facies association of the upper portion of the columnar profile (Fig.5). A) Aeolian dunes paleotopography preserved by basaltic volcanic flows (By). Sandstone with original sedimentary structures deformed (Sda). B) Preservation and deformation of aeolian dunes by dacitic flows (Dfs). Sandstone with deformed structures (Sda). C) Large trough cross-stratification (Sta) in residual deposits of aeolian dunes. D) Low-angle aeolian stratifications (Sla) grading to trough cross-stratification (Sta).

5. DEPOSICIONAL MODELS AND STRATIGRAPHIC SUCCESSION

Guará Formation represents the distal portion of a braided fluvial system that migrated to southwest recording three cycles of typical multistorey channels deposits

associated with wet aeolian deposits (Fig. 9 A). The system discharge was variable, so that the conglomeratic facies (Gm) of bottom cycle I did not repeat during the next cycles II and III. Furthermore, the predominance of intraclasts and quartz clasts in the Gm facies indicate recurrent erosion of the floodplain exposed after periods of flooding. The shallow erosive surfaces resulted from shallow channels typical of seasonal flood discharges associated with wind action. This was installed recurrently, whose record was controlled by the variation in the water table. The restricted lateral continuity and the few occurrences of aeolian sand sheet deposits (Profiles 1 and 23) suggest that the availability of sedimentary supply and the existence of frankly arid conditions were incipient.

A thin precursor flow, 3 m thick, overlayed the braided fluvial deposits of cycle III in a restricted way (P02 and P04). While the river system was finished in the rest of the area, at these points a unique ephemeral river system was installed, represented by cycle IV (Figure 9B). The bottom deposits of this cycle are monomictic, consisting exclusively of very thick volcanic clasts with boulder to pebble sizes. The cycle ends with medium to coarse sandstone facies, with trough cross-stratification (St) and climbing cross lamination (Sr) denoting a rapid current deceleration (Miall, 1977; Stear, 1985; Langford and Braken, 1987). This ephemeral system was erosively conditioned exclusively over a volcanic flow, showing fewer confining channels towards the top.

The ephemeral fluvial cycle, represented by cycle IV, it is restricted to profiles P02 and P04, and cycle III of the braided fluvial system with the other profiles were supplanted by the wind system registered by cycle V, belonging to Botucatu Formation (Figure 9C), showing the establishment of arid climate. In two profiles (P01 and P18) the abrupt and flat contact occurs over medium sandstones with climbing cross-lamination (Sr), in the others, over medium sandstones with trough cross-stratification (St), showing that there was no erosion. Therefore, it is reasonable to infer that the change from one depositional system to another was brief. At the bottom, the cycle exposes sandstones formed by deposition in straight crest dune beds superimposed by sinuous crest dunes, registering an increase in the sedimentary supply.

The basaltic flows of Serra Geral Formation covered the aeolian dunes bed of Botucatu Formation, which contact has a duniform (wavy) geometry preserving the paleotopography (Figure 9C). A volcano-aeolic system was installed in which an increase in aridity and volcanic activity was verified, evidenced by the absence of humid facies and recurrence of flows. This successions of five cycles, the last two ones are at the top

of dacitic cycles, show that the development of aeolian beds was conditioned by volcanic quiescence.

Although many authors consider the existence of a nonconformity surface, hence necessarily erosive (Boggs, 2016) between the Guará and Botucatu Formations (Zerfass et al., 2007; Godoy et al., 2011, 2016, 2018; Reis, 2016, 2020; Reis et al., 2019), no erosion surface feature was evidenced in the study area. On the other hand, Scherer and Lavina (2005, 2006) described this contact as being a surface with non-depositional features, such as mud cracks and silcretes. However, such features, although denoting a diastema, are not enough to represent a large gap that would lead to the interpretation of a paraconformity. In the present study, the contact was abrupt, flat and between different facies, named St and Sr sandstones of Guará Formation underlying the Sta and Spa sandstones of Botucatu Formation, therefore not supporting the interpretation of a large gap. Furthermore, the occurrence of intercalated basic flows in the sandstones at the top of Guará Formation (see Figure 3, P02 and P04) and the subsequent intercalation of flows with aeolian sandstones demonstrates contemporaneity between the fluvio-aeolic, aeolian and volcanic systems. However, the paleogeographic configuration of these systems can distribute them differently, justifying regional differences. Thus, the age assigned by Zerfass et al. (2007) for the top of Guará and Botucatu Formations is Lower Cretaceous, as the flows of Serra Geral Formation belong to this epoch (Thiede and Vasconcellos, 2010).

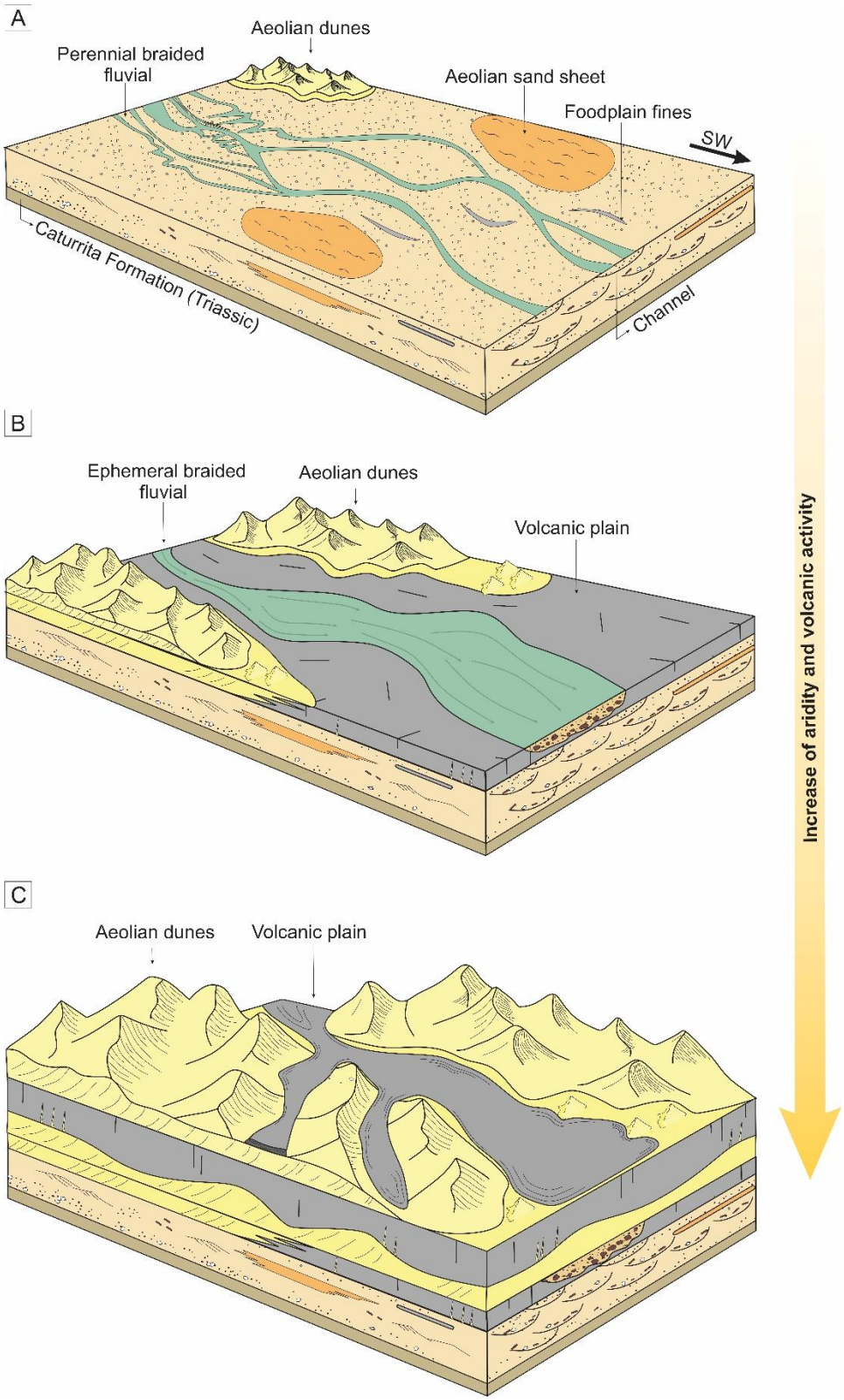

Figure 9: Proposed paleoenvironmental evolution for the Upper Jurassic – Lower Cretaceous of Paraná Basin (Modified from Rabelo, 2019).

6. CONCLUSION

The identification of three depositional systems characterized by their respective cycles, facies associations as being fluvial-aeolic for Guará Formation, aeolian for Botucatu Formation and volcano-aeolic for Serra Geral Formation, demonstrated to be synchronous at least in one of its development phases occurred during the Lower Cretaceous. The stratigraphic configuration shows the intercalation of flows through Guará Formation and wind fields in Serra Geral Formation which consistently supports this assumption. Furthermore, the contact surfaces between the formations do not show prolonged gaps.

The fluvio-eolian system of Guará Formation, characterized by three cycles of braided channels that culminate in floods, developed, in a unique way, also over a volcanic plain that preceded the lava flow represented by Serra Geral Formation. The deposits formed there represent a system of ephemeral channels, whose boulder to pebble size clasts are exclusively from the volcanic bed in which they were installed. This flow and the superimposed deposits constitute a stratigraphic marker, as they represent the first occurrence of volcanic flows, the last occurrence of a river system and arid conditions towards the top.

The transition between the fluvio-aeolic system to the frankly aeolian system of Botucatu Formation took place abruptly and in a short period of time, so that persistent arid conditions prevailed during the lava flows of Serra Geral Formation. For this reason, the intercalation of flows and aeolian successions was controlled by the quiescence of volcanic flows and, in the area investigated here, extended to the beginning of acid flows.

Acknowledgments

The first author acknowledges to all who contributed to this work, specially to Conselho Nacional de Desenvolvimento Científico e Tecnológico (CNPq, grant number: 141345/2017-9) for the grant awarded at the period of this doctorate program.

7. BIBLIOGRAPHIC REFERENCES

Allen, J.P., Fielding, C.R., Rygel, M.C., Gibling, M.R., 2013. Deconvolving signals of tectonic and climatic controls from continental basins: an example from the Late Paleozoic Cumberland Basin, Atlantic Canada. J. Sediment. Res. 83, 847–872. doi: https://doi.org/10.2110/jsr.2013.58

Almeida, E.F.M., 1954. Botucatu, um deserto triássico da América do Sul. DNPM Div. Geo. Min., Notas Prel. E Estudos, 86.

Almeida, E.F.M., Melo, C., 1981. A Bacia do Paraná e o vulcanismo no Mesozóico. In: Bistrichi, C.A., Carneiro, C.D.R., Dantas, A.S.L., Ponçano, W.L. (Eds.), Mapa geológico do Estado de São Paulo, nota explicativa. Instituto de Pesquisas Tecnológicas, 1, 46-77.

Amarante, F.B., Scherer, C.M.S., Goso Aguilar, C.A., Reis, A.D., Mesa, V., Soto, M., 2019. Fluvial-eolian deposits of the Tacuarembó Formation (Norte basin – Uruguay): depositional models and stratigraphic succession. J. South Am. Earth Sci. 90, 355–376. doi: https://doi.org/10.1016/j.jsames.2018.12.024

Andreis, R.R., Bossi, G. E., Montardo, D.K., 1980 O Grupo Rosário do Sul (Triássico) no Rio Grande do Sul. In: Congresso Brasileiro de Geologia, 31, Balneário Camboriú. Anais... Balneário Camboriú. SBG. 659-673.

Baksi, A.K., 2018. Paraná flood basalt volcanism primarily limited to ~ 1 Myr beginning at 135 Ma: New40Ar/39Ar ages for rocks from Rio Grande do Sul, and critical evaluation of published radiometric data. J. Volcanol. Geotherm. Res. 355, 66–77. doi:10.1016/j.jvolgeores.2017.02.016

Bigarella, J.J., 1979. Botucatu and Sambaiba sandstones of South America (Jurassic and Cretaceous); and Cave sandstone and similar sandstone of Southern Africa (Triassic). In: McKee, F.D. (Ed.), A Study of Global Sand Seas. U.S. Geological Survey Professional Paper, 1052, 233-238.

Bigarella, J.J., Salamuni, R., 1961. Early Mesozoic wind patterns as suggested by dune bedding in the Botucatu Sandstone of Brazil and Uruguai. Geol. Soc. Amer. Bull., 72, 1089-1106.

Bigarella, J.J., Salamuni, R., 1967. Botucatu Formation. In: Bigarella, J.J., Becker, R.D., Pinto, I.D. (Eds.), Problems in Brazilian Gondwana Geology, Curitiba, pp. 197–206.

Boggs, S.Jr., 2016. Principles of sedimentology and stratigraphy. 5ed. London, Pearson. 585 p.

Brito, I.M., 1979. Bacias sedimentares e formações pós–paleozóicas do Brasil. Rio de Janeiro, Interciência, 175p.

Bristow, C.S. 1987. Brahmaputra river: channel migration and deposition. In: Ethridge, F.G.; Flores, R.M.; Harvey, M.D. (Eds.). Recent developments in fluvial

sedimentology. SEPM Special Publication, 39, 83-91. doi: https://doi.org/10.2110/pec.87.39.0063

Brookfield, M.E., Silvestro, S., 2010. Eolian Systems. In: James, N. & Dalrymple, R.W. 2010. Facies Models 4. St. John's, Geological Association of Canada, pp. 139-166.

Chakraborty, T., Chaudhuri, A.K., 1993. Fluvial aeolian interactions in a Proterozoic alluvial plain: example from Mancheral Quartzite, Sullavai Group, Pranhita-Godavari Valley, India. In: Dynamics and Environmental Context of Aeolian Sedimentary Systems (Ed. Pye, K.), Spec. Publ. geol. Soc. London, No. 72, pp. 127–141. Geological Society of London, Bath. doi: https://doi.org/10.1144/GSL.SP.1993.072.01.12

Dadd, K.A., Van Wagoner, N.A., 2002. Magma composition and viscosity as controls on peperite texture: an example from Passamaquoddy Bay, southeastern Canada. In: Skilling, I.P., White, J.D.L., McPhie, J. (Eds.), Peperite: Processes and Products of Magma-Sediment Mingling. J. Volcanol. Geotherm. Res. 114, 63-80. doi: https://doi.org/10.1016/S0377-0273(01)00288-8

Fernandes, M.A., Carvalho, I.S., 2008. Revisão diagnóstica para a icnoespécie 683 de tetrápode Mesozóico Brasilichnium elusivum (Leonardi, 1981) 684 (Mammalia) da Formação Botucatu, Bacia do Paraná, Brasil. 685 Ameghiniana, 45(1), 167–173. apa1317.qxd (ufrj.br)

Fernandes, A.C.S., Carvalho, I.S., Guimarães–Netto, R., 1990. Icnofósseis de invertebrados da Formação Botucatu, São Paulo (Brasil). Anais da Academia Brasileira de Ciências, 62 (1), 45–49. 2_3.pdf (ufrj.br)

Fernandes, M.A., Fernandes, L.B.R., Souto, P.R.F., 2004. Occurrence of urolites related to dinosaurs in the Lower Cretaceous of the Botucatu Formation, Paraná Basin, São Paulo State, Brazil. Revista Brasileira de Paleontologia, 7(2), 263–268. Artigo20_Fernandes.p65 (sbpbrasil.org)

Francischini, H., Dentzien-Dias, P.C., Fernandes, M.A. Schultz, C.L., 2015. Dinosaur ichnofauna of the Upper Jurassic/Lower Cretaceous of the Paraná Basin (Brazil and Uruguay). Journal of South American Earth Sciences 63, 180-190. doi: https://doi.org/10.1016/j.jsames.2015.07.016

Fryberger, S.G., Ahlbrandtt, T.S., Andrews, S., 1979. Origin, sedimentary features, and significance of low-angle eolian 'sand sheet' deposits, Great Sand Dunes

National Monument and vicinity, Colorado. J. Sedm. Petrol 49, 733–746. doi: 10.1306/212F782E-2B24-11D7-8648000102C1865D

Godoy, M. M., Binotto, R. B., Silva, R. C., Zerfass, H., 2011. Geologia e Recursos Minerais do Geoparque Quarta Colônia, estado do Rio Grande do Sul, escala 1:100.000. Porto Alegre, Serviço Geológico do Brasil, CPRM. 54p.

Godoy, M. M., Scherer, O. L. B., Binotto, R. B., Gross, A. O. M., Dreher, A. M., 2016. Geologia e Recursos Minerais da Folha Sobradinho – SH.22-V-C-II, estado do Rio Grande do Sul, escala 1:100:000. Porto Alegre Serviço Geológico do Brasil, CPRM. 107p.

Godoy, M.M., Scherer, O. L. B., Binotto, R. B., Kischlat, E. E., Dreher, A. M., 2018. Geologia e Recursos Minerais da Folha Santa Maria – SH.22-V-C-IV, estado do Rio Grande do Sul, escala 1:100:000. Porto Alegre Serviço Geológico do Brasil, CPRM. 179p.

Hunter, R.E., 1977. Basic types of stratification in small eolian dunes. Sedimentology 24, 361–387. doi: https://doi.org/10.1111/j.1365-3091.1977.tb00128.x

Janasi, V.D.A., de Freitas, V.A., Heaman, L.H., 2011. The onset of flood basalt volcanism, Northern Paraná Basin, Brazil: a precise U-Pb baddeleyite/zircon age for a Chapecó-type dacite. Earth and Planetary Science Letters, 302(1), 147-153. doi: 10.1016/j.epsl.2010.12.005.

Jerram, D.A., Moutney, N.P., Howell, J.A., Long, D., Stolhofen, H., 2000. Death of a sand sea: an active aeolian erg systematically buried by the Etendeka flood basalts of NW Namibia. J. Geol. Soc. London. 157, 513–516. doi:10.1144/jgs.157.3.513

Kocurek, G., 1981. Significance of interdune deposits and bounding surfaces in aeolian dune sands. Sedimentology 28, 753–780. doi: https://doi.org/10.1111/j.1365-3091.1981.tb01941.x

Kocurek, G., 1991. Interpretation of ancient eolian sand dunes. Annu. Rev. Earth Planet Sci. 19, 43–75. doi: https://doi.org/10.1146/annurev.ea.19.050191.000355

Kocurek, G., 1996. Desert aeolian systems. In: Reading, H.G. (Ed.), Sedimentary Environments: Processes, Facies and Stratigraphy. Blackwell Science, Oxford, pp. 125–153.

Kocurek, G., Fielder, G., 1982. Adhesion structures. J. Sediment. Petrol. 51, 1229–1241.

Kocurek, G., Havholm, K.G. 1993. Eolian sequence stratigraphy - a conceptual framework. In: Weimer, P. & Posamentier, H.W. (Eds.). Siliciclastic sequence stratigraphy: recent developments and application. Soc. Econ. Paleont. Miner. Special publication, 52, pp.393-409. doi: https://doi.org/10.1306/M58581C16

Kocurek, G., Lancaster, N., 1999. Aeolian system sediment state: Theory and Mojave Desert Kelso dune field example. Sedimentology, 46**,** 505-515. doi: https://doi.org/10.1046/j.1365-3091.1999.00227.x

Kocurek, G., Nielson, J., 1986. Conditions favorable for the formation of warm-climate aeolian sand sheets. Sedimentology 33, 495–816.

Lancaster, N. 1988. Development of Linear Dunes in the Southwestern Kalahari, Southern-Africa. Journal of Arid Environments, 14, 233-244. doi: https://doi.org/10.1016/S0140-1963(18)31070-X

Lancaster, N. 1995. Geomorphology of Desert Dunes, London, Routledge. doi: https://doi.org/10.1017/S0016756800008931

Langford, R., Bracken, B., 1987. Medano Creek, Colorado, a model for upper-flow-regime fluvial deposition. J. Sediment. Petrol. 57, 863–870.

Leonardi, G., Oliveira, F.H., 1990. A revision of the Triassic and Jurassic tetrapod footprints of Argentina and a new approach on the age and meaning of the Botucatu Formation footprints (Brazil). Revista Brasileira de Geociências, 20(1–4), 216–229. doi: Microsoft Word - 2001216.rtf (siteoficial.ws)

McPhie, J., Doyle, M.G., Allen, R.L., 1993. Volcanic Textures: A Guide to the Interpretation of Textures in Volcanic Rocks. Centre for Ore Deposit and Exploration Studies, University of Tasmania, Hobart (198 p.).

Miall, A.D., 1977. A review of the braided-river depositional environment. Earth Sci. Rev. 13, 1–62. doi: https://doi.org/10.1016/0012-8252(77)90055-1

Miall, A.D. 1988. Facies Architecture in clastic sedimentary basins. In: Kleinspehn, K.L. & Paola, C. New perspectives in basin analysis, Berlin, Spriger-Verlag, p.67-81.

Miall, A.D., 1996. The geology of fluvial deposits: sedimentary facies. In: Basin Analysis and Petroleum Geology Springer-Verlag, New York, pp. 582.

Michelin, C.R.L. 2014. Ágata do Distrito Mineiro de Salto do Jacuí (Rio Grande do Sul, Brasil) - uma caracterização com base em técnicas estratigráficas, petrográficas, geoquímicas e isotópicas. PhD Thesis, Programa de Pós-Graduação em

Geociências, Instituto de Geociências, Universidade Federal do Rio Grande do Sul.

Milani, E.J., 1997. Evolução tectono-estratigráfica da Bacia do Paraná e seu relacionamento com a geodinâmica fanerozóica do Gondwana Sul-ocidental. PhD Thesis, Programa de Pós-Graduação em Geociências, Instituto de Geociências, Universidade Federal do Rio Grande do Sul.

Milani, E.J., Faccini, U.F., Scherer, C.M., Araújo, L.M., Cupertino, J.A., 1998. Sequences and Stratigraphic Hierarchy of the Paraná Basin (Ordovician to Cretaceous), Southern Brazil. BoI. IG USP, Série Científica, 29, 125-173. doi: http://dx.doi.org/10.11606/issn.2316-8986.v29i0p125-173

Milani, E.J.; Melo, J.H.G.; Souza, P.A.; Fernandes, L.A.; França, A.B. 2007. Bacia do Paraná. Boletim de Geociências da Petrobras, 15(2): 265-287. doi: https://www.researchgate.net/publication/279547262_Parana_basin.

Perea, D., Soto, M., Veroslavsky, G., Martínez, S., Ubilla, M., 2009. A late jurassic fossil assemblage in Gondwana: biostratigraphy and correlations of the Tacuarembó Formation, Paraná Basin, Uruguay. J. South Am. Earth Sci. 28, 168–179. doi: https://doi.org/10.1016/j.jsames.2009.03.009

Pires, E.F., Guerra–Sommer, M., Scherer, C.M.S., Santos, A.R., Cardoso, E., 2011. Early Cretaceous coniferous woods from a paleoerg (Paraná Basin, Brazil). Journal of South American Earth Sciences, 32, 96–109. doi: https://doi.org/10.1016/j.jsames.2011.04.001

Rabelo, C. E. N., 2019. A sucessão Jurássica-Eocretácea da Bacia do Parnaíba, NE do Brasil: paleoambiente, diagênese e correlação com os eventos magmáticos do Atlântico Central (CAMP). PhD Thesis, Programa de Pós-Graduação em Geologia e Geoquímica, Universidade Federal do Pará.

Reis, G.S., Mizusaki, A.M.P., Roisenberg, A., Rubert, R.R., 2014. Formação Serra Geral (Cretáceo da Bacia do Paraná): um análogo para os reservatórios ígneo-básicos da margem continental brasileira. Pesquisas em Geociências, 41(2), 155-168. doi: https://doi.org/10.22456/1807-9806.78093.

Reis, A. D., 2016. Análise arquitetural de depósitos fluviais da Formação Guará (Jurássico Superior-Cretáceo Inferior) na borda sudeste da Bacia do Paraná. M.Sc. dissertation. Universidade Federal do Rio Grande do Sul, RS, Brasil

Reis, A. D., 2020. O sistema fluvial distributivo da Formação Guará, Jurássico Superior, Gondwana Ocidental. PhD Thesis, Programa de Pós-Graduação em Geociências, Instituto de Geociências, Universidade Federal do Rio Grande do Sul

Reis, A. D. dos, Scherer, C. M. dos S., Amarante, F. B., Rossetti, M. M. M., Kifumbi, C., Souza, E. G., Owen, A., 2019. Sedimentology of the proximal portion of a large-scale, Upper Jurassic fluvial-aeolian system in Paraná Basin, southwestern Gondwana. Journal of South American Earth Sciences, 102248. doi: https://doi.org/10.1016/j.jsames.2019.102248

Renne, P.R., Ernesto, M., Pacca, I.G., Coe, R.S., Glen, J.M.G., Prevot, M., Perrin, M., 1992. The Age of Parana Flood Volcanism, Rifting of Gondwanaland, and the Jurassic-Cretaceous Boundary. Science (80-.). 258, 975–979. doi:10.1126/science.258.5084.975

Rios, F.R., Mizusaki, A.M.P., Michelin, C.R.L., 2018. Feições de interação vulcano-sedimentares – exemplos na Bacia do Paraná (RS). UNESP, Geociências, 37(3), 483-495. doi: https://doi.org/10.5016/geociencias.v37i3.12172

Rocha, B.C., Davies, J.H.F.L., Janasi, V.A., Schaltegger, U., Nardy, A.J.R., Greber, N.D., Lucchetti, A.C.F., Polo, L.A., 2020. Rapid eruption of silicic magmas from the Paraná magmatic province (Brazil) did not trigger the Valanginian event. Geology, 48(12): 1174-1178. doi: https://doi.org/10.1130/G47766.1

Scherer, C.M.S. 2000. Eolian dunes of the Botucatu Formation (Cretaceous) in Southernmost Brazil: morphology and origin. Sedimentary Geology, 137: 63–84. doi: 10.1016/S0037-0738(00)00135-4

Scherer, C.M.S. 2002. Preservation of aeolian genetic units by lava flows in the Lower Cretaceous of the Paraná Basin, southern Brazil. Sedimentology, 49, 97-116. doi: 10.1046/j.1365-3091.2002.00434.x.

Scherer, C. M. S.; Lavina, E. L., 1997. Aloformação Guará: uma nova unidade estratigráfica mesozóica na porção meridional da Bacia do Paraná. In: Simpósio sobre cronoestratigrafia da Bacia do Paraná, 3, Barra do Garças. Resumos, Barra do Garças: SBG, 1997. p. 36-37.

Scherer, C.M.S., Faccini, U.F., Lavina, E.L., 2000. Arcabouço estratigráfico do Mesozóico da Bacia do Paraná. In: Holz, M., De Ros, L.F. (Eds.), Geologia do

Rio Grande do Sul, Editora da Universidade/UFRGS, Porto Alegre, pp. 335–354.

Scherer, C.M.S., Lavina, E.L.C., 2005. Sedimentary cycles and facies architecture of aeolian-fluvial strata of the Upper Jurassic Guará Formation, southern Brazil. Sedimentology 52, 1323–1341. doi: https://doi.org/10.1111/j.1365-3091.2005.00746.x

Scherer, C.M.S., Lavina, E.L., 2006. Stratigraphic evolution of a fluvial–eolian succession: the example of the Upper Jurassic - lower cretaceous Guará and Botucatu formations, Paraná Basin, southernmost Brazil. Gondwana Res. 9 (4), 475–484. doi: https://doi.org/10.1016/j.gr.2005.12.002

Schumm, S.A. 1972. Fluvial paleochannels. In: Rigby, J.K. & Hamblin, W.K. (Eds). Recognition of ancient sedimentary environments. Soc. Econ. Paleontol. Mineral. Spec. Publ., 16, pp.98-107.

Skilling, I.P., White, J.D.L., McPhie, J., 2002. Peperite: a review of magma–sediment mingling. J. Volcanol. Geotherm. Res. 114, 1–17. doi: https://doi.org/10.1016/S0377-0273(01)00278-5

Soares, P.C., 1975. Divisão estratigráfica no Mesozóico no Estado de São Paulo. Ver. Bras. Geoc., 5, 251-267.

Soto, M., Perea, D., 2010. Late Jurassic lungfishes (Dipnoi) from Uruguay, with comments on the systematics of Gondwanan ceratodontiforms. Journal of Vertebrate Paleontology, 30(4), 1049–1058. doi: https://doi.org/10.1080/02724634.2010.483540

Stear, W.M., 1985. Comparison of the bedform distribution and dynamics of modern and ancient sandy ephemeral flood deposits in the southwestern Karoo region, South Africa: Sedimentary Geology, v. 45, p. 209-230. doi: https://doi.org/10.1016/0037-0738(85)90003-X

Suguio, K., Coimbra, A.M., 1972. Madeira fóssil silicificada na Formação Botucatu. Ciência e Cultura, 24, 1049–1055. http://memoria.bn.br/DocReader/DocReader.aspx?bib=003069&Pesq=petri,%20setembrino&pagfis=11852

Thiede, D.S., Vasconcelos, P.M., 2010. Paraná flood basalts: rapid extrusion hypothesis confirmed by new 40Ar/39Ar results. Geology, 38, 747-750. doi: https://doi.org/10.1130/G30919.1

Waichel, B., Scherer, C., Frank, H., 2008. Basaltic lava flows covering active aeolian dunes in the Paraná Basin in southern Brazil: features and emplacement aspects. J. Volcanol. Geotherm. Res. 171, 59–72. doi: https://doi.org/10.1016/j.jvolgeores.2007.11.004

Walker, R.G., James, N.P., 1992. Fácies Models: Response to Level Sea Change. Geology Association of Canada, St. John's 410 pp.

Zalán, P.V., Wolff, S., Astolfi, M.A.M., Vieira, I.S., Conceição, J.C.J., Appi, V.T., Neto, E.V.S., Cerqueira, J.R., Marques, A., 1990. The Paraná Basin, Brazil. Tulsa: AAPG Memoir, 51: 681- 708.

Zerfass, H., Sander, A., Flores, A. E., 2007. Geologia da Folha Agudo - SH.22-V-C-V, escala 1:100.000. Porto Alegre. Serviço Geológico do Brasil, CPRM. 98p.

6.3 VOLCANOCLASTIC AND EPICLASTIC DIAGENESIS OF SANDSTONES ASSOCIATED WITH VOLCANO-SEDIMENTARY DEPOSITS FROM THE UPPER JURASSIC AND LOWER CRETACEOUS, PARANÁ BASIN, SOUTHERN BRAZIL

This is an automated message.

VOLCANOCLASTIC AND EPICLASTIC DIAGENESIS OF SANDSTONES ASSOCIATED WITH VOLCANO-SEDIMENTARY DEPOSITS FROM THE UPPER JURASSIC, LOWER CRETACEOUS, PARANÁ BASIN, SOUTHERN BRAZIL

Dear MSc. Rios,

We have received the above referenced manuscript you submitted to Journal of South American Earth Sciences. It has been assigned the following manuscript number: SAMES-D-23-00099.

To track the status of your manuscript, please log in as an author at https://www.editorialmanager.com/sames/, and navigate to the "Submissions Being Processed" folder.

Thank you for submitting your work to this journal.

Kind regards,
Journal of South American Earth Sciences

More information and support

You will find information relevant for you as an author on Elsevier's Author Hub: https://www.elsevier.com/authors

FAQ: How can I reset a forgotten password?
https://service.elsevier.com/app/answers/detail/a_id/28452/supporthub/publishing/
For further assistance, please visit our customer service site: https://service.elsevier.com/app/home/supporthub/publishing/
Here you can search for solutions on a range of topics, find answers to frequently asked questions, and learn more about Editorial Manager via interactive tutorials. You can also talk

VOLCANOCLASTIC AND EPICLASTIC DIAGENESIS OF SANDSTONES ASSOCIATED WITH VOLCANO-SEDIMENTARY DEPOSITS FROM THE UPPER JURASSIC AND LOWER CRETACEOUS, PARANÁ BASIN, SOUTHERN BRAZIL

Fernando Rodrigues RIOS[a*], Ana Maria Pimentel MIZUSAKI[a], Cassiana Roberta Lizzoni MICHELIN[b], Isaque Conceição RODRIGUES da Silva[a]

[a]UFRGS, Instituto de Geociências, Programa de Pós-Graduação em Geociências, Campus do Vale – Porto Alegre (RS).
[b]UFRGS, Instituto de Geociências, Departamento de Mineralogia e Petrologia, Campus do Vale – Porto Alegre (RS).

ABSTRACT

The opening of South Atlantic Ocean produced an immense volume of lava that covered an active aeolian system during Lower Cretaceous. The contact of Botucatu Formation sandstones with the Serra Geral volcanic flows generated a variety of volcano-sedimentary features and deposits. During volcanism, volcanoclastic features and deposits were formed by temperature contrasts between lava and wet or water-saturated sediments. In moments of magmatic quiescence, epiclastic deposits were generated due to the return of sedimentation. Volcanoclastic deposits are characterized by volcanic breccias with sandy matrix, and epiclastic deposits are characterized by conglomerates and conglomeratic sandstones with intraclasts. Quantitative petrography of sandy matrix samples of these deposits was analyzed, in order to discuss the paragenesis of volcano-sedimentary interactions. Regular burial diagenetic processes were discussed for epiclastic sandstones and contact diagenesis processes for volcanoclastic sandstones. The original composition of volcanoclastic and epiclastic sandstones is heterogeneous. However, the main difference between them is the presence of textural fluidization indicators found in the volcanoclastic sandstones, along the lava-sediment interface. These textural characteristics indicate that the unconsolidated sediments were probably wet or saturated in water during the interaction with the volcanic flow. Epiclastic sandstones have infiltrated clays and neoformed smectites as their main diagenetic constituent due to alteration of available volcanic lithoclasts. For volcanoclastic sandstones, the formation of opal, chalcedony and megaquartz cements through burial is unlikely, due to the intergranular volume occupied by these cements, indicating early conditions near the surface. Therefore, the cementation, mainly of chalcedony, was formed through mechanisms of dissolution and reprecipitation of the siliceous fluids incorporated in the system. Furthermore, zeolite cementation, which occurs along the lava-sediment contact, is another important indicator of contact diagenesis for volcanoclastic sandstones. During telodiagenesis the formation of secondary porosity by dissolution of volcanic lithoclasts and detrital K-feldspar grains was of great importance in volcanoclastic and epiclastic sandstones.

Keywords: Contact diagenesis, lava-sediment interaction, Chalcedony cement, Zeolite cement, Paraná Basin.

1. INTRODUCTION

Sedimentary basins register dynamic processes that control the lithosphere deformation and its interaction with the deep mantle, sediments transformation into sedimentary rocks, burial, tectonic subsidence, volcanic events and surface processes (Miall, 2000; Cloetingh and Ziegler, 2007; Allen and Allen, 2013; Weissmann et al., 2015).

In this regard, Paraná Basin stands out in the South American Platform, where there is an important cretaceous volcanic event, related to the break of Gondwana and the South Atlantic Ocean formation. This event is related to Serra Geral Formation, characterized by a huge volume of lavas and associated intrusions that covered and interacted with an extensive active wind system, the Botucatu Formation, generating deposits and volcano-sedimentary features (Milani et al., 1998; Scherer, 2002; Petry et al., 2007; Waichel et al., 2008; Michelin, 2014; Reis et al., 2014; Rios et al., 2018).

Understanding the genesis and subsequent processes related to lava-sediment interaction is necessary, as they are common in other sedimentary basins. The research of the sedimentary stratigraphic range of probable contacts with volcanic rock, their different scales, their possible effects on diagenesis, information about sediments fluidization and paleoenvironmental contexts are extremely important. As well as clarify the effects of volcanism in the features diagenesis and deposits in Paraná Basin. The features and deposits formed through interaction are essential for diagenetic and paleoenvironmental studies, as they develop in a variety of sedimentary successions in which sedimentation and volcanism are contemporaneous (Macdonald, 1939; Branney & Suthren, 1988; Allen, 1992; Boulter, 1993; McPhie et al., 1993; Skilling et al., 2002; Rios et al., 2018).

Furthermore, understanding the diagenesis, associated with volcanism, supply the knowledge for the order in which the grains framework was altered and the authigenic phases were precipitated and, perhaps, subsequently dissolved, and thus reveal the post-depositional history of these features and volcano-sedimentary deposits affected by volcanic flows. This work aims to delineate the main textural and mineralogical sandstones characteristics related to volcanoclastic and epiclastic features and deposits. In addition, to discuss and explain the origin, distribution and chronology of your diagenetic alterations.

2. GEOLOGICAL SETTING

The Botucatu and Serra Geral Formations are part of the volcano-sedimentary filling of Paraná Basin. Paraná Basin is the largest Paleozoic basin in the South American Platform (Fig. 1A) and records successive processes of subsidence, uplift, sedimentation and magmatism from Ordovician to Cretaceous (Zalán et al., 1990; Milani, 1997; Milani et al., 1998, 2007). There are approximately 7,000 m of volcano-sedimentary succession at the basin's depocenter, covering an area of 1,400,000 km^2 in Brazil, Paraguay, Uruguay and Argentina (Milani, et al., 2007) (Fig. 1B). The evolution of the basin is related to the break of Gondwana and the South Atlantic Ocean opening (Milani et al., 2007). The lithological record evolves from transgressive-regressive marine cycles to continental features associated with magmatism, resulting in six different Supersequences, according to Milani et al. (2007).

The aeolian sedimentation is attributed to Botucatu Formation and the intense magmatism related to Serra Geral Formation, comprising the Gondwana III Supersequence (Neo-Jurassic to Eo-Cretaceous), where volcano-sedimentary interactions are set (Milani, 1997).

Botucatu Formation siliciclastic deposits comprehend well sorted, pinkish quartz sandstones, fine to medium granulometry and rounded grains associated with large cross-stratification that indicate residual deposits of aeolian dunes. (Scherer, 2000, 2002). The Botucatu Formation erg is covered by lavas of Serra Geral Formation, which comprise basic and, secondarily, acid flows related to the initial distension processes and the break of Gondwana. The age for these successions is in Lower Cretaceous of approximately 134 Ma (Renne et al., 1992; Thiede and Vasconcellos, 2010; Janasi et al., 2011; Baksi, 2018; Rocha et al., 2020).

The top sedimentary portion of Botucatu Formation exposes a contemporary event between the overlying lava flows from the Serra Geral Formation forming volcano-sedimentary interaction along with the contact between these two units. In this regard, two geological processes can be considered about the interaction genesis. The first refers to hot lava flowing over the sediments, the temperature contrast with the humidity or water saturation of the sediments are the main controls in the formation of volcanoclastic rocks. Moreover, the second process during the return of sedimentation and quiescence of volcanic activity, forming epiclastic deposits (McPhie et al., 1993; Milani et al., 1998;

Petry et al., 2007; Waichel et al., 2008; Michelin, 2014; Reis et al., 2014; Rios et al., 2018).

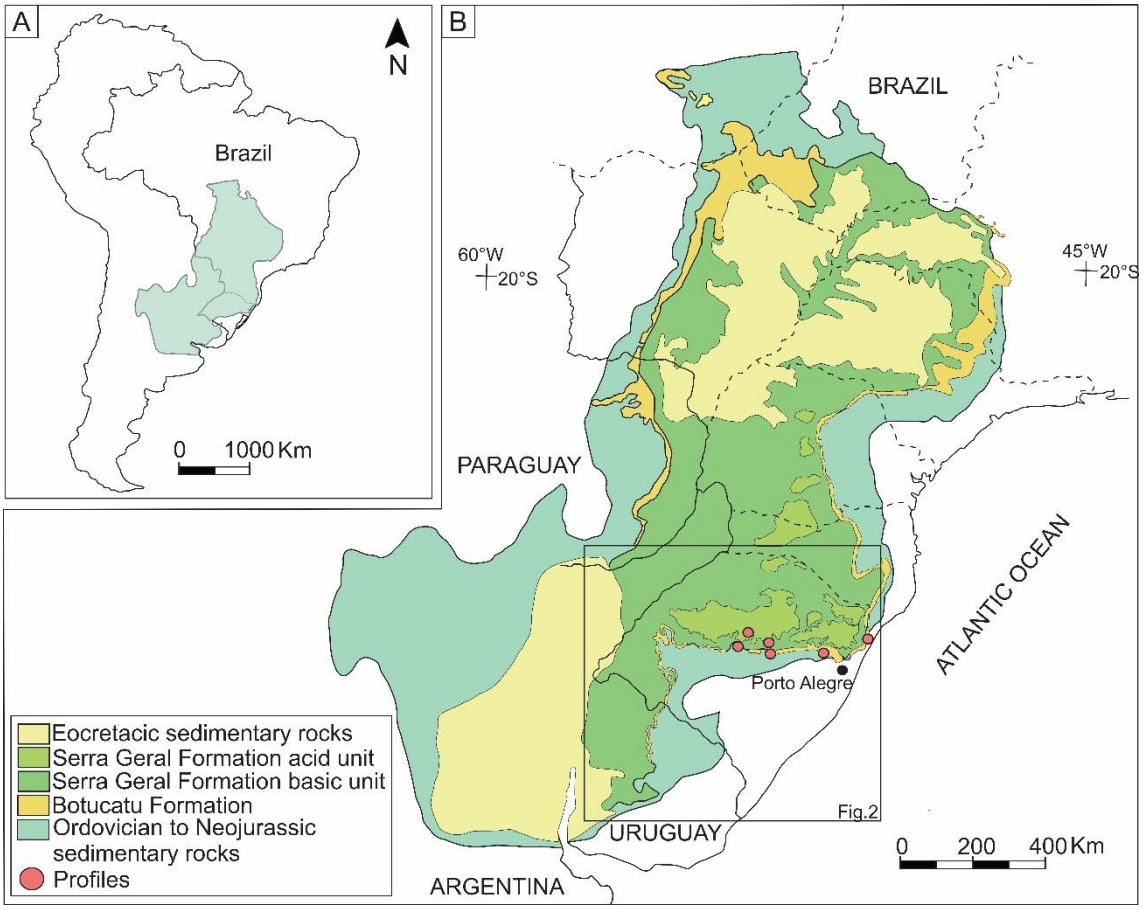

Figure 1: A) Paraná Basin, South American Platform. B) Detail of the Paraná Basin and location of the analyzed profiles (modified from Janasi et al., 2011; Rossetti et al., 2018; Reis et al., 2019).

3. MATERIALS AND METHODS

The study used the identification and description of features and volcano-sedimentary deposits from previously proposed vertical profiles on the current southeastern border of Paraná Basin, in Rio Grande do Sul state, southern Brazil (Fig. 2). In the vertical profiles, the features of interest were observed and samples were selected for macroscopic and petrographic description. The samples for petrography are from the sandy matrix of the region's volcanoclastic and epiclastic deposits.

Thirty samples were selected for quantitative petrography. The samples were impregnated with blue resin in order to highlight the porosity. Thin sections were initially exposed to a solution of alizarin red S and potassium ferrocyanide (Dickson, 1966) for

the identification of carbonate minerals. Petrography was performed at the Departamento de Mineralogia e Petrologia do Instituto de Geociências of Universidade Federal do Rio Grande do Sul with a conventional petrographic microscope and Petroledge® software (De Ros and Goldberg, 2007). The modal composition was obtained by counting 300 points per thin section, according to the Gazzi-Dickinson method (Zuffa, 1985). The petrography included textural, mineralogical and porosity description, but preferably the focus was on the diagenetic components and their relationships.

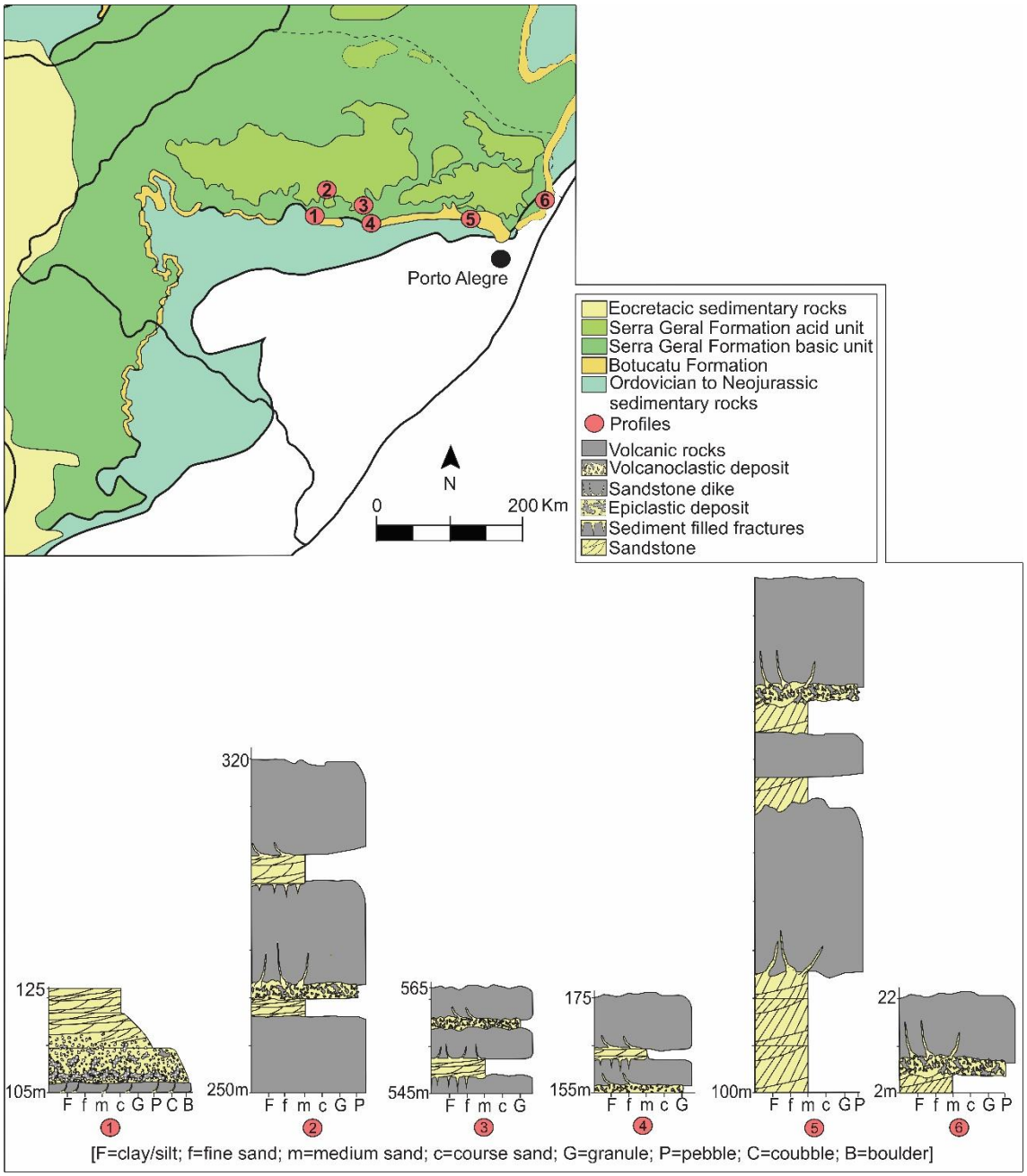

Figure 2: Location and representation of the vertical profiles in the current southeastern border of Paraná Basin, Rio Grande do Sul state, through their topographic dimensions

(see Fig. 1B); Profile (1) 29°28'55" S/ 53°28'33" W; (2) 29°06'05" S/ 53°13'49" W; (3) 29°30'12" S/ 52°39'00" W; (4) 29°41'30" S/ 52°23'23" W; (5) 29°37'54" S/ 51°08'49" W; (6) 29°21'27" W/ 49°44'02" W (modified from Rios et al., 2023 submitted)

4. VOLCANOCLASTIC AND EPICLASTIC ANALYZED DEPOSITS AND FEATURES

Interaction features and volcanoclastic deposits concomitant with volcanism and later or at periods between volcanic flows, called epiclastic features and deposits, were identified (Fig. 3A-D).

The classification of volcanoclastic rocks can be based on the size and morphology of the volcanic clasts, mineralogical types and composition of the matrix sediments (Folk, 1968), and, when possible, based on the genesis (McPhie et al., 1993; Lorenz, 1984; Busby-Spera and White, 1987; Skilling et al., 2002).

Underneath volcanic flows and along the lava-sediment interface, volcanoclastic deposits are formed (profiles 2, 3, 4, 5, 6, see Fig. 2). These deposits are named, macroscopically, in a descriptive way using the term breccia associated with the volcanic clasts and sedimentary matrix compositions (Folk, 1968; Rosa et al., 2016). The occurrences show multiple and discordant geometries of the sedimentary bedding. The volcanic clasts granulometry varies from 0.2 mm to 40 cm, with angular (Fig. 3C, D), fluid and globular morphologies. Associated or not with volcaniclastic breccias, there are sandstone dykes (profiles 1 to 6, see Fig 2) (Michelin, 2014; Rios et al., 2018). They are fractures filled by sandstone, displaying centimetric thicknesses and straight or irregular limits. These features occur at the bottom of the volcanic flow, superimposed on a sediment layer, and may extend until the top.

Above the volcanic flows, there is an active sedimentary system and the features and deposits were considered as epiclastic because they are the result of pre-existing rocks reworking. It contains fragments derived from syn-eruptions and post-eruptions, through weathering and erosion processes (Fisher, 1960; Cas and Wright 1987; McPhie et al., 1993). The fractures filled by sediments, for example, occur at the top of basaltic flows (profiles 2, 3 and 4, see Fig 2). The epiclastic deposit (profile 1, see Fig. 2) holds a lenticular geometry and it is characterized by conglomerates and conglomeratic sandstones with intraclasts. The bottom of the deposit is in contact with the basalt through an erosive surface, with intraclasts from 0.2 mm to 35 cm, exposing irregular shapes and

that may display vesicles filled with zeolite (Fig. 3A). The top of the deposit is marked by a trough cross-stratification and the decrease of the fragments granulometry (Fig. 3B).

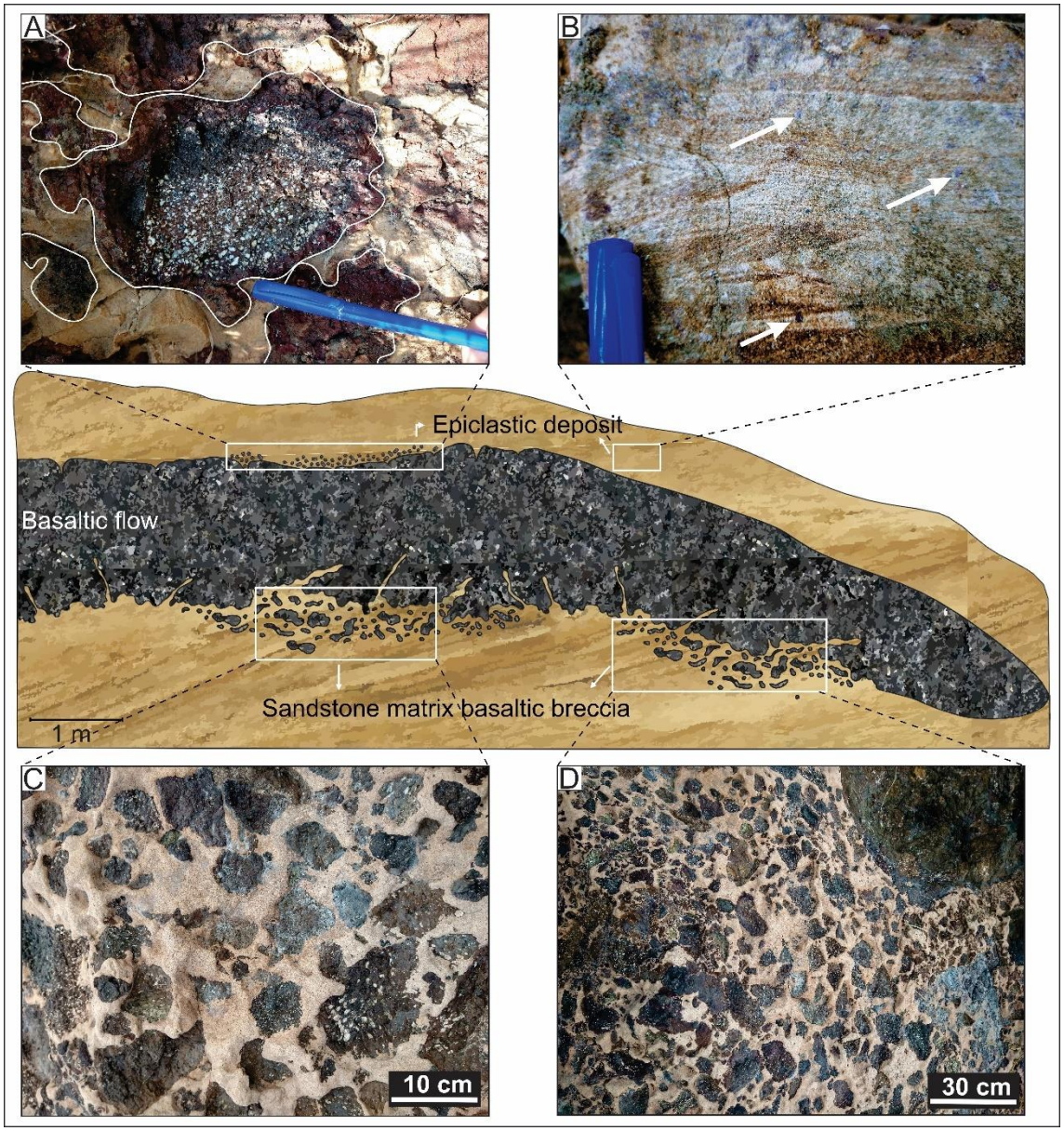

Figure 3: Modes of occurrence of the deposits, volcanoclastic superimposed on the flow and epiclastic underlying A) Epiclastic conglomerate with irregular intraclasts with vesicles filled with zeolite. B) Conglomeratic sandstone with trough cross-stratification and volcanic fragments (white arrows). C) and D) Basaltic breccia of sandy matrix with angular morphological clasts.

5. MATRIX OF VOLCANOCLASTIC FEATURES AND DEPOSITS

5.1 Detrital texture, composition and provenance

The analyzed samples vary texturally from muddy sandstones to conglomeratic sandstones, with a predominance of fine to coarse sandstones and moderately sorted (Figs. 4A, B). The samples are predominantly massive or with foliation, evidenced by the concentration of detrital clay forming planes along the lava-sediment interface (Fig. 4B). The grains are mostly sub-rounded and the packing varies from loose to normal, with point, long and rarely concave-convex contacts.

Quartz grains are mainly monocrystalline and secondarily metamorphic polycrystalline (Tab. 1). The detrital feldspars are predominantly microcline and subordinately orthoclase (Tab. 1). Fragments of volcanic rock represent the second most abundant detrital constituent, while fragments of plutonic, metamorphic and sandstone rock are less common (Table 1). Volcanic lithoclasts can be substituted and/or oxidized, with angular morphologies, mainly, globular and fluidal (Figs. 4C, D). The detrital clay grains are mostly oxidized forming foliations parallel to the lava-sediment contact (Tab.1; Fig. 4B). Biotite and muscovite are the most common accessories (Table 1).

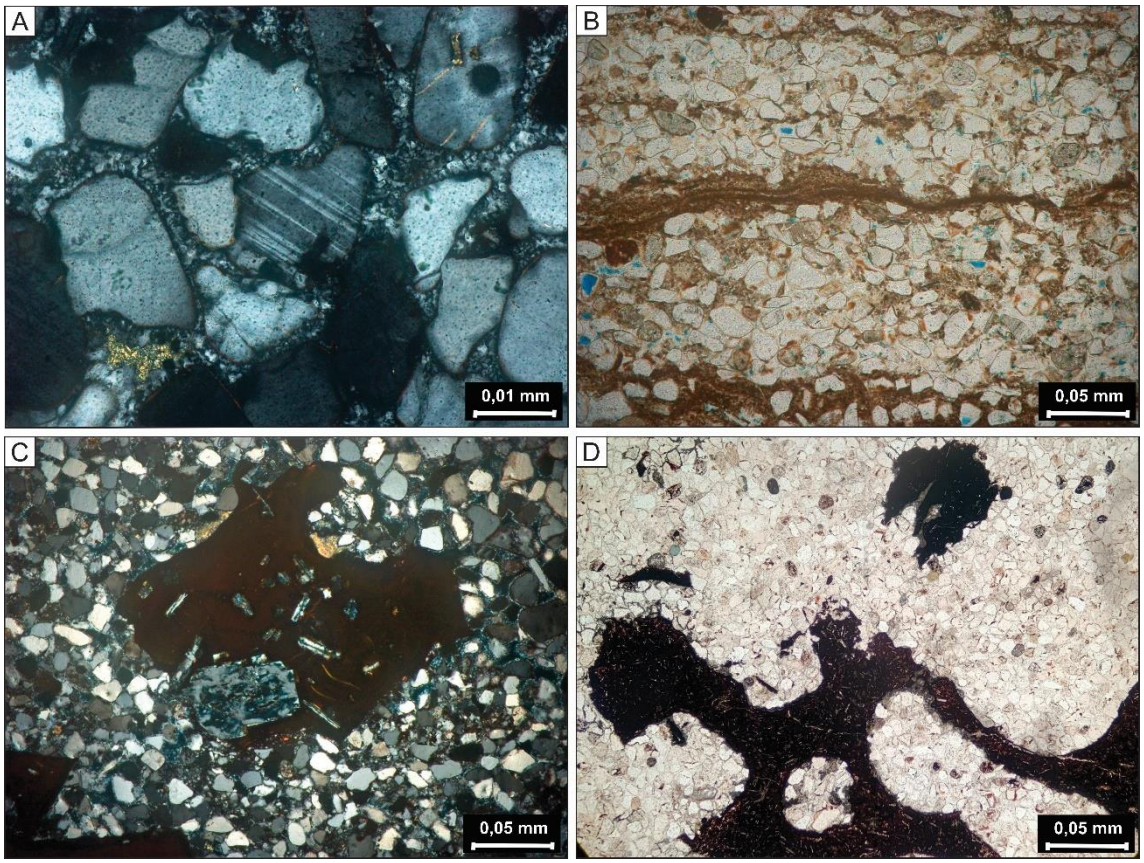

Figure 4: Main textural aspects and detrital composition of the sandstones from volcanoclastic features and deposits. A) Moderately sorted and massive lithic arkoseum (crossed polarizers, XP). B) Fine to medium feldspathic litharenite, moderately sorted, with foliation marked by the concentration of detrital clays near the lava-sediment contact

(uncrossed polarizers, //P). C) Litharenite fine to coarse volcanic sandstone, massive, with angular basaltic fragments (XP). C) Massive conglomeratic volcanic litharenite, with vitreous volcanic lithoclasts of fluidal and globular morphologies (XP).

Primary main constituents	Maximum (%)	Average (%)
Monocrystalline quartz grains	44.00	33.52
Policrystalline quartz grains	6.00	3.75
Detrital microcline grains	14.33	6.22
Detrital orthoclase grains	3.67	<1
Volcanic rock fragments	44.67	12.46
Plutonic rock fragments	5.67	<1
Metamorphic rock fragments	3.00	<1
Sandstone fragments	1.33	<1
Detrital clay	15.67	4.21
Biotite	2.00	<1
Muscovite	1.00	<1

Table 1: Simplified petrographic quantification of the primary constituents of the sandstones from volcanoclastic features and deposits.

The original composition of the analyzed samples is heterogeneous, with the sandstones predominantly classified as feldspathic litharenite, followed by volcanic sandstone, lytic arkose and, subordinately, arkose and sublitharenite *sensu* Folk (1968) (Fig. 5A). The current composition (Fig. 5B) is relatively more enriched in quartz when compared to the original composition (Fig. 5A), due to the replacement of volcanic fragments by chalcedony, zeolite, authigenic titanium minerals, hematite, calcite, and also by the dissolution and replacement of detrital feldspar grains by kaolinite. The original composition corresponds to a provenance predominantly of recycled orogen, which may be influenced by transitional continental tectonic environments and transitional arc *sensu* Dickinson (1985) (Fig. 5C).

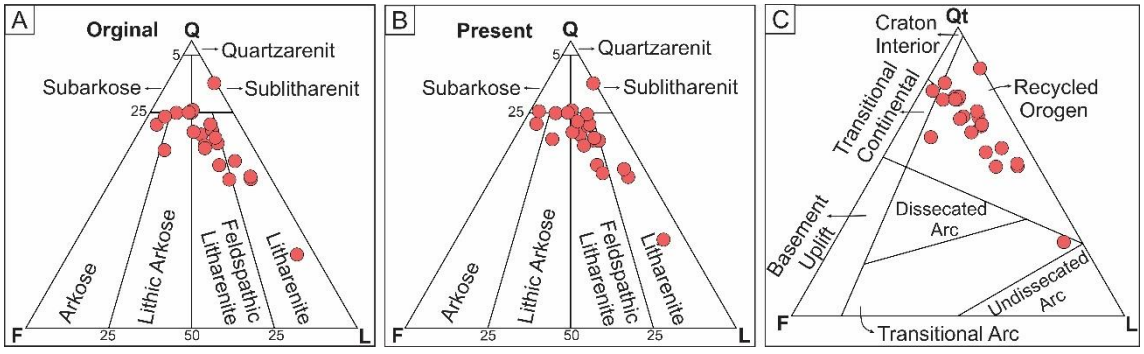

Figure 4: Sandstone compositions of the volcanoclastic features and deposits analyzed and plotted in Folk's diagram (1968): A) Original detrital composition of the sandstones. B) Current sandstones composition. C) Original detrital composition plotted on Dickinson's (1985) provenance diagram.

5.2 Diagenetic constituents

Quartz cement – Chalcedony is the most abundant cement in the analyzed sandstones (Table 2). It occurs mainly as cryptocrystalline crystals (Figs. 6A) and fibro-radial habit (Figs. 6B), predominantly in intergranular pores and, secondarily, in fracture porosity where there is formation of well-developed fibro-radial habits. They form on the framework grains in continuous or discontinuous rims, and may develop on chalcedony rims forming a zoning. They also develop on other diagenetic constituents such as hematite coatings, infiltrated clays (Figs. 6A, B), zeolite and opal (Table 2). Chalcedony can occur in microcrystalline and intragranular form replacing volcanic fragments. The cementation of megaquartz (Table 2) was observed after the cementation of chalcedony, forming a mosaic of pseudohexagonal crystals, where the size of the crystals increases towards the center of the pores. These mosaics fill pores along the lava-sediment interface (Fig. 6C) and, mainly, fractures present in the sandstone, associated with opal cements, chalcedony, zeolite (Fig. 6C) and calcite (Tab. 2). In intergranular or fracture pores cementation of poikilotopic opal can occur, and it is possible to observe impurities in the opal delimiting the pulses of its cementation. The opal cement (Table 2) is posterior to the infiltrated clays around the grains and previous to the chalcedony and megaquartz cements. Syntax quartz overgrowths (Tab. 2) occur mainly in monocrystalline grains, as well as prismatic outgrowths (Fig. 6D).

Zeolite - Cementation by zeolite (Table 2) occurs mainly as large prismatic crystals, in thick mosaic and filling the intergranular pores, mainly in the lava-sediment contact and near the contact (Fig. 6C). Discontinuous prismatic rims of zeolite over detrital (quartz grains, volcanic fragments) and diagenetic (autigenic clays, hematite and zeolite coatings) constituents are common (Figs. 6C, E, F). A sequence of up to three steps was observed in the evolution of cementation and subsequent pore filling by zeolites: 1) small prismatic zeolite crystals are formed in the intergranular space; 2) poikilotopic or thick mosaic zeolite crystals encompass the existing prismatic crystals, filling the intergranular porosity; 3) a rim of prismatic zeolite aggregates form around the mosaic crystals (Figs.

6E, F). Zeolites also occur replacing volcanic fragments and filling intragranular porosity. Along the sandstone-basalt interface, sediment-filled and zeolite-cemented vesicles may occur.

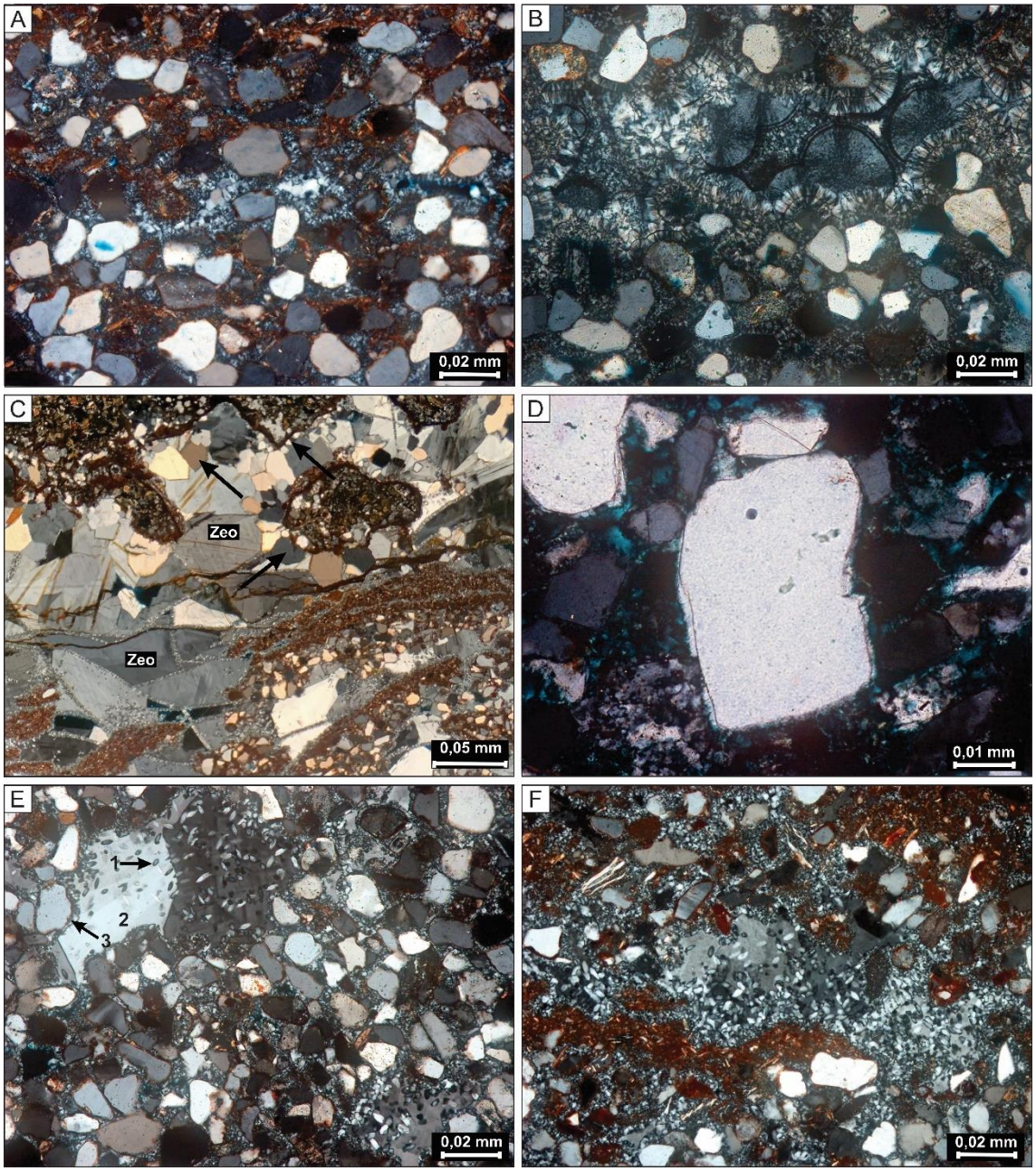

Figure 6: A) Microcrystalline chalcedony filling the intergranular porosity (crossed polarizers, XP). B) Well-developed fiber-radial chalcedony (XP). C) Megaquartz (black arrows) formed along lava-sediment interface associated with prismatic zeolite (Zeo) crystals (XP). D) Prismatic quartz outgrowths (XP). E) and F) Sequence of three steps in cementation (1, 2, 3) and filling of the intergranular porosity with zeolites (XP).

Hematite - Hematite occurs as continuous coatings and as inherited coatings in the most concave and less salient portions of the grains (Table 2). Hematite also occurs in small

crystalline clusters in intergranular spaces, mixed with detrital clay (Figs. 6A, C, F) and on cementation of chalcedony and opal (Tab. 2). It also occurs filling fractures in zeolite cements and close to the lava-sediment contact (Fig. 6C). They replace volcanic debris and heavy minerals.

Clay infiltration and mixed-layers illite-smectite - Infiltrated smectite clays can directly cover hematite grains and coatings, commonly filling intergranular pores and pore linings (Fig. 7A). Volcanic fragments can be completely dissolved, leaving only the mold pore formed by the coatings of infiltrated clays. The mixed I/S layers partially replaced the infiltrated clays forming simple rims and hair-like projections. The infiltrated clays predate the cementation of chalcedony, calcite and zeolite (Fig. 7A).

Authigenic titanium minerals - Authigenic titanium minerals occur as discrete prismatic crystals of TiO_2 and as cryptocrystalline to microcrystalline aggregates, mainly filling intergranular pores (Table 2). They replace volcanic fragments, heavy mineral grains and locally authigenic clays. In some samples they are preferentially located near the lava-sediment interface, where they are engulfed by zeolite or chalcedony cement (Table 2).

Other diagenetc constituents - Calcite occurs filling intergranular pores (Fig. 7A) and in volcanic fragments altering zeolite (Tab. 2; Fig. 7B). They fill the intergranular pores with a poikilotopic habit (Fig. 7A) and thick mosaic. Authigenic K-feldspar may occur as outgrowths around microcline grains preferentially (Tab. 2). In some samples, such outgrowths were preserved from the late dissolution that affected the feldspar grains. Celadonite occurs in micaceous aggregates that develop on chalcedony filling intergranular pores (Tab.2; Figs 7C). The celadonite cement stains the chalcedony, leaving it with a greenish color (Fig. 7D). Kaolinite occurs as booklets replacing micaceous metamorphic fragments and feldspar grains (Tab. 2).

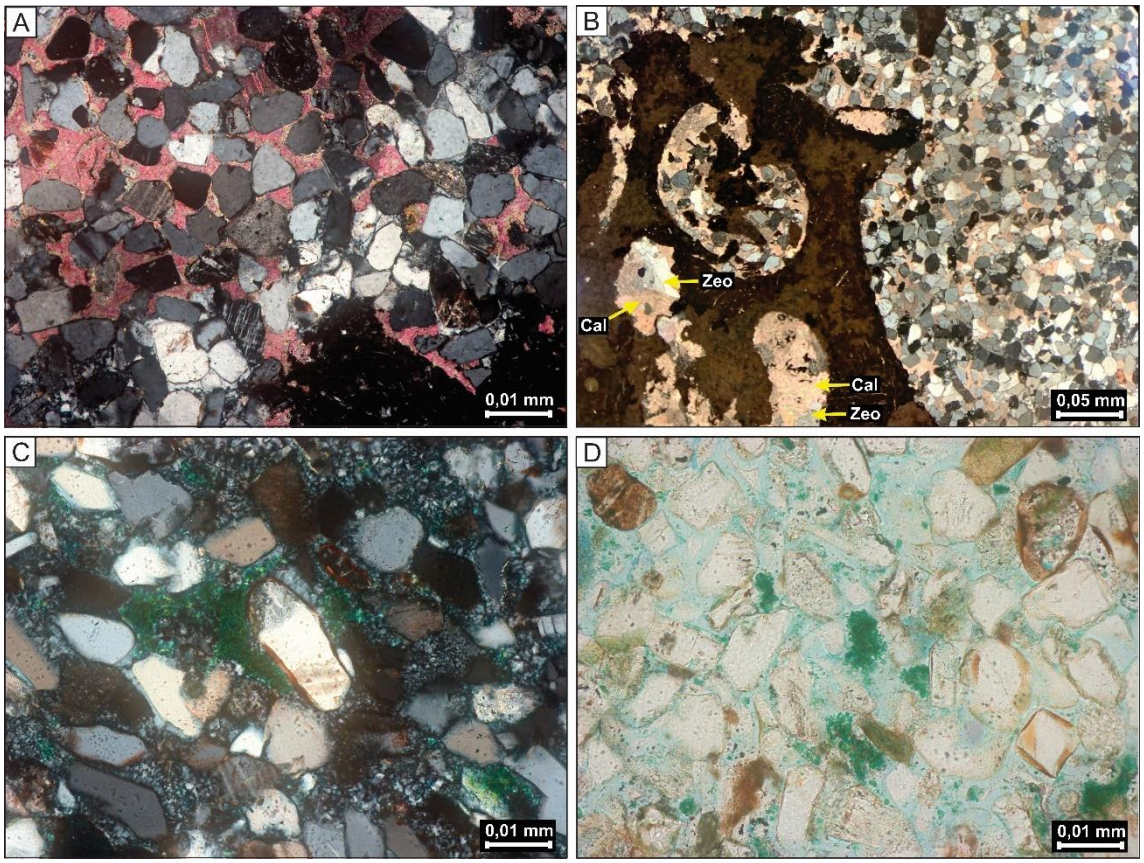

Figure 7: A) Poikilotopic calcite filling intergranular porosity (crossed polarizers, XP). B) Intragranular calcite (Cal) in volcanic fragment altering the zeolite (Zeo) (XP). C) Celadonite micaceous aggregates developed on chalcedony, filling intergranular porosity (XP). D) Cement of chalcedony dyed green by subsequent cementation of celadonite (uncrossed polarizers, //P).

Diagenetic main constituents and porosity	**Maximum (%)**	**Average (%)**
Total quartz cement	**34.67**	**18.74**
Intergranular chalcedony	34.67	15.86
Intragranular chalcedony	3	<1
Overgrowths or outhgrowths	9	1.10
Opal	17.67	<1
Prismatic quartz	8	<1
Total zeolite	**41.00**	**7.19**
Intergranular zeolite	41.00	6.92
Intragranular zeolite	4.67	<1
Hematite	**6.00**	**2.81**
Infiltrated clay	**22.67**	**2.48**
Total TiO_2	**15.66**	**1.35**

Intergranular TiO_2	12.66	<1
Intragranular TiO_2	7.00	<1
Intergranular ilite-smectite	**<1**	**<1**
K-feldspar	**<1**	**<1**
Total Calcite	**12.67**	**<1**
Intergranular calcite	2.67	<1
Intragranular calcite	10.00	<1
Celadonite	**7.33**	**<1**
Caulinite	**1.67**	**<1**
Total porosity	**15.00**	**4.64**
Intergranular pore	12.33	3.95
Intragranular pore	5.67	1.28
Other pores (Mouldic, fracture, intracristaline)	4.67	<1

Table 2: Maximum and average values of the main diagenetic constituents and the sandstones types of porosity from volcanoclastic features and deposits.

5.3 Compaction, porosity and fluidization

Compaction in the sandstones is quite homogeneous, packing varies from loose to normal, with a predominance of normal packing. Petrographic evidence of mechanical compaction includes fracturing of quartz, feldspar and zeolite cement grains along the lava-sediment interface. Chemical compaction was limited, as indicated by point intergranular contacts, long and sparse concave-convex contacts.

The primary intergranular porosity (Table 2) is more plenty far from the lava-sediment contact (Figs. 8A). However, there may be sediment-filled and/or zeolite-cemented vesicles along the lava-sediment interface (Figs. 8B). Intragranular porosity (Table 2) due to partial or total dissolution of unstable grains of the framework occurs mainly in volcanic fragments, secondarily in feldspars. Less common types of pores include moldic, grain-fracturing, and intracrystalline (Tab. 2). Moldic pores were generated by the dissolution, mainly, of volcanic grains, whereas intracrystalline pores occur, especially, in plagioclase crystals in volcanic fragments (Fig. 8 C).

Along the lava-sediment interface it is possible to observe characteristics in the sediments that indicate fluidization: sediments with vesicles along the contact (Figure 8B, D), flow foliation in detrital clays (Fig.8D) and vesicles with sediments included in the

volcanic flow. The different morphologies of volcanic lithoclasts represent active fluidization processes (Figs.4C, D, 8C).

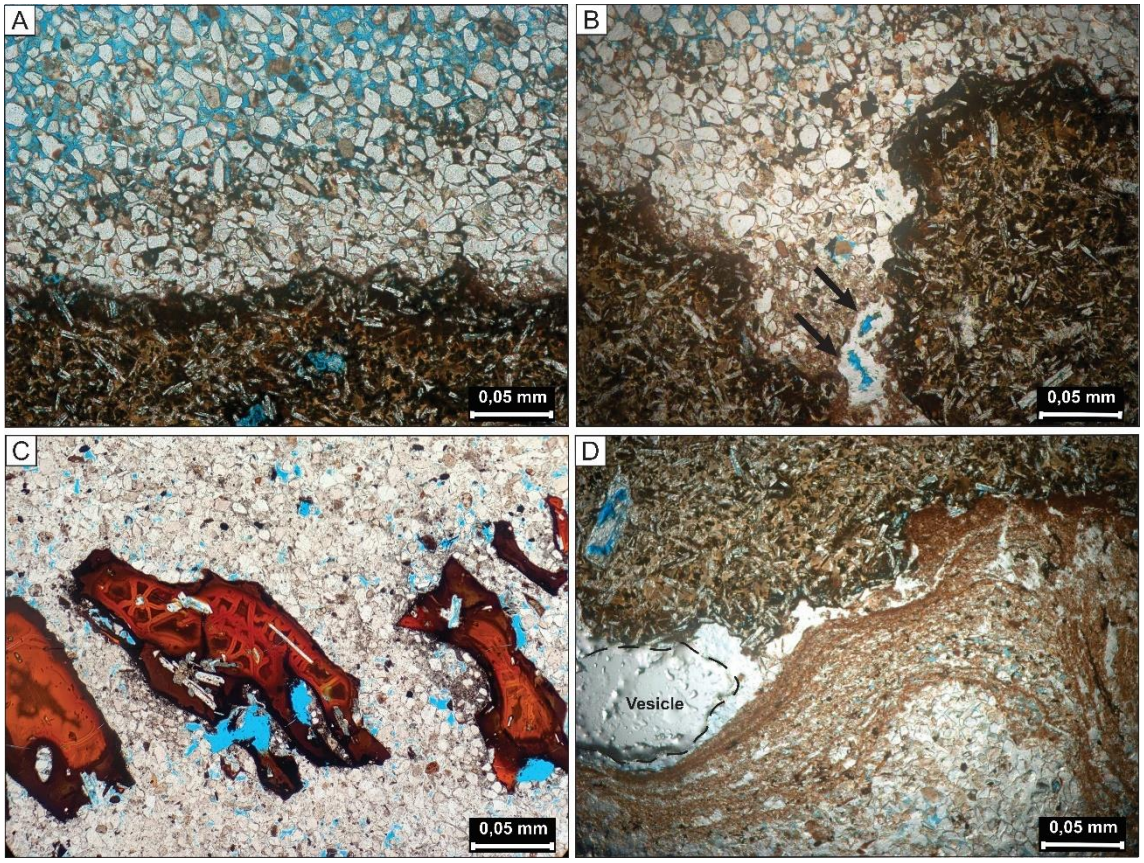

Figure 8: A) The intergranular porosity is preserved outside the basalt contact zone (uncrossed polarizers, //P). B) Cementation by zeolite along the basalt-sandstone interface and vesicles (black arrows) in the sediments near the contact (//P). C) Vitreous, angular volcanic fragments with intracrystalline porosity in palgioclase crystals (//P). D) Foliation by fluidization marked by detrital clays and occurrence of vesicles along the lava-sediment contact (//P).

6. MATRIX OF THE FEATURES AND EPICLASTIC DEPOSITS

6.1 Detrital texture, composition and provenance

The analyzed samples vary texturally from very fine to very coarse sandstones, with a predominance of fine to coarse sandstones, predominantly moderately sorted. The samples are predominantly laminated, evidenced by the granulometric variation of the grains and, secondarily, massive. The grains are predominantly subrounded. Packing varies from loose to normal, with point, long, and rare concave-convex contacts.

Quartz grains are mainly monocrystalline and, secondarily, polycrystalline (Tab. 3). Detrital feldspars are essentially microcline with rare orthoclases (Tab. 3). Many feldspar grains could not be identified due to their intense dissolution. Volcanic lithoclasts are the second most abundant detrital constituent. However, metamorphic rock fragments are more common when compared to plutonic and sandstone fragments (Table 3). The few grains of detrital clay are oxidized forming parallel laminations (Tab.3). Muscovite is the most common accessory grain (Table 3).

Primary main constituents	Maximum (%)	Average (%)
Monocrystalline quartz grains	44.67	34.71
Policrystalline quartz grains	13.00	8.92
Detrital microcline grains	6.66	3.25
Detrital orthoclase grains	<1	<1
Volcanic rock fragments	11.00	8.42
Plutonic rock fragments	<1	<1
Metamorphic rock fragments	1.67	<1
Sandstone fragments	<1	<1
Detrital clay	<1	<1
Muscovite	<1	<1

Table 3: Simplified petrographic quantification of the main primary constituents of the sandstones from epiclastic features and deposits.

The original composition of the analyzed samples is heterogeneous, with the sandstones predominantly classified as litharenite volcanic sandstone followed by feldspathic litharenite, sublitharenite and subarkose *sensu* Folk (1968) (Figs. 9A, Figs 10A, B). The current composition (Fig. 9B) is essentially more enriched in quartz when compared to the original composition (Fig. 9A), due to the replacement of volcanic fragments by smectite, illite-smectite, hematite, titanium authigenic minerals, zeolite, and also by intense dissolution and replacement of detrital feldspar grains, mostly by smectite. The original composition mainly corresponds to a recycled orogen provenance *sensu* Dickinson (1985) (Fig. 7).

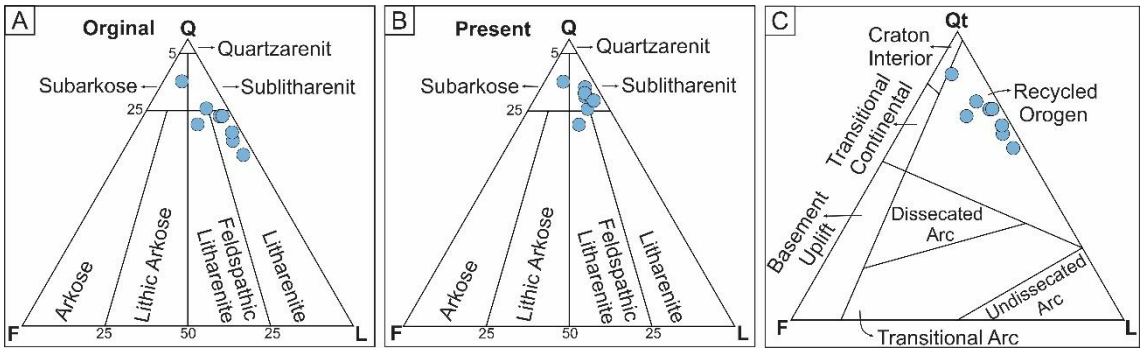

Figure 9: Compositions of the analyzed sandstones plotted in Folk's diagram (1968): A) Original detrital composition of the sandstones. B) Current composition of the sandstones. C) Original detrital composition plotted on Dickinson's (1985) provenance diagram.

6.2 Diagenetic constituents

Clay infiltration and mixed-layers illite-smectite - The infiltrated smectite clays, including mixed layers of illite-smectite (I/S) represent the main cement of sandstones with epiclastic features and deposits (Table 4). They occur in a variety of habits, being able to directly cover the grains (Fig. 10C) and hematite coatings, simple rims, double rims or replacing them with microcrystalline and fibrous aggregates filling the intergranular porosity such as geopetal (pendular) aggregates and meniscus (Table 4; Figs. 10D, 11A). Volcanic fragments and detrital feldspars may be completely dissolved, leaving only the mold pore formed by coatings and illite-smectite rims (Table 4). Single and double rims may show contraction and expansion of volume due to grain surface detachment (Fig. 11A). Intragranular aggregates of smectite and illite-smectite (Tab.4) are microcrystalline and fibrous, occurring mainly replacing volcanic fragments (Fig. 11A)., feldspars and heavy minerals.

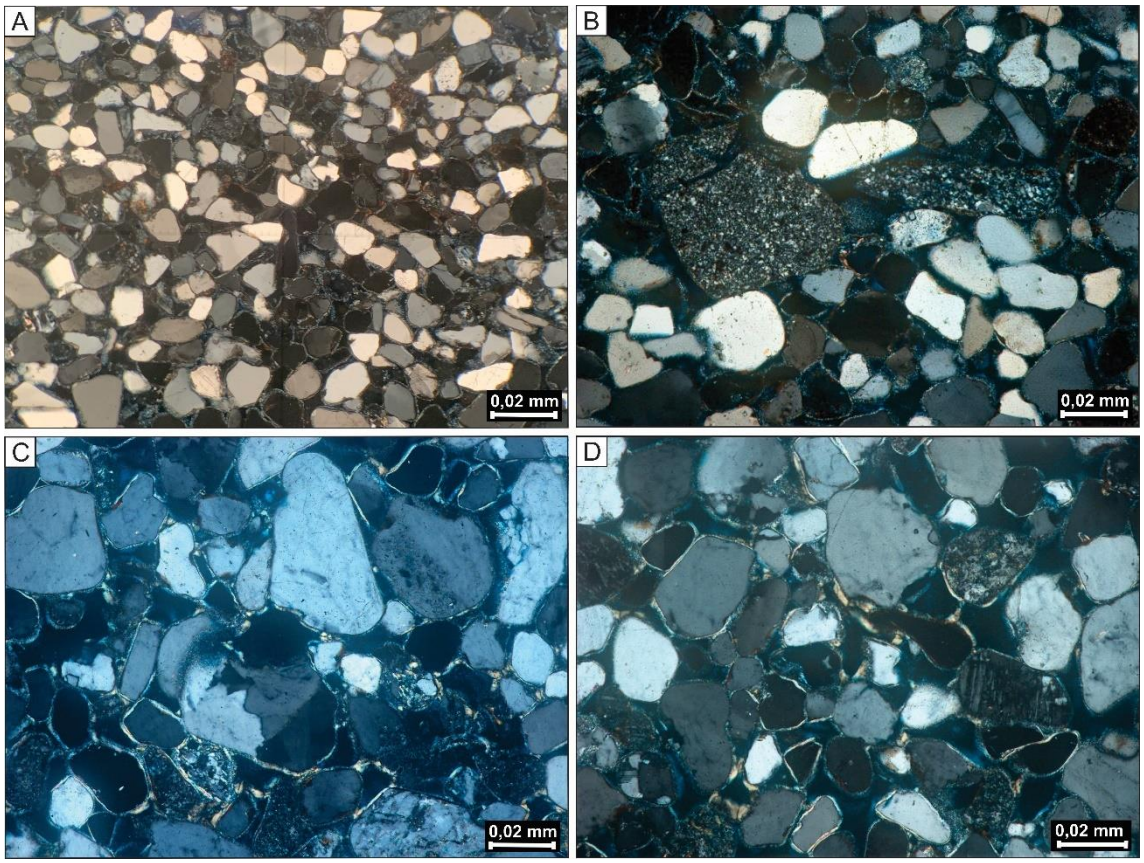

Figure 10: A) Fine to medium litharenite volcanic sandstone, moderately sorted, massive, with subrounded grains (crossed polarizers, XP). B) Litharenite volcanic sandstone with point and long contacts (XP). C) Smectite coatings and illite-smectite interstratified covering the framework grains (XP). D) Coatings and smectite fibrous aggregates filling the intergranular porosity with pendular shapes (XP).

Zeolite - Zeolite (Table 4) occurs mainly as substitutive intragranular form, replacing volcanic lithoclasts and filling the intragranular porosity. Prismatic zeolite rims may occur on authigenic clays and on hematite coatings or directly on volcanic fragments and detrital quartz grains.

Hematite - Hematite occurs mainly as continuous coatings and as inherited coatings in the most concave and least bulging portions of the grains (Table 4; Fig. 11B). They replace volcanic fragments, heavy minerals. Hematite coatings can form mold porosity by delimiting the contour of fully dissolved grains.

Quartz cement - Quartz cement occurs mainly as syntax overgrowths, and outgrowths may also occur (Table 4; Fig. 11C). Likewise, K-feldspar grains (Tab. 4) may show outgrowths (Fig. 11C), in many cases the K-feldspar grains were completely dissolved with only the outgrowths remaining.

Authigenic titanium minerals - Authigenic titanium minerals occur as prismatic, acicular crystals and as microcrystalline aggregates specially replacing volcanic fragments (Figs. 11A, B) and heavy mineral grains (Tab.4)

Calcite – Calcite cement fills intergranular pores with blocky habits (Table 4). Calcite forms on hematite coatings and rims of authigenic clays (Fig. 11D).

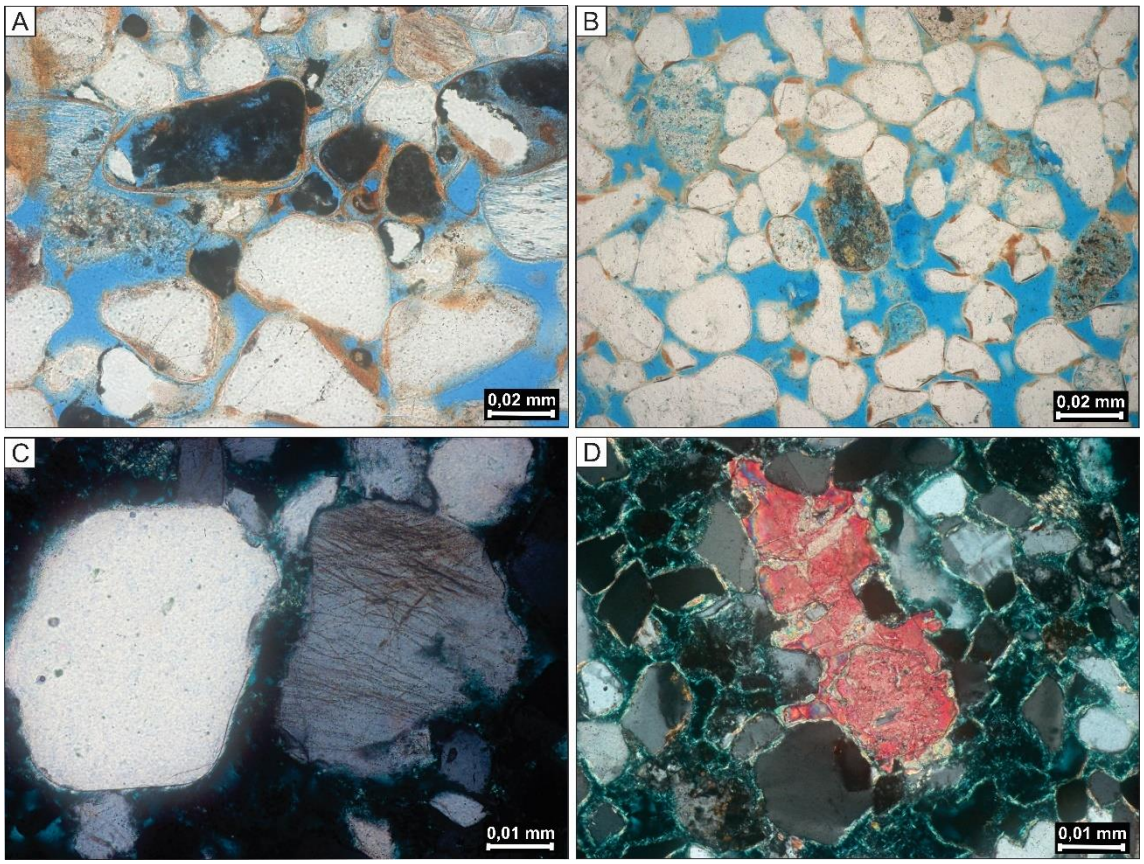

Figure 11: A) Coatings and smectite fibrous aggregates with signs of expansion/contraction and pendular shapes. Dissolved and volcanic K-feldspar fragments being dissolved and replaced by authigenic smectite and titanium, forming intragranular and moldic porosities (uncrossed polarizers, //P). B) Inherited hematite coatings and replacement of volcanic grains by smectite and authentic titanium. Intergranular, intragranular and mold porosities (//P). C) Prismatic quartz and K-feldspar outgrowths (crossed polarizers, XP). D) Cementation of block calcite, filling the intergranular porosity, following the smectite and illite-smectite rims on the framework grains (XP).

Diagenetic main constituents and porosity	Maximum (%)	Average (%)
Infiltrated clay and ilite-smectite	**30.00**	**23.7**
Intragranular smectite, ilite-smectite	**6.00**	**2.09**
Total zeolite	**8.67**	**2.79**
Intergranular zeolite	3.00	<1
Intragranular zeolite	8.67	2.33
Hematite	**4.67**	**2.08**
Quartz cement	**16.00**	**2.00**
Intragranular TiO_2	**4.34**	**1.38**
Intergranular Calcite.	**4.67**	**<1**
K-feldspar	**2.34**	**<1**
Total porosity	**13**	**9.33**
Intergranular pore	12.33	3.95
Intragranular pore	5.67	1.28
Mouldic pore	4.67	<1

Table 4: Maximum and average values of the main diagenetic constituents and types of porosity (epiclastic).

6.3 Compaction and porosity

Compaction in the sandstones is quite homogeneous, and packing ranging from loose to normal, with a predominance of normal packing. Petrographic evidence of mechanical compaction includes fracturing of quartz and feldspar grains. The chemical compaction occurred in a restricted way, consistent with point intergranular contacts, long and rare concave-convex contacts.

Primary intergranular porosity is more abundant when compared to intragranular and mold porosities (Table 4). The concentration of authigenic clays allowed greater preservation of intergranular porosity (Figs. 10C, D). Partial dissolution of volcanic fragments and K-feldspar grains represent intragranular porosity (Tab. 4; Figs. 11A, B). Moldic pores (Tab. 4; Figs. 11A, B) were formed by the dissolution of volcanic lithoclasts.

7. DISCUSSION

7.1 Main textural and compositional detrital differences

The original composition is heterogeneous for both of sandstones with volcanoclastic features and deposits, and for sandstones with epiclastic features and deposits. However, there is a predominance of feldspathic litharenites for the volcanoclastics, followed by volcanic sandstone litharenites for the epiclastics. In both, volcanic lithoclasts represent the second most abundant detrital constituent and are found dissolved, replaced and/or oxidized. Furthermore, detrital feldspar grains are essentially microcline and, subordinately, orthoclase. Despite the different proportions of existing detrital clay between both, the main distinction between them is the presence of textural fluidization indicators. The presence of volcanic clasts with angular, globular and fluidal morphologies (Figs. 4C, D, 8C), as well as the foliation of detrital micas (Fig. 8D), sediments with vesicles (Figs. 8B, D) and vesicles with included sediments in the volcanic flow along the lava-sediment contact, indicate a strong influence of fluidization on the detrital texture of sandstones related to features and volcanoclastic deposits (Kokelaar, 1982, Skilling et al., 2002)

7.2 Main diagenetic differences

There are substantial differences in the patterns of diagenetic changes that have affected volcanoclastic sandstones from epiclastic sandstones. The main difference is related to the contact diagenesis (McKinley et al., 2001; Bernet and Gaupp, 2005) the volcanoclastic sandstones were submitted, which allowed extensive cementation of chalcedony, followed by zeolite. The effects of volcanic flows and intrusions into sedimentary rocks are outside of normal burial diagenetic processes (McKinley et al., 2001; Bernet and Gaupp, 2005). Whereas, the epiclastic sandstones underwent regular burial diagenetic processes, where the main diagenetic constituent of these sandstones are the infiltrated and interstratified illite-smectite clays.

The textural characteristics indicative of fluidization, found at the lava-sediment interface, point to unconsolidated sediments, influenced by surface diagenetic changes and that were probably wet or saturated in water during the interaction with the volcanic

flow. These sediments underwent thermal episodes and fluid percolation defined by the volcanic flows that covered them.

7.3 Paragenetic sequence and diagenetic environments

Some diagenetic processes that affected the analyzed sandstones are eodiagenetic, pre-compactional, and prior to the lava-sediment interaction, in the case of the volcanoclastic sandstones, since they occurred right after deposition and under the direct influence of surface conditions.

Volcanoclastic and epiclastic sandstones have quartz grains with continuous hematite coatings representing the oldest eodiagenetic process that is previous to the autigenesis of most other minerals (Fig. 12). They were formed under loose packing conditions, near the depositional surface. Inherited hematite coatings cover the available spaces of the grains and are absent in the convex grain portions, representing part of the recycled framework, being formed earlier and outside the depositional site (Gregory, 1950; Walker, 1979; Doelling et al., 1989; Bush, 2020). Oxidation of volcanic lithoclasts took place under telodiagenetic conditions (Fig. 12).

In the epiclastic sandstones (Figs.3A, B), the remarkable quantity of subrounded grains of volcanic origin and detrital constituents, indicates the transport of volcanic material during the quiescence of volcanism and the active contemporary sedimentary system. Although infiltrated clays occur in both analyzed sandstones, they constitute an important coating of epiclastic sandstones. These clays are formed under eodiagenetic conditions under semi-arid to arid climatic conditions (McKinley et al., 2003) (Fig. 12). They were infiltrated into the sediments by runoff, due to the lowering of the water table and settled in the vadose zone, which was confirmed by the presence of fibrous and microcrystalline aggregates filling the intergranular porosity with pendular shapes and in meniscus, in the epiclastic sandstones. Complex aggregates of coatings and rims in these sandstones may represent alterations of volcanic materials and the subsequent autigenesis of smectite, as well as the replacement of these fragments in smectite (Surdam and Boles, 1979; Hawlader, 1990; Moraes and De Ros, 1992; De Ros et al., 1997; McKinley et al., 2003). Thus, smectites possibly occur by mechanical infiltration and also by neoformation, due to the alteration of volcanic materials available during eodiagenesis (Fig. 12). With burial and increasing temperature, smectites were partially transformed

by mixed illite-smectite (I/S) layers under mesodiagenetic conditions (Moraes and De Ros, 1992; Worden and Morad, 2003) (Fig. 12).

The small number of overgrowths and outgrowths of quartz and K-feldspar in both sandstones, volcanoclastic and epiclastic, was possibly promoted by the smectite coatings on the framework grains, which inhibited the autigenesis of this cement (Ajdukiewicz and Larese, 2012), mainly in the epiclastics. In addition, the low rate of compaction of these sandstones, evidenced by the spatial relations of the loose to normal packing, with punctual, long and rare concave-convex contacts, allows inferring the eodiagenetic origin of these cements. Overgrowths and outgrowths of quartz and K-feldspar are posterior to the coatings and rims of smectite, making it impossible to assess, among quartz and K-feldspar cements, which one is the precursor (Fig. 12). Quartz overgrowths can be found engulfed by chalcedony, evidencing their earlier origin, in the volcanoclastic sandstones. Dissolution of detrital feldspar grains occurs mainly during telodiagenesis, forming secondary porosity (Fig. 12).

For volcanoclastic sandstones, the formation of opal, chalcedony and megaquartz cements through burial is unlikely, due to the intergranular volume occupied by these cements in the sandstones, indicating early conditions close to the surface. Furthermore, for quartz and its polymorphs (opal and chalcedony) the solubility increases slightly with temperature, thus decreasing the probability of significant precipitation from them at elevated burial temperatures (Mackenzie and Bricker, 1971). The pH of diagenetic fluids exerts a great influence on the formation of quartz and amorphous silica (opal), with pH values below 9 favoring their precipitation (Scholle and Scholle, 1978). However, the relative high proportion of quartz cement (18.74%) and the spatial relationships of the framework allow considering the possibility of elevated temperatures in surface conditions. Thus, the siliceous cement would have been provided by contact diageneses conditions induced by the volcanic event, where effective cementation inhibited a possible effective compaction (Fig. 12). Through the heat of the overlying lavas or in contact with the sandstones, fluids rich in silica were progressively incorporated into the system through the dissolution of volcanic fragments and the devitrification of the glassy matrix of the associated volcanic material (Nogueira et al., 2021). The heating produced by the volcanic flows increased the temperature and pressure on the sediments, increasing the solubility of the quartz polymorphs, thus providing a greater amount of silica-rich fluids available for cementation (Dove and Rimstidt, 1994;

Nogueira et al.., 2021). This situation would have provided a cyclic mechanism of dissolution and reprecipitation of opal and chalcedony cements. Allowing the formation of zoned opal and chalcedony cements, indicating a formation in multiple episodes during contact diagenesis. The first siliceous polymorph to precipitate is opal, causing a decrease of silica concentration in solution and consequently promoting later crystallization of cryptocrystalline and microcrystalline forms of silica, such as chalcedony. Favoring the development of chalcedony over opal cements. Megaquartz cementation occurs after chalcedony, with a decrease in silica saturation in the fluid, forming larger and more developed crystals. It occurs mainly along the lava-sediment contact and is related to the zeolite, being prior to it (Fig 6C).

In volcanoclastic sandstones, mainly along the lava-sediment interface, zeolite cementation occurs. In these sandstones the cementation of zeolite, as well as the cementation of silica polymorphs, originated before the burial of the sediments as evidenced by the spatial relationships of the framework, indicating a cementation near the surface. The sequence of three stages in the evolution of cementation of zeolites and the subsequent filling of the porosity along the lava-sediment contact were formed during the thermal episode that provided the interaction of lava with wet or water-saturated sediment during contact diagenesis (Fig. 12). In epiclastic sandstones cementation by intergranular and intragranular zeolite occurred under eodiagenetic conditions, being determined by temperature conditions, availability of reactive precursor material such as volcanic glass, volcanic clasts and plagioclase, as well as the existence of a highly alkaline environment (Ghent,1979; Iijima, 1988; Remy, 1994; Bernet and Gaupp, 2005) (Fig. 12).

The alteration of the zeolite cement and subsequent cementation by poikilotopic calcite and coarse mosaic was observed in the volcanoclastic sandstones (Fig. 7B). In turn, zeolites were replaced and calcite could precipitate when pore fluid conditions changed due to a decrease in temperature and an increase in PCO2 (Helmold and Van de Kamp, 1984; Rabelo et al., 2019). Indicating that this process occurred at the end of contact diagenesis in the volcanoclastic sandstones (Fig. 12). However, in epiclastic sandstones the conditions for the precipitation of block calcite occurred during eodiagenesis, where the interaction of meteoric water with volcanic lithoclasts allowed its formation (Fig. 12).

In epiclastic sandstones, authigenic titanium minerals were formed by the alteration of volcanic fragments during eodiagenesis (Fig. 12). Later, during

mesodiagenesis, with the remobilization of the eodiagenetic minerals formed, there was the transformation of small eodiagenetic minerals into other larger mesodiagenetic minerals (Fig. 12). In the volcanoclastic sandstones, the authigenic titanium minerals were formed at the end of contact diagenesis and later during mesodiagenesis (Fig. 12).

Celadonite cement, in volcanoclastic sandstones, was characterized as a telodiagenetic process, formed due to significant oxidation of basalt by surface water, reflecting the high ferric iron content of this mineral (Velde, 2014) (Fig. 12). For volcanoclastic and epiclastic sandstones, there was an important formation of secondary porosity during telodiagenesis with the dissolution and oxidation of detrital constituents such as volcanic lithoclasts and the dissolution of detrital K-feldspar grains (Fig. 12). Furthermore, the dissolution of contact diageneses constituents such as chalcedony and zeolite cements occurred in the volcanoclastic sandstones.

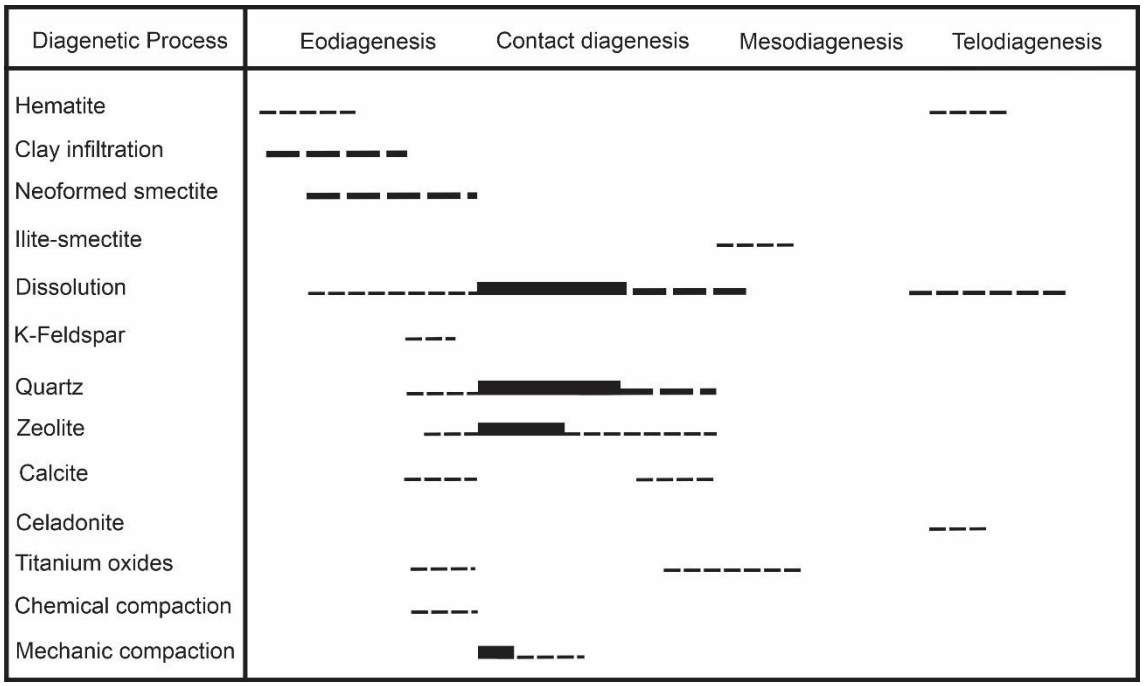

Figure 12: Simplified paragenetic sequence for volcanoclastic and epiclastic sandstones. The thickness of the lines indicates the importance of each process.

8. CONCLUSIONS

The analyzes of the volcanoclastic sandstones and epiclastic sandstones revealed that:

I. Although the detrital compositions of both are heterogeneous, the main difference between them is the presence of textures characteristic of fluidization in volcanoclastic

sandstones. Such evidence, in these sandstones, indicates that the lava-sediment interaction occurred with humid or water-saturated sediments.

II. Volcanoclastic sandstones, under eodiagenetic conditions, were initially cemented by hematite coatings, followed by infiltrated clays, overgrowths and outgrowths of quartz and K-feldspar. Moreover, the epiclastic sandstones, under the same conditions, were cemented primarily by coatings of hematite, infiltrated clays, neoformed smectites, overgrowths and outgrowths of quartz and K-feldspar, calcite, zeolite, authigenic titanium minerals.

III. The spatial relationships in the framework of volcanoclastic sandstones allowed us to observe that due to the intergranular volume occupied by quartz cements and zeolites, the conditions for their formation were by contact diagenesis.

IV. Under contact diagenesis conditions, the volcanoclastic sandstones were cemented by opal, chalcedony and megaquartz through dissolution and reprecipitation mechanisms of siliceous fluids incorporated in the system. Cementation of zeolite occurred preferentially along the lava-sediment contact zone, and could be replaced by calcite at the end of the contact diagenesis. Autigenic titanium minerals were formed at the end of these conditions.

V. In volcanoclastic and epiclastic sandstones, mesodiagenesis is marked by the formation of interstratified illite-smecite and remobilization and formation of authigenic titanium minerals.

VI. The diagenetic process of secondary porosity formation by dissolution of volcanic lithoclasts and detrital K-feldspar grains was of great importance in volcanoclastic and epiclastic sandstones during telodiagenesis. The dissolution of contact diagenesis constituents (chalcedony and zeolite) and formation of celadonite cement occurred during the telodiagenesis of volcanoclastic sandstones.

Acknowledgments

The first author thanks the Conselho Nacional de Desenvolvimento Científico e Tecnológico (CNPq) for the scholarship granted during this doctoral period (Process: 141345/2017-9). Special thanks to professors Luiz Fernando De Ros and Amanda Goulart Rodrigues for their provided knowledge.

9. BIBLIOGRAPHIC REFERENCES

Ajdukiewicz, J.M., Larese, R.E., 2012. How clay grain coats inhibit quartz cement and preserve porosity in deeply buried sandstones: Observations and experiments. AAPG Bull. 96, 2091–2119. doi: 10.1306/02211211075

Allen, R.L., 1992. Reconstruction of the tectonic, volcanic and sedimentary setting of strongly deformed Zn-Cu massive sulfide deposits at Benambra, Victoria, Australia. Econ. Geol. 87, 825-854. https://doi.org/10.2113/gsecongeo.87.3.825.

Allen, P.A., Allen, J.R., 2013. Basin Analysis: Principles and Application to Petroleum Play Assessment. 3rd edition. Chichester, Wiley-Blackwell 642p. Allen: Basin analysis: Principles and application... - Google Acadêmico

Baksi, A.K., 2018. Paraná flood basalt volcanism primarily limited to ~ 1 Myr beginning at 135 Ma: New40Ar/39Ar ages for rocks from Rio Grande do Sul, and critical evaluation of published radiometric data. J. Volcanol. Geotherm. Res. 355, 66–77. doi: 0.1016/j.jvolgeores.2017.02.016

Bernet, M., Gaupp, R., 2005. Diagenetic history of Triassic sandstone from the Beacon Supergroup in central Victoria Land, Antarctica. New Zealand Journal of Geology and Geophysics. 48, 447 - 458. doi: https://doi.org/10.1080/00288306.2005.9515125

Boulter, C.A., 1993. High-level peperitic sills at Rio Tinto, Spain: implications for stratigraphy and mineralization. Trans. Inst. Min. Metall. 102, B30-B38.

Branney, M., Suthren, R., 1988. High-level peperitic sills in the English Lake District: distinction from block lavas, and implications for Borrowdale Volcanic Group stratigraphy. Geol. J. 23, 171-187. doi: https://doi.org/10.1002/gj.3350230206.

Busby-Spera, C.J., White, J.D.L., 1987. Variation in peperito textures associated with di¡ering host-sediment properties. Bull. Volcanol. 49, 765-775. doi: 10.1007/BF01079827.

Busch, B., 2020. Pilot study on provenance and depositional controls on clay mineral coatings in active fluvio-eolian systems, western USA. Sedimentary Geology, 105721. doi: https://doi.org/10.1016/j.sedgeo.2020.105721

Cas, R.F., Wright, J.V., 1987. Volcanic Succession: Modern and ancient: London, Allen & Unwin, 528 p.

Cloetingh, S., Ziegler, P.A., 2007. Tectonic Models for the Evolution of Sedimentary Basins. Treatise on Geophysics, 485–611. doi: https://doi.org/10.1016/B978-044452748-6.00109-7

De Ros, L.F., Morad, S., Al-Aasm, I.S., 1997. Diagenesis of siliciclastic and volcaniclastic sediments in the Cretaceous and Miocene sequences of NW African margin (DSDP Leg 47A, Site 397). Sedimentary Geology 112, 137-156. doi: https://doi.org/10.1016/S0037-0738(97)00030-4

De Ros, L.F., Goldberg, K., 2007, Reservoir petrofacies: a tool for quality characterization and prediction: AAPG Annual Conference and Exhibition, Long Beach, CA, Extended Abstracts Vol. 6 pp. 1. Microsoft Word - AAPG07_Petrofacies_extended5.doc (endeeper.com)

Dickson J.A.D., 1966. Carbonate identification and genesis as revealed by staining. Journal of Sedimentary Petrology, 36(2): 491-505. doi: https://doi.org/10.1306/74D714F6-2B21-11D7-8648000102C1865D

Dickinson, W.R., 1985. Interpreting provenance relations from detrital modes of sandstones, in: Zuffa, G.G. (Ed.), Provenance of Arenites. NATO-ASI Series C: Mathematical and Physical Sciences, v. 148, D. Reidel Publishing Co., Dordrecht, The Netherlands, pp. 333–361. doi: 10.1007/978-94-017-2809-6_15

Doelling, H.H., Davis, F.D., Brandt, C.J., 1989. The Geology of Kane County, Utah: Geology, Mineral Resources, Geologic Hazards: Bulletin 124. Utah Geological and Mineral Survey, Salt Lake City, UT. Doelling: The geology of Kane County, Utah: Geology,... - Google Acadêmico

Dove, P.M., Rimstidt, J.D., 1994. Silica-water interactions. In: Heaney, P.J., Prewitt, C.T., Gibbs, G.V. (Eds.), Silica: Physical Behavior, Geochemistry and Materials Applications, 29. MSA Rev. Mineral, pp. 259–308. doi: https://doi.org/10.1515/9781501509698-013

Fischer, R.V., 1960. Classification of volcanic breccias. Geologic Society American Bulletin, 71: 973-982. doi: https://doi.org/10.1130/0016-7606(1960)71[973:COVB]2.0.CO;2.

Folk, R.L. 1968. Petrology of Sedimentary Rocks. Hemphill's, Austin, Texas, 107 pp.

Ghent, E.D., 1979. Problems in zeolite facies geothermometry, geobarometry and fluid compositions. In: Scholle PA, Schluger PR ed.Aspects of diagenesis. Society of

Economic Paleontologists and Mineralogists Special Publication 26: 81-87. doi: https://doi.org/10.2110/pec.79.26.0081

Gregory, H.E., 1950. Geology and Geography of the Zion Park Region, Utah and Arizona. A comprehensive report on a scenic and historic region of the southwest. Professional Paper, 220. USGS, Washington, D.C., 200 pp. Gregory: Geology and geography of the Zion Park region,... - Google Acadêmico

Hawlader, H.M., 1990. Diagenesis and reservoir potential of volcanogenic sandstones - Cretaceous of the Surat Basin, Australia. Sedimentary Geology 66, 181-195. doi: https://doi.org/10.1016/0037-0738(90)90059-3

Helmold, K.P., Van de Kamp, P.C., 1984. Diagenetic mineralogy and controls on albitization and laumontite formation in Paleogene arkoses, Santa Ynez Mountains, California. In: McDonald, D.A., Surdam, R.C. (Eds.), Clastic Diagenesis. Mem., Am. Assoc. Pet. Geol., 37, pp. 239–276. doi: https://doi.org/10.1306/M37435C15

Iijima, A., 1988. Chapter 3 Diagenetic Transformations of Minerals As Exemplified By Zeolites and Silica Minerals-A Japanese View. Developments in Sedimentology, 147–211. doi: https://doi.org/10.1016/S0070-4571(08)70008-6

Janasi, V.D.A., de Freitas, V.A., Heaman, L.H., 2011. The onset of flood basalt volcanism, Northern Paraná Basin, Brazil: a precise U-Pb baddeleyite/zircon age for a Chapecó-type dacite. Earth and Planetary Science Letters, 302(1), 147-153. doi: 10.1016/j.epsl.2010.12.005.

Kokelaar, B.P., 1982. Fluidization of wet sediments during the emplacement and cooling of various igneous bodies. J. Geol. Soc. London 139, 21-33. doi: https://doi.org/10.1144/gsjgs.139.1.0021

Lorenz, B.E., 1984. Mud-magma interactions in the Dunnage Mélange, Newfoundland. In: Kokelaar, B.P., Howells, M. (Eds.), Volcanic and Associated Sedimentary and Tectonic Processes in Modern and Ancient Marginal Basins, Geol. Soc. London. Spec. Publ. 16, pp. 271-277. doi: https://doi.org/10.1144/GSL.SP.1984.016.01.20

Macdonald, G.A., 1939. An intrusive peperite at San Pedro Hill, California. Calif. Univ. Publ. Dept. Geol. Sci. Bull. 24, 329-338.

MacKenzie, F.T., Bricker, O.P., 1971. Cementation of sediments by carbonate minerals. In Bricker, O.P. (ed.), Carbonate Cements. Baltimore, MD: Johns Hopkins Press, pp. 239–246.

Mckinley, J.M., Worden, R.H., Ruffell, A.H., 2001. Contact Diagenesis: The Effect of an Intrusion on Reservoir Quality in the Triassic Sherwood Sandstone Group, Northern Ireland. Journal of Sedimentary Research, 71(3), 484–495. doi: 10.1306/2DC40957-0E47-11D7-8643000102C1865D

McKinley, J.M., Worden, R. and Ruffell, A.H., 2003. Smectite in sandstones: a review of the controls on occurrence and behaviour during diagenesis, in: Worden, R. H., Morad, S. (Eds.), Clay Cements in Sandstones. IAS Special Publication, Blackwell Scientific Publications, Oxford, UK, pp. 109-128. doi: https://doi.org/10.1002/9781444304336.ch5

McPhie, J., Doyle, M.G., Allen, R.L., 1993. Volcanic Textures: A Guide to the Interpretation of Textures in Volcanic Rocks. Centre for Ore Deposit and Exploration Studies, University of Tasmania, Hobart (198 p.).

Miall, A.D., 2000. Principles of Sedimentary Basin Analysis. 3rd Updated and Enlarged edition. Springer, Berlin (616 pp.). Miall: Principles of sedimentary basin analysis - Google Acadêmico

Michelin, C.R.L. 2014. Ágata do Distrito Mineiro de Salto do Jacuí (Rio Grande do Sul, Brasil) - uma caracterização com base em técnicas estratigráficas, petrográficas, geoquímicas e isotópicas. PhD Thesis, Programa de Pós-Graduação em Geociências, Instituto de Geociências, Universidade Federal do Rio Grande do Sul.

Milani, E.J., 1997. Evolução tectono-estratigráfica da Bacia do Paraná e seu relacionamento com a geodinâmica fanerozóica do Gondwana sul-ocidental. PhD Thesis, Programa de Pós-Graduação em Geociências, Instituto de Geociências, Universidade Federal do Rio Grande do Sul.

Milani, E.J., Faccini, U.F., Scherer, C.M., Araújo, L.M., Cupertino, J.A., 1998. Sequences and Stratigraphic Hierarchy of the Paraná Basin (Ordovician to Cretaceous), Southern Brazil. BoI. IG USP, Série Científica, 29, 125-173. http://dx.doi.org/10.11606/issn.2316-8986.v29i0p125-173

Milani, E.J., Melo, J.H.G., Souza, P.A., Fernandes, L.A., França, A.B. 2007. Bacia do Paraná. Boletim de Geociências da Petrobras, 15(2): 265-287. doi: https://www.researchgate.net/publication/279547262_Parana_basin.

Moraes, M.A.S., De Ros L.F., 1992. Depositional, infiltrated and authigenic clays in fluvial sandstones of the Jurassic Sergi Formation, Recôncavo Basin, northeastern Brazil, in: D. W. Houseknecht, E. W. Pittman. (Eds.), Origin, Diagenesis and Petrophysics of Clay Minerals in Sandstones. SEPM Special Publication, pp. 197-208. doi: https://doi.org/10.2110/pec.92.47.0197

Nogueira, A. C. R., Rabelo, C. E. N., Góes, A. N., Cardoso, A. R., Bandeira, J., Rezende, G. L., dos Santos, R. F. S., Truckenbrodt, W., 2021. Evolution of Jurassic intertrap deposits in the Parnaíba Basin, northern Brazil: The last sediment-lava interaction linked to the CAMP in West Gondwana, Palaeogeography, Palaeoclimatology, Palaeoecology. 572, 110370. doi: https://doi.org/10.1016/j.palaeo.2021.110370.

Petry, K., Jerram, D.A., Almeida, D.P.M., Zerfass, H., 2007. Volcanic-sedimentary features in the Serra Geral Fm., Paraná Basin, southern Brazil: Examples of dynamic lava-sediment interactions in an arid setting. J. Volcanol. Geotherm. Res., 159: 313–325. doi: https://doi.org/10.1016/j.jvolgeores.2006.06.017.

Rabelo, C.E.N., Cardoso, A.R., Nogueira, A.C.R., Soares, J.L., Góes, A.M., 2019. Genesis of poikilotopic zeolite in aeolianites: an example from the Parnaíba Basin, NE Brazil. Sediment. Geol. 385, 61–78. doi:https://doi.org/10.1016/j.sedgeo.2019.03.013

Reis, G.S., Mizusaki, A.M.P., Roisenberg, A., Rubert, R.R., 2014. Formação Serra Geral (Cretáceo da Bacia do Paraná): um análogo para os reservatórios ígneo-básicos da margem continental brasileira. Pesquisas em Geociências, 41(2), 155-168. doi: https://doi.org/10.22456/1807-9806.78093.

Reis, A. D. dos, Scherer, C. M. dos S., Amarante, F. B., Rossetti, M. M. M., Kifumbi, C., Souza, E. G., Owen, A., 2019. Sedimentology of the proximal portion of a large-scale, Upper Jurassic fluvial-aeolian system in Paraná Basin, southwestern Gondwana. Journal of South American Earth Sciences, 102248. doi: https://doi.org/10.1016/j.jsames.2019.102248

Remy, R.R., 1994. Porosity reduction and major controls on diagenesis of Cretaceous Paleocene volcaniclastic and arkosic sandstone, Middle Park Basin, Colorado. J. Sediment. Res. 64, 797–806.

Renne, P.R., Ernesto, M., Pacca, I.G., Coe, R.S., Glen, J.M.G., Prevot, M., Perrin, M., 1992. The Age of Parana Flood Volcanism, Rifting of Gondwanaland, and the Jurassic-Cretaceous Boundary. Science (80-.). 258, 975–979. doi:10.1126/science.258.5084.975

Rios, F.R., Mizusaki, A.M.P., Michelin, C.R.L., 2018. Feições de interação vulcano-sedimentares – exemplos na Bacia do Paraná (RS). UNESP, Geociências, 37(3), 483-495. doi: https://doi.org/10.5016/geociencias.v37i3.12172

Rios, F.R., Mizusaki, A.M.P., Michelin, C.R.L., 2018, Rodrigues, I.C.S., 2023. Volcano-sedimentary interactions - a key to understand Cretaceous paleoenvironments in the Paraná Basin (southern Brazil). Journal of Volcanology and Geothermal Research. Manuscript number: VOLGEO-D-23-00040.

Rocha, B.C., Davies, J.H.F.L., Janasi, V.A., Schaltegger, U., Nardy, A.J.R., Greber, N.D., Lucchetti, A.C.F., Polo, L.A., 2020. Rapid eruption of silicic magmas from the Paraná magmatic province (Brazil) did not trigger the Valanginian event. Geology, 48(12): 1174-1178. doi: https://doi.org/10.1130/G47766.1

Rosa, C.J.P., McPhie, J., Relvas, J.M.R.S., 2016. Distinguishing peperite from other sediment-matrix igneous breccias: Lessons from the Iberian Pyrite Belt. J. Volcanol. Geotherm. Res. 315, 28–39. doi: https://doi.org/10.1016/j.jvolgeores.2016.02.007

Rossetti, L., Lima, E. F., Waichel, B. L., Hole, M. J., Simões, M. S., Scherer, C. M. S., 2018. Lithostratigraphy and volcanology of the Serra Geral Group, Paraná Etendeka Igneous Province in Southern Brazil: Towards a formal stratigraphical framework. Journal of Volcanology and Geothermal Research, 355, 98–114. doi: https://doi.org/10.1016/j.jvolgeores.2017.05.008

Scherer, C.M.S. 2000. Eolian dunes of the Botucatu Formation (Cretaceous) in Southernmost Brazil: morphology and origin. Sedimentary Geology, 137: 63–84. doi: 10.1016/S0037-0738(00)00135-4

Scherer, C.M.S. 2002. Preservation of aeolian genetic units by lava flows in the Lower Cretaceous of the Paraná Basin, southern Brazil. Sedimentology, 49, 97-116. doi: https://doi.org/10.1046/j.1365-3091.2002.00434.x

Scholle, P.A., Ulmer-Scholle, D., 1978. Cements and cementation. In: Middleton, G.V., Church, M.J., Coniglio, M., Hardie, L.A., Longstaffe, F.J. (eds) Encyclopedia of Sediments and Sedimentary Rocks. Encyclopedia of Earth Sciences Series. Springer, Dordrecht. doi: https://doi.org/10.1007/978-1-4020-3609-5_40

Skilling, I.P., White, J.D.L., McPhie, J., 2002. Peperite: a review of magma–sediment mingling. J. Volcanol. Geotherm. Res. 114, 1–17. doi: https://doi.org/10.1016/S0377-0273(01)00278-5

Surdam, R.C., Boles, J.R., 1979. Diagenesis of volcanic sandstones. In: Scholle, P.A., Schluger, P.R. (Eds.), Aspects of Diagenesis, 26. Society of Economic Paleontologists and Mineralogists Special Publication, pp. 227–242 doi: https://doi.org/10.2110/pec.79.26.0227

Thiede, D.S., Vasconcelos, P.M., 2010. Paraná flood basalts: rapid extrusion hypothesis confirmed by new 40Ar/39Ar results. Geology, 38, 747-750. doi: https://doi.org/10.1130/G30919.1.

Velde, B., 2014. Green Clay Minerals. Treatise on Geochemistry, 351–364. doi: https://doi.org/10.1016/B978-0-08-095975-7.00712-9

Waichel, B., Scherer, C., Frank, H., 2008. Basaltic lava flows covering active aeolian dunes in the Paraná Basin in southern Brazil: features and emplacement aspects. J. Volcanol. Geotherm. Res. 171, 59–72. doi: https://doi.org/10.1016/j.jvolgeores.2007.11.004

Walker, T.R., 1979. Red color in dune sands. In: McKee, E.D. (Ed.), A Study of Global Sand Seas. Geological Survey Professional Paper. U.S. Government Printing Office, Washington, D.C., pp. 61 - 81. Walker: Red color in dune sand - Google Acadêmico

Weissmann, G.S., Hartley, A.J., Scuderi, L.A., Nichols, G.J., Owen, A., Wright, S., Felicia, A.L., Holland, F., Anaya, F. M. L., 2015. Fluvial geomorphic elements in modern sedimentary basins and their potential preservation in the rock record: A review. Geomorphology, 250, 187–219. doi: https://doi.org/10.1016/j.geomorph.2015.09.005

Worden, R.H., Morad, S. 2003. Clay minerals in sandstones: controls on formation distribution and evolution, in: Worden, R. H., Morad, S. (Eds.). Clay minerals cements in Sandstones, International Association of Sedimentologists Special

Publication 34, Blackwell Publishing, Oxford, pp. 109–128. doi: https://doi.org/10.1002/9781444304336.ch1

Zalán, P.V., Wolff, S., Astolfi, M.A.M., Vieira, I.S., Conceição, J.C.J., Appi, V.T., Neto, E.V.S., Cerqueira, J.R., Marques, A., 1990. The Paraná Basin, Brazil. Tulsa: AAPG Memoir, 51: 681- 708.

Zuffa, G.G., 1985. Optical analysis of arenites: Influence of methodology on compositional results,in: Zuffa, G.G. (Ed.), Provenance of Arenites. NATO-ASI Series C: Mathematical and Physical Sciences, v. 148, D. Reidel Publishing Co., Dordrecht, The Netherlands, pp. 165–189. Optical-Analyses-of-Arenites-Influence-of-Methodology-on-Compositional-Results.pdf (researchgate.net)

CAPÍTULO 7 - CONCLUSÕES

7. CONCLUSÕES

A identificação de três sistema deposicionais caracterizados por seus respectivos ciclos, associações de fácies e fácies como sendo flúvio-eólico, pertencente à Formação Guará, eólico, pertencente à Formação Botucatu e vulcano-eólico, da Formação Serra Geral demonstraram-se síncronos pelo menos em uma de suas fases de desenvolvimento ocorridas durante o Cretáceo Inferior. Além disso, as superfícies de contato entre as formações não evidenciam hiatos prolongados.

O sistema flúvio-eólico da Formação Guará, foi caracterizado por três ciclos de canais entrelaçados que culminam com inundações, desenvolveu-se, de forma singular também sobre uma planície vulcânica precursora do extravasamento de lavas representado pela Formação Serra Geral. Os depósitos ali formados representam um sistema de canais efêmeros instalados sobre uma planície vulcânica. Esse derrame e os depósitos sobrepostos representam a primeira ocorrência de derrames vulcânicos, a última de um sistema fluvial e a vigência de condições áridas em direção ao topo. A transição entre o sistema flúvio-eólico para o francamente eólico da Formação Botucatu deu-se de forma abrupta e em um intervalo de tempo curto

Ao comparar a morfologia do sistema eólico da Formação Botucatu com os ambientes eólicos atuais, propõe-se um aumento na quantidade de água e/ou umidade para oeste dos perfis estudados na borda atual da Bacia do Paraná, não sendo possível estimar os teores de água (%) que estavam presentes. Este fato é confirmado pelo aparecimento de frações silto-argilosas, bem como pelo aumento da granulometria dos sedimentos associados aos lençóis de areia eólicos, com indícios de canais fluviais efêmeros, a oeste dos perfis estudados. Além disso, a fragmentação da lava e a erosão do substrato vulcânico, formando clastos vulcânicos com diferentes morfologias e com distintas granulometrias, registrados em cada domínio, aponta, principalmente, para aspectos relacionados a diferenças de umidade e saturação em água entre os domínios propostos.

As análises dos arenitos referentes a feições e depósitos vulcanoclásticos e dos arenitos de feições e depósitos epiclásticos revelaram que apesar de as composições detríticas de ambos serem heterogêneas, a principal diferença entre eles é a presença de

texturas características de fluidização nos arenitos vulcanoclásticos. Tais evidências, nesses arenitos, apontam que a interação lava-sedimento ocorreu com sedimentos úmidos ou saturados em água. Os arenitos vulcanoclásticos, sob condições eodiagenéticas, foram cimentados inicialmente por cutículas de hematita, seguidas por argilas infiltradas, overgrowths e outgrowths de quartzo e K-feldspato. Ademais, os arenitos epiclásticos, sob as mesmas condições, foram cimentados primeiramente por cutículas de hematita, argilas infiltradas, esmectitas neoformadas, overgrowths e outgrowths de quartzo e K-feldspato, calcita, zeólita, minerais de titânio autigênicos.

As relações espaciais no arcabouço dos arenitos vulcanoclásticos permitiram observar que, devido ao volume intergranular ocupado pelos cimentos quartzosos e de zeólitas, as condições para suas formações foi por diagênese de contato. Sob condições de diagênese de contato os arenitos vulcanoclásticos foram cimentados por opala, calcedônia e megaquartz através de mecanismos de dissolução e reprecipitação dos fluidos silicosos incorporados no sistema. A cimentação de zeólita ocorreu preferencialmente ao longo da zona de contato lava-sedimento, podendo ser substituída por calcita ao final da diagênese de contato. Minerais autigênicos de titânio foram formados ao final dessas condições.

Nos arenitos vulcanoclásticos e epiclásticos a mesodiagênese é marcada pela formação de interestratificado ilita-esmecita e remobilização e formação de minerais autigênicos de titânio. O processo diagenético de formação de porosidade secundária por dissolução dos litoclastos vulcânicos e de grãos de K-feldspato detrítico foi de grande importância nos arenitos vulcanoclásticos e epiclásticos durante a telodiagênese. A dissolução de constituintes diagenéticos de contato (calcedônia e zeólita) e formação do cimento de celadonita ocorreu durante a telodiagênese dos arenitos vulcanoclásticos.

CAPÍTULO 8 - REFERÊNCIAS BIBLIOGRÁFICAS

Allen, R.L., 1992. Reconstruction of the tectonic, volcanic and sedimentary setting of strongly deformed Zn-Cu massive sulfide deposits at Benambra, Victoria, Australia. Econ. Geol. 87, 825-854.

Almeida, E.F.M., 1954. Botucatu, um deserto triássico da América do Sul. DNPM Div. Geo. Min., Notas Prel. E Estudos, 86.

Almeida, E.F.M., Melo, C., 1981. A Bacia do Paraná e o vulcanismo no Mesozóico. In: Bistrichi, C.A., Carneiro, C.D.R., Dantas, A.S.L., Ponçano, W.L. (Eds.), Mapa geológico do Estado de São Paulo, nota explicativa. Instituto de Pesquisas Tecnológicas, 1, 46-77.

Amarante, F.B., Scherer, C.M.S., Goso Aguilar, C.A., Reis, A.D., Mesa, V., Soto, M., 2019. Fluvial-eolian deposits of the Tacuarembó Formation (Norte basin – Uruguay): depositional models and stratigraphic succession. J. South Am. Earth Sci. 90, 355–376.

Andreis, R.R., Bossi, G. E., Montardo, D.K., 1980 O Grupo Rosário do Sul (Triássico) no Rio Grande do Sul. In: Congresso Brasileiro de Geologia, 31, Balneário Camboriú. Anais... Balneário Camboriú. SBG. 659-673.

Arioli, E.E., Licht, O.A.B., Vasconcellos, E.M.G., Bonnet, K.L., Santos, E.M., 2008. Faciologia vulcânica da Formação Serra Geral na região de Guarapuava, Paraná. In: IV Simpósio de Vulcanismo e Ambientes Associados, 4., 2008. Foz do Iguaçu. Anais. Foz do Iguaçu, SBG. 1CDROM.

Artur, P.C., Soares, P.C., 2002. Paleoestruturas e petróleo na Bacia do Paraná, Brasil. Revista Brasileira de Geociências, 32(4): 433-448.

Ballén, O.A.R., Góes, A.M., Negri, F.A., Maziviero, M.V., Teixeira, V.Z.S., 2013. Sistema eólico úmido nas sucessões sedimentares interderrames da Formação Mosquito, Jurássico da Província Parnaíba, Brasil. Brazi. J. Geol. 43, 695–710.

Baksi, A.K., 2018. Paraná flood basalt volcanism primarily limited to ~ 1 Myr beginning at 135 Ma: New40Ar/39Ar ages for rocks from Rio Grande do Sul, and critical evaluation of published radiometric data. J. Volcanol. Geotherm. Res. 355, 66– 77.

Bellieni, G., Comin-Chiaramonti, P., Marques, L, S., Melfi, A. J., Piccirillo, A. J. R., Roisemberg, A., 1984. High-and-low-TiO2 flood basalts from the Paraná Plateau (Brazil): petrology and geochemical aspects bearing on their mantle origin. Neues Jahrbuch fur Mineralogie, 150(3), 273-306.

Betiollo, L.M., 2006. Caracterização estrutural, hidrogeológica e hidroquímica dos sistemas aquiferos Guarani e Serra Geral no nordeste do Rio Grande do Sul, Brasil. Porto Alegre, 117p. Dissertação de Mestrado, Programa de Pós-graduação em Geociências, Instituto de Geociências, Universidade Federal do Rio Grande do Sul.

Bigarella, J.J., 1979. Botucatu and Sambaiba sandstones of South America (Jurassic and Cretaceous); and Cave sandstone and similar sandstone of Southern Africa (Triassic). In: McKee, F.D. (Ed.), A Study of Global Sand Seas. U.S. Geological Survey Professional Paper, 1052, 233-238.

Bigarella, J.J., Salamuni, R., 1961. Early Mesozoic wind patterns as suggested by dune bedding in the Botucatu Sandstone of Brazil and Uruguai. Geol. Soc. Amer. Bull., 72, 1089-1106.

Bigarella, J.J., Salamuni, R., 1967. Botucatu Formation. In: Bigarella, J.J., Becker, R.D., Pinto, I.D. (Eds.), Problems in Brazilian Gondwana Geology, Curitiba, pp. 197–206.

Boulter, C.A., 1993. High-level peperitic sills at Rio Tinto, Spain: implications for stratigraphy and mineralization. Trans. Inst. Min. Metall. 102, B30-B38.

Branney, M., Suthren, R., 1988. High-level peperitic sills in the English Lake District: distinction from block lavas, and implications for Borrowdale Volcanic Group stratigraphy. Geol. J. 23, 171-187.

Branney, M., Bonnichsen, B., Andrews, G., Ellis, B., Barry, T., McCurry, M., 2008. Snake River (SR)-type'volcanism at the Yellowstone hotspot track: distinctive products from unusual, high-temperature silicic super-eruptions: Bulletin of Volcanology, 70, 293-314.

Brito, I.M., 1979. Bacias sedimentares e formações pós–paleozóicas do Brasil. Rio de Janeiro, Interciência, 175p.

Brooks, E.R., 1995. Palaeozoic Fluidization, folding and peperito formation, northern Sierra Nevada, California. Can. J. Earth. Sci. 32, 314-324.

Brooks, E.R., Wood, M.M., Garbutt, P., L, 1982. Origin and metamorphism of peperite and associated rocks in the Devonian Elwell Formation, northern Sierra Nevada, California. Geol. Soc. Am. Bull. 93, 1208-1231.

Brown, D.J., Bell, B.R., 2007. How do you grade peperites? J. Volcanol. Geotherm. Res., 159, 409-420.

Busby-Spera, C.J., White, J.D.L., 1987. Variation in peperite textures associated with differing host-sediment properties. Bull. Volcanol. 49, 765-775.

Cas, R.F., Wright, J.V., 1987. Volcanic Succession: Modern and ancient: London, Allen & Unwin, 528 p.

Cas, R.A.F., Edgar, C., Allen, R.L., Bull, S., Cliford, B.A., Giordano, G., Wright, J.V., 2001. Influence of magmatism and tectonics on sedimentation in an extensional lake basin: the Upper Devonian Bunga Beds, Boyd Volcanic Complex, southeastern Australia. In: White, J.D.L., Riggs, N.R. (Eds.), Volcaniclastic Sedimentation in Lacustrine Settings, Int. Assoc. Sediment. Spec. Publ. 30, 83-108.

Dadd, K.A., Van Wagoner, N.A., 2002. Magma composition and viscosity as controls on peperite texture: an example from Passamaquoddy Bay, southeastern Canada. In: Skilling, I.P., White, J.D.L., McPhie, J. (Eds.), Peperite: Processes and Products of Magma-Sediment Mingling. J. Volcanol. Geotherm. Res., 114, 63-80.

De Ros, L.F., Goldberg, K., 2007, Reservoir petrofacies: a tool for quality characterization and prediction: AAPG Annual Conference and Exhibition, Long Beach, CA, Extended Abstracts Vol. 6 pp. 1.

Donaire, T., Saez, R., Pascual, E., 2002. Rhyolitic globular peperites from the Aznalcollar mining district (Iberian Pyrite belt, Spain): physical and chemical controls. In: Skilling, I.P., White, J.D.L. and McPhie, J. (Eds.), Peperite: Processes and Products of Magma-Sediment Mingling. J. Volcanol. Geotherm. Res. 114, 119-128.

Doyle, M.G., 2000. Clast shape and textural associations in peperite as a guide to hydromagmatic interactions: Upper Permian basaltic and basaltic andesite examples from Kiama, Australia. Aust. J. Earth Sci. 47, 167-177.

Druitt, T.H., 1995. Settling behavior of concentrated dispersions and some volcanological applications. J. Volcanol. Geotherm. Res. 65, 27–39.

Druitt, T.H., Bruni, G., Lettieri, P., Yates, J.G., 2004. The fluidization behaviour of ignimbrite at high temperature and with mechanical agitation. Geophys. Res. Lett. 31, 136–152.

Druitt, T., Avard, G., Bruni, G., Lettieri, P., Maes, F., 2007. Gas retention in fine-grained pyroclastic flow materials at high temperatures. Bull. Volcanol. 69, 881–901.

Erkül, F., Helvaci, C., Sözbilir, H., 2006. Olivine basalt and trachyandesite peperites formed at the subsurface/surface interface of a semi-arid lake: an example from

the Early Miocene Bigadiç basin, western Turkey. J. Volcanol. Geotherm. Res. 149, 240–262.

Famelli, N., Millett, J.M., Hole, M.J., Lima, E.F., Carmo, I.O., Jerram, D.A., Jolley, D.W., Pugsley, J.H., Howell, J.A., 2021. Characterizing the nature and importance of lavasediment interactions with the aid of field outcrop analogues. J. S. Am. Earth Sci. 108, 103108.

Fernandes, M.A., Carvalho, I.S., 2008. Revisão diagnóstica para a icnoespécie 683 de tetrápode Mesozóico Brasilichnium elusivum (Leonardi, 1981) 684 (Mammalia) da Formação Botucatu, Bacia do Paraná, Brasil. 685 Ameghiniana, 45(1), 167–173.

Fernandes, A.C.S., Carvalho, I.S., Guimarães–Netto, R., 1990. Icnofósseis de invertebrados da Formação Botucatu, São Paulo (Brasil). Anais da Academia Brasileira de Ciências, 62 (1), 45–49.

Fernandes, M.A., Fernandes, L.B.R., Souto, P.R.F., 2004. Occurrence of urolites related to dinosaurs in the Lower Cretaceous of the Botucatu Formation, Paraná Basin, São Paulo State, Brazil. Revista Brasileira de Paleontologia, 7(2), 263–268.

Fischer, R.V., 1960. Classification of volcanic breccias. Geologic Society American Bulletin, 71: 973-982.

Francischini, H., Dentzien-Dias, P.C., Fernandes, M.A. Schultz, C.L., 2015. Dinosaur ichnofauna of the Upper Jurassic/Lower Cretaceous of the Paraná Basin (Brazil and Uruguay). Journal of South American Earth Sciences 63, 180-190.

Frank, H.T., Elisa, M., Gomes, B., Luiz, M., Formoso, L., 2009. Review of the areal extent and the volume of the Serra Geral Formation, Paraná Basin, South America. Pesqui. em Geociencias 36, 49–57.

Gifkins, C.C., McPhie, J., Allen, R.L., 2002. Pumiceous peperito in ancient submarine volcanic successions. In: Skilling, I.P., White, J.D.L., McPhie, J. (Eds.), Peperite: processes and products of magma-sediment mingling. J. Volcanol. Geotherm. Res. 114, 181-203.

Gihm, Y.S., Kwon, C.W., 2017. Textural variations and fragmentation processes in peperite formed between felsic lava flow and wet substrate: An example from the Cretaceous Buan Volcanics, southwest Korea. J. Volcanol. Geotherm. Res. 331, 92–101.

Girolami, L., Druitt, T.H., Roche, O., Khrabrykh, Z., 2008. Propagation and hindered settling of laboratory ash flows. J. Geophys. Res. 113: B02202.

Godoy, M. M., Binotto, R. B., Silva, R. C., Zerfass, H., 2011. Geologia e Recursos Minerais do Geoparque Quarta Colônia, estado do Rio Grande do Sul, escala 1:100.000. Porto Alegre, Serviço Geológico do Brasil, CPRM. 54p.

Godoy, M. M., Scherer, O. L. B., Binotto, R. B., Gross, A. O. M., Dreher, A. M., 2016. Geologia e Recursos Minerais da Folha Sobradinho – SH.22-V-C-II, estado do Rio Grande do Sul, escala 1:100:000. Porto Alegre Serviço Geológico do Brasil, CPRM. 107p.

Godoy, M.M., Scherer, O. L. B., Binotto, R. B., Kischlat, E. E., Dreher, A. M., 2018. Geologia e Recursos Minerais da Folha Santa Maria – SH.22-V-C-IV, estado do Rio Grande do Sul, escala 1:100:000. Porto Alegre Serviço Geológico do Brasil, CPRM. 179p.

Goto, Y., McPhie, J., 1996. A Miocene basanite peperitic dyke at Stanley, northwestern Tasmania, Australia. J. Volcanol. Geotherm. Res. 74, 111-120.

Hanson, R.E., 1991. Quenching and hydroclastic disruption of andesitic to rhyolitic intrusions in a submarine island-arc sequence, northern Sierra Nevada, California. Geol. Soc. Am. Bull. 103, 804-816.

Hanson, R.E., Wilson, T.J. 1993. Large-scale rhyolitic peperitos (Jurassic, southern Chile). Journal of Volcanology and Geothermal Research, 54: 247-264.

Hanson, R.E., Hargrove, U.S., 1999. Processes of magma/wet sediment interaction in a large-scale Jurassic andesitic peperite complex, northern Sierra Nevada, California. Bull. Volcanol. 60, 610-626.

Hartmann, L.A., Duarte, L.C., Massonne, H.-J., Michelin, C., Rosenstengel, L.M., Bergmann, M., Theye, T., Pertille, J., Arena, K.R., Duarte, S.K., Pinto, V.M., Barboza, E.G., Rosa, M.L.C.C., Wildner, W., 2012a. Sequential opening and filling of cavities forming vesicles, amygdales and giant amethyst geodes in lavas from the southern Paraná volcanic province, Brazil and Uruguay. International Geology Review, 54: 1–14. 43

Hartmann, L.A., Arena, K.R., Duarte, S.K., 2012b. Geological relationships of basalts, andesites and sand injectites at the base of the Paraná volcanic province, Torres, Brazil. Journal of Volcanology and Geothermal Research, 237-238: 97–111.

Hole, M., Jolley, D., Hartley, A., Leleu, S., John, N., BalL, M., 2013, Lava–sediment interactions in an Old Red Sandstone basin, NE Scotland. Journal of the Geological Society, 170: 641-655.

Holz, M., Soares, A.P., Soares P.C., 2008. Preservation of aeolian dunes by pahoehoe lava: An example from the Botucatu Formation (Early Cretaceous) in Mato Grosso do Sul state (Brazil), western margin of the Paraná Basin in South America. Journal of South American Earth Sciences, v. 25, p. 398–404.

Hunns, S.R., McPhie, J., 1999. Pumiceous peperite in a submarine volcanic succession at Mount Chalmers, Queensland, Australia. J. Volcanol. Geotherm. Res. 88, 239-254.

Jamtveit B., Svensen H., Podladchikov Y.Y., 2004. Hydrothermal vent complexes associated with sill intrusions in sedimentary basins. In: Physical Geology of High-Level Magmatic Systems (Ed. C. Breitkreuz & N. Petford), vol. 234. Geological Society, London, Special Publications.

Janasi, V.D.A., de Freitas, V.A., Heaman, L.H., 2011. The onset of flood basalt volcanism, Northern Paraná Basin, Brazil: a precise U-Pb baddeleyite/zircon age for a Chapecó-type dacite. Earth and Planetary Science Letters, 302(1), 147-153.

Jeon Y., Sohn, Y.K., 2022. Interactions of pāhoehoe and ‘a‘ā lavas and fluvial sediments on an alluvial plain (the Cretaceous Gyeongsang Basin, Republic of Korea). J. Volcanol. Geotherm. Res.432, 107699.

Jerram, D., Stollhofen, H., 2002. Lava/sediment interaction in desert settings: are all peperite-like textures the result of magma-water interaction? In: Skilling, I.P., White, J.D.L., McPhie, J. (Eds.), Peperite: Processes and Products of Magma-Sediment Mingling. J. Volcanol. Geotherm. Res. 114, 231-249.

Jerram, D.A., Mountney, N., Holzförster, F., Stollhofen, H., 1999a. Internal stratigraphic relationships in the Etendeka Group in the Huab Basin, NW Namibia. Journal of Geodynamics, 28: 393-418.

Jerram, D.A., Mountney, F., Stollhofen, H., 1999b. Facies architecture of the Etjo Sandstone Formation and its interaction with the basal Etendeka Flood Basalts of northwest Namibia: implications for offshore prospectivity. In: Cameron, N.R., Bate, R.H., Clure, V.S. (Eds.), The Oil and Gas Habitats of the South Atlantic. Geological Society London, Special Publications, 153: 367- 380.

Jerram, D., Mountney, N., Howell, J.A., Long, D., Stollhofen, H., 2000. Death of a sand sea: an active aeolian erg systematically buried by the Etendeka flood basalts of NW Namibia. Journal of the Geological Society, 157: 513-516.

Jolly R.J.H., Lonergan L., 2002. Mechanisms and controls on the formation of sand intrusions. Journal of the Geological Society, 159, 605–617.

Kano, K., 1989. Interactions between andesitic magma and poorly consolidated sediments: examples in the Neogene Shirahama Group, south Izu, Japan. J. Volcanol. Geotherm. Res. 37, 59-75.

Kokelaar, B.P., 1982. Fluidization of wet sediments during the emplacement and cooling of various igneous bodies. J. Geol. Soc. London 139, 21-33.

Kwon, C.W., Gihm, Y.S., 2017. Fluidization of host sediments and its impacts on peperitos forming processes, the Cretaceous Buan Volcanics, Korea. J. Volcanol. Geotherm Res. 341: 84–93.

Leonardi, G., Oliveira, F.H., 1990. A revision of the Triassic and Jurassic tetrapod footprints of Argentina and a new approach on the age and meaning of the Botucatu Formation footprints (Brazil). Revista Brasileira de Geociências, 20(1–4), 216–229.

Lorenz, B.E., 1984. Mud-magma interactions in the Dunnage Mélange, Newfoundland. In: Kokelaar, B.P., Howells, M. (Eds.), Volcanic and Associated Sedimentary and Tectonic Processes in Modern and Ancient Marginal Basins, Geol. Soc. London. Spec. Publ. 16, pp. 271-277.

Lorenz, V., Zimanowski, B., Buettner, R., 2002. On the formation of deep-seated subterranean peperite-like magma–sediment mixtures. Journal of Volcanology and Geothermal Research, 114: 107-118.

Luchetti, A. C. F., Nardy, A. J. R., Machado, F. B., Madeira, J. E. O., Arnosio, J. M., 2014. Peperites and sedimentary deposits within the silicic volcanic sequences of the PMP. Solid Earth, 5: 121–130.

Macdonald, G.A., 1939. An intrusive peperite at San Pedro Hill, California. Calif. Univ. Publ. Dept. Geol. Sci. Bull. 24, 329-338.

Machado, F.B., Nardy, A.J.R., Rocha Jr., E.R.V., Marques, L.S., Oliveira, M.A.F., 2009. Geologia e litogeoquímica da Formação Serra Geral nos estados de Mato Grosso e Mato Grosso do Sul. Geociências-Universidade Estadual Paulista, 28: 523–540.

Mazzini A., Jonk R., Duranti D., Parnell J., Cronin B.T., Hurst A., 2003. Fluid escape from reservoirs: implications from cold seeps, fractures and injected sands. Part I: the fluid flow system. Journal of Geochemical Exploration, 78, 293–296.

McLean, C.E., Brown, D.J., Rawcliffe, H.J., 2016. Extensive soft-sediment deformation and peperite formation at the base of a rhyolite lava: Owyhee Mountains, SW Idaho, USA.Bull Volcanol. 78, 42.

McPhie, J., Doyle, M.G., Allen, R.L., 1993. Volcanic Textures: A Guide to the Interpretation of Textures in Volcanic Rocks. Centre for Ore Deposit and Exploration Studies, University of Tasmania, Hobart (198 p.).

Melfi, A.J., Piccirillo, E.M., Nardy, A.J.R., 1988. Geological and magmatic aspects of the Paraná Basin: an introduction. In: Piccirillo, E.M., Melfi, A.J. (Eds.). The Mesozoic flood volcanism of the Paraná Basin: petrogenetic and geophisycal aspects. Instituto Astronômico e Geofísico, Universidade de São Paulo, p 1-13.

Michelin, C.R.L., 2007. Sequência de formação das cavidades no basalto e seu preenchimento com zeólitas, arenito, ágata e ametista, Derrame Miolo, São Martinho da Serra, Rio Grande do Sul, Brasil. Porto Alegre, 50p. Dissertação de Mestrado, Programa de Pós-Graduação em Geociências, Instituto de Geociências, Universidade Federal do Rio Grande do Sul.

Michelin, C.R.L. 2014. Ágata do Distrito Mineiro de Salto do Jacuí (Rio Grande do Sul, Brasil) - uma caracterização com base em técnicas estratigráficas, petrográficas, geoquímicas e isotópicas. PhD Thesis, Programa de Pós-Graduação em Geociências, Instituto de Geociências, Universidade Federal do Rio Grande do Sul.

Milani, E.J., 1997. Evolução tectono-estratigráfica da Bacia do Paraná e seu relacionamento com a geodinâmica fanerozóica do Gondwana sul-ocidental. PhD Thesis, Programa de Pós-Graduação em Geociências, Instituto de Geociências, Universidade Federal do Rio Grande do Sul.

Milani, E.J., Faccini, U.F., Scherer, C.M., Araújo, L.M., Cupertino, J.A., 1998. Sequences and Stratigraphic Hierarchy of the Paraná Basin (Ordovician to Cretaceous), Southern Brazil. BoI. IG USP, Série Científica, 29, 125-173.

Milani, E.J., Melo, J.H.G., Souza, P.A., Fernandes, L.A., França, A.B., 2007. Bacia do Paraná. Boletim de Geociências da Petrobras, 15(2): 265-287.

Mizusaki, A.M.P., 1986. A utilização do microscópio eletrônico de varredura no estudo de rochas reservatório de hidrocarbonetos. Seminário de Geologia, Rio de Janeiro, Petrobrás/Depex, 1: 322-331.

Mountney, N., Howell, J., 2000. Aeolian architecture, bedform climbing and preservation space in the Cretaceous Etjo Formation, NW Namibia. Sedimentology, 47: 825–849.

Mountney, N., Howell, J., Flinth, S., Jerram, D.A., 1998. Aeolian and alluvial deposition within the Mesozoic Etjo Sandstone Formation, northwest Namibia. Journal of African Earth Science, v. 27, p. 175–192.

Mountney, N., Howell, J., Flinth, S., Jerram, D.A., 1999. Relating eolian bounding-surface geometries to the bed forms that generated them: Etjo Formation, Cretaceous, Namibia. Geology, 27: 159–162.

Nichols G.T., Wyllie P.J., Stern C.R., 1994. Subduction zone melting of pelagic sediments constrained by melting experiments. Nature, 371, 785–788.

Nogueira, A. C. R., Rabelo, C. E. N., Góes, A. N., Cardoso, A. R., Bandeira, J., Rezende, G. L., dos Santos, R. F. S., Truckenbrodt, W., 2021. Evolution of Jurassic intertrap deposits in the Parnaíba Basin, northern Brazil: The last sediment-lava interaction linked to the CAMP in West Gondwana, Palaeogeography, Palaeoclimatology, Palaeoecology. 572, 110370.

Peate, D. W., 1989. Stratigraphy and Petrogenesiso of the Parana Continental Flood Basalts, Southern Brazil. Doctoral Tesis. The Open University. 359 p.

Peate, D.W., Hawkesworth, C.J., Mantovani, M.S.M., 1992. Chemical stratigraphy of the Parand lavas (South America): classification of magma types and their spatial distribution. Bulletin Volcanology, 55, 119-139.

Perea, D., Soto, M., Veroslavsky, G., Martínez, S., Ubilla, M., 2009. A Late Jurassic fossil assemblage in Gondwana: biostratigraphy and correlations of the Tacuarembó Formation, Paraná Basin, Uruguay. J. South Am. Earth Sci. 28, 168–179.

Perinotto, J.A.J., Etchebehere, M.L.C., Simões, L.S.A., Zanardo, A., 2008. Diques clásticos na Formação Corumbataí no nordeste da Bacia do Paraná, SP: Análise sistemática e significações estratigráficas, sedimentológicas e tectônicas. Geociências, 27: 469–491.

Petry, K., 2006. Feições de interação vulcano-sedimentares: seu uso como indicadores de contemporaneidade no magmatismo Rodeio Velho (Meso-Ordoviciano) e no vulcanismo Serra Geral (cretáceo inferior). São Leopoldo, 88p. Dissertação de Mestrado em Geociências, Universidade do Vale do Rio do Sinos.

Petry, K., Jerram, D.A., Almeida, D.P.M., Zerfass, H., 2007. Volcanic-sedimentary features in the Serra Geral Fm., Paraná Basin, southern Brazil: Examples of dynamic lava-sediment interactions in an arid setting. J. Volcanol. Geotherm. Res., 159: 313–325.

Pettijohn, F.J., 1975. Sedimentary rocks. New York, Harper & Row, 628p.

Piccirillo, E.M., Melfi, A.J., 1988. The Mesozoic flood volcanism from the Paraná Basin (Brazil): petrogenetic and geophysical aspects. Instituto Astronômico e Geofísico, Universidade de São Paulo, 600p.

Picheler, E., 1952. Diques de arenitos em Salto Grande, rio Paranapanema. Boletim da Sociedade Brasileira de Geologia, 1:15-22.

Pires, E.F., Guerra–Sommer, M., Scherer, C.M.S., Santos, A.R., Cardoso, E., 2011. Early Cretaceous coniferous woods from a paleoerg (Paraná Basin, Brazil). Journal of South American Earth Sciences, 32, 96–109.

Rabelo, C. E. N., 2019. A sucessão Jurássica-Eocretácea da Bacia do Parnaíba, NE do Brasil: paleoambiente, diagênese e correlação com os eventos magmáticos do Atlântico Central (CAMP). PhD Thesis, Programa de Pós-Graduação em Geologia e Geoquímica, Universidade Federal do Pará.

Rabelo, C.E.N., Nogueira, A.C.R., 2015. The sistema desértico húmido do Jurássico Superior da Bacia do Parnaíba, região entre Formosa da Serra Negra e Montes Altos, Estado do Maranhão, Brasil. Geol. USP 15, 3–21.

Rabelo, C.E.N., Cardoso, A.R., Nogueira, A.C.R., Soares, J.L., Góes, A.M., 2019. Genesis of poikilotopic zeolite in aeolianites: an example from the Parnaíba Basin, NE Brazil. Sediment. Geol. 385, 61–78.

Rawcliffe, H. J., 2016. Lava-water-sediment interaction: processes, products and petroleum systems. PhD Thesis, School of Geographical and Earth Sciences, College of Science and Engineering, University of Glasgow.

Rawlings, D.J., 1993. Mafic peperite from the Gold Creek Volcanics in the Middle Proterozoic McArthur Basin, Northern Territory. Aust. J. Earth Sci. 40, 109-113.

Reis, G.S., 2013. A Formação Serra Geral (Cretáceo, Bacia do Paraná) como análogo para os reservatórios ígneo-básicos da margem continental brasileira. Porto Alegre, 2013. 100p. Dissertação (Mestrado em Geociências) - Instituto de Geociências, Universidade Federal do Rio Grande do Sul.

Reis, G.S., Mizusaki, A.M.P., Roisenberg, A., Rubert, R.R., 2014. Formação Serra Geral (Cretáceo da Bacia do Paraná): um análogo para os reservatórios ígneo-básicos da margem continental brasileira. Pesquisas em Geociências, 41(2), 155-168.

Reis, A. D., 2016. Análise arquitetural de depósitos fluviais da Formação Guará (Jurássico Superior-Cretáceo Inferior) na borda sudeste da Bacia do Paraná. M.Sc. dissertation. Universidade Federal do Rio Grande do Sul, RS, Brasil

Reis, A. D., 2020. O sistema fluvial distributivo da Formação Guará, Jurássico Superior, Gondwana Ocidental. PhD Thesis, Programa de Pós-Graduação em Geociências, Instituto de Geociências, Universidade Federal do Rio Grande do Sul

Reis, A. D. dos, Scherer, C. M. dos S., Amarante, F. B., Rossetti, M. M. M., Kifumbi, C., Souza, E. G., Owen, A., 2019. Sedimentology of the proximal portion of a large-scale, Upper Jurassic fluvial-aeolian system in Paraná Basin, southwestern Gondwana. Journal of South American Earth Sciences, 102248

Renne, P.R., Ernesto, M., Pacca, I.G., Coe, R.S., Glen, J.M.G., Prevot, M., Perrin, M., 1992. The Age of Parana Flood Volcanism, Rifting of Gondwanaland, and the Jurassic-Cretaceous Boundary. Science (80-.). 258, 975–979.

Rios, F.R., 2017. Feições de interação vulcano-sedimentares – exemplos na Bacia do Paraná (RS). Porto Alegre, 69p. Dissertação de Mestrado, Programa de Pós-Graduação em Geociências, Instituto de Geociências, Universidade Federal do Rio Grande do Sul.

Rios, F.R., Mizusaki, A.M.P., Michelin, C.R.L., 2018. Feições de interação vulcano-sedimentares – exemplos na Bacia do Paraná (RS). UNESP, Geociências, 37(3), 483-495.

Rocha, B.C., Davies, J.H.F.L., Janasi, V.A., Schaltegger, U., Nardy, A.J.R., Greber, N.D., Lucchetti, A.C.F., Polo, L.A., 2020. Rapid eruption of silicic magmas from the Paraná magmatic province (Brazil) did not trigger the Valanginian event. Geology, 48(12): 1174-1178.

Roche, O., Druitt, T.H., Cas, R.A.F., 2001. Experimental aqueous fluidization of ignimbrite. J. Volcanol. Geotherm. Res. 112, 267–280

Rosa, C.J.P., McPhie, J., Relvas, J.M.R.S., 2016. Distinguishing peperite from other sediment-matrix igneous breccias: Lessons from the Iberian Pyrite Belt. J. Volcanol. Geotherm. Res. 315, 28–39.

Ross, P.S., White, J.D.L., 2005. Unusually large clastic dykes formed by elutriation of a poorly sorted, coarser grained source. J. Geol. Soc. Lond. 162: 579–582.

Rossetti, L., Lima, E. F., Waichel, B. L., Hole, M. J., Simões, M. S., Scherer, C. M. S., 2018. Lithostratigraphy and volcanology of the Serra Geral Group, Paraná Etendeka Igneous Province in Southern Brazil: Towards a formal stratigraphical framework. Journal of Volcanology and Geothermal Research, 355, 98–114.

Scherer, C.M.S., 1998. Análise estratigráfica e litofaciológica da Formação Botucatu (Cretáceo Inferior da Bacia do Paraná) no Rio Grande do Sul. Porto Alegre, 202p. Tese de Doutorado, Programa de Pós-graduação em Geociências, Instituto de Geociências, Universidade Federal do Rio Grande do Sul.

Scherer, C.M.S. 2000. Eolian dunes of the Botucatu Formation (Cretaceous) in Southernmost Brazil: morphology and origin. Sedimentary Geology, 137: 63–84.

Scherer, C.M.S., 2002. Preservation of aeolian genetic units by lava flows in the Lower Cretaceous of the Paraná Basin, southern Brazil. Sedimentology, 49, 97-116.

Scherer, C. M. S.; Lavina, E. L., 1997. Aloformação Guará: uma nova unidade estratigráfica mesozóica na porção meridional da Bacia do Paraná. In: Simpósio sobre cronoestratigrafia da Bacia do Paraná, 3, Barra do Garças. Resumos, Barra do Garças: SBG, 1997. p. 36-37.

Scherer, C.M.S., Lavina, E.L.C., 2005. Sedimentary cycles and facies architecture of aeolian-fluvial strata of the Upper Jurassic Guará Formation, southern Brazil. Sedimentology 52, 1323–1341.

Scherer, C.M.S., Lavina, E.L., 2006. Stratigraphic evolution of a fluvial–eolian succession: the example of the upper Jurassic - lower cretaceous Guará and Botucatu formations, Paraná Basin, southernmost Brazil. Gondwana Res. 9 (4), 475–484.

Scrope, G.P., 1827. Memoir on the Geology of Central France; Including the Volcanic Formations of Auvergne, the Velay and the Vivarais. Longman, Rees, Orme, Brown and Green, London, p. 79.

Skilling, I.P., White, J.D.L., McPhie, J., 2002. Peperite: a review of magma–sediment mingling. J. Volcanol. Geotherm. Res. 114, 1–17.

Snyder, G.L., Fraser, G.D., 1963. Pillow lavas I: Intrusive layered lava pods and pillowed lavas, Unalaska Island, Alaska. U.S. Geol. Surv. Prof., 454-B: 1-23.

Soares, P.C., 1975. Divisão estratigráfica no Mesozóico no Estado de São Paulo. Ver. Bras. Geoc., 5, 251-267.

Soto, M., Perea, D., 2010. Late Jurassic lungfishes (Dipnoi) from Uruguay, with comments on the systematics of Gondwanan ceratodontiforms. Journal of Vertebrate Paleontology, 30(4), 1049–1058.

Squire, R.J., McPhie, J., 2002. Characteristics and origin of peperite involving coarse-grained host sediment. In: Skilling, I.P., White, J.D.L., McPhie, J. (Eds.), Peperite: Processes and Products of Magma-Sediment Mingling. J. Volcanol. Geotherm. Res. 114, 45-61.

Strugale, M., Rostirolla, S. P.; Mancini, F., Portela Filho, C. V.; Ferreira, F.J.F.; Freitas, R.C., 2007. Structural framework and Mesozoic-Cenozoic Evolution os Ponta Grossa Arch, Paraná Basin, southern Brazil. Journal of South American Earth Sciences, 24: 203-227.

Suguio, K., Coimbra, A.M., 1972. Madeira fóssil silicificada na Formação Botucatu. Ciência e Cultura, 24, 1049–1055.

Suguio, K., Fulfaro, J.V., 1974. Diques clásticos e outras feições de contato entre arenitos e basaltos da formação Serra Geral. In: Congresso Brasileiro de Geologia, 28, Porto Alegre, 1974. Anais, Porto Alegre, SBG, v.2, p. 107-112.

Svensen H., Jamtveit B., Planke S., Chevallier L., 2006. Structure and evolution of hydrothermal vent complexes in the Karoo Basin, South Africa. Journal of the Geological Society, 163, 671–682.

Svensen H., Aarnes I., Podladchikov Y.Y., Jettestuen E., Harstad C.H., Planke S. 2010. Sandstone dikes in dolerite sills: Evidence for high pressure gradients and sediment mobilization during solidification of magmatic sheet intrusions in sedimentary basins. Geosphere, 6 (3): 211-224.

Thiede, D.S., Vasconcelos, P.M., 2010. Paraná flood basalts: rapid extrusion hypothesis confirmed by new 40Ar/39Ar results. Geology, 38, 747-750.

Tucker, D.S., Scott, K.M., 2009. Structures and facies associated with the flow of subaerial basaltic lava into a deep freshwater lake: The Sulphur Creek lava flow, North Cascades, Washington: Journal of Volcanology and Geothermal Research, 185, 311-322.

Tuffen, H., Gilbert, J., McGarvie, D., 2001. Products of an effusive subglacial rhyolite eruption: Bláhnúkur, Torfajökull, Iceland. Bull. Volcanol. 63, 179–190.

Waichel, B.L., Lima, E.F., Lubachesky, R., Sommer, C.A. 2006. Pahoehoe flows from the central Paraná Continental Flood Basalts. Bulletin of Volcanology, 68(7/8): 599-610.

Waichel, B.L., Lima, E.F., Sommer, C.A., Lubachesky, R., 2007. Peperite formed by lava flows over sediments: An example from the central Paraná Continental Flood Basalts, Brazil. Journal of Volcanology and Geothermal Research, 159: 343-354.

Waichel, B.L., Scherer, C.M.S., Frank, H.T., 2008. Basaltic lavas covering active Aeolian dunes in the Paraná Basin in Southern Brazil: features and emplacement aspects. J. Volcanol. Geotherm. Res. 169, 59–72.

Walker, R.G., James, N.P., 1992. Fácies Models: Response to Level Sea Change. Geology Association of Canada, St. John's 410 pp.

White, J., Houghton, B., 2006, Primary volcaniclastic rocks: Geology, 34, 677-680.

White, J.D.L., McPhie, J., Skilling, I.P., 2000. Peperite: a useful geneticterm. Bull. Volcanol., 62: 65-66.

Wilson, C.J.N., 1980. The role of fluidization in the emplacement of pyroclastic flows: an experimental approach. J. Volcanol. Geotherm. Res. 8, 231–249.

Wilson, C.J.N., 1984. The role of fluidization in the emplacement of pyroclastic flows, 2: experimental results and their interpretation. J. Volcanol. Geotherm. Res. 20, 55–84.

Zalán, P.V., Conceição, J.C., Wolff, S., Astolfi, M.A., Vieira, I.S., Appi, V.T., Neto, E.V.S., Cerqueira, J.R., Zanotto, O.A., Paumer, M.L., Marques, A., 1986. Análise da Bacia do Paraná. Rio de Janeiro, Petrobras/DEPEX/CENPES, 195p.

Zalán, P.V., Wolff, S., Conceição, J.C.J., Astolfi, M.A.M., Vieira, I.S., Appi, V.T., Zanotto, O.A., 1987. Tectônica e sedimentação da Bacia do Paraná. In: Simpósio Sul-Brasileiro de Geologia, 3., 1987, Porto Alegre. Anais... Porto Alegre, SBG, v.1, p. 441-473

Zalán, P.V., Wolff, S., Astolfi, M.A.M., Vieira, I.S., Conceição, J.C.J., Appi, V.T., Neto, E.V.S., Cerqueira, J.R., Marques, A., 1990. The Paraná Basin, Brazil. Tulsa: AAPG Memoir, 51: 681- 708.

Zalán, P.V., Wolff, S., Conceição, J.C.J., Marques, A., Astolfi, M.A.M., Vieira, I.S., Appi, V.T., Zanotto, O.A., 1991. Bacia do Paraná. In: Gabaglia, G.R. & Milani, E.J. (Eds.) Origem e evolução de bacias sedimentares. Rio de Janeiro, Petrobrás, p.135-168.

Zerfass, H., Sander, A., Flores, A. E., 2007. Geologia da Folha Agudo - SH.22-V-C-V, escala 1:100.000. Porto Alegre. Serviço Geológico do Brasil, CPRM. 98p.

Zimanowski, B., Büttner, R., 2002. Dynamic mingling of magma and liquefied sediments. In: Skilling, I.P., White, J.D.L., McPhie, J. (Eds.), Peperite: Processes and Products of Magma-Sediment Mingling. J. Volcanol. Geotherm. Res. 37-44.

Zuffa, G.G., 1985. Optical analysis of arenites: Influence of methodology on compositional results,in: Zuffa, G.G. (Ed.), Provenance of Arenites. NATO-ASI Series C: Mathematical and Physical Sciences, v. 148, D. Reidel Publishing Co., Dordrecht, The Netherlands, pp. 165–189.